2016

The Role Of Ferric Oxide Particles As Sources And Sinks Of Reactive Oxygen Species During The Autoxidation Of Ferrous Iron

Shengnan Meng
University of South Carolina

THE ROLE OF FERRIC OXIDE PARTICLES AS SOURCES AND SINKS OF REACTIVE OXYGEN SPECIES DURING THE AUTOXIDATION OF FERROUS IRON

by

Shengnan Meng

Bachelor of Engineering
Beijing University of Technology, 2004

Master of Engineering
Beijing University of Technology, 2007

Submitted in Partial Fulfillment of the Requirements

For the Degree of Doctor of Philosophy in

Chemistry

College of Arts and Sciences

University of South Carolina

2016

Accepted by:

John Ferry, Major Professor

Timothy Shaw, Committee Chair

Andrew Greytak, Committee Member

Alicia Wilson, Committee Member

Lacy Ford, Senior Vice Provost and Dean of Graduate Studies

DEDICATION

To my parents.

ABSTRACT

The oxic portion of the biosphere is a metastable mixture of different oxidation states of carbon, sulfur and oxygen energetically poised from equilibrium by the net rate differentials between photosynthetic carbon fixation and its metabolic or abiotic oxidation. The direct reaction of dioxygen with reduced carbon or sulfur is spin forbidden and therefore kinetically slow, but ferric and ferrous iron species serve as catalysts for enabling their oxidation and therefore play critical roles in the environment. This thesis reports exploratory and hypothesis driven research that seeks a better understanding of the physical and chemical limitations on the effectiveness of iron to catalyze interaction between the different oxidation states of these elements. These include studies of the relationship between iron speciation and its ability to generate reactive oxygen species (Chapter 1); the role of heterogeneous iron oxide suspensions in controlling reactive oxygen species yield during the spontaneous reaction of Fe(II) and O_2 (Chapter 2), an exploration of the system of natural iron-containing soils, sulfide and oxygen and how they produce superoxide and hydrogen peroxide (Chapter 3) and a preliminary report of reactive oxygen species and antioxidant enzyme formation in the salt marsh muds (Chapter 4). The results are showing that ferric iron catalyzed oxidation of hydrogen sulfide is an important reservoir for the generation of reactive oxygen species except for the photoinduced processes. The ferrous iron oxidation in the presence of ferric oxides shows a faster oxidation rate and produces a higher yield of reactive

oxygen species, which is indicating the catalysis of the process by removing ferric species from the iron cycle.

TABLE OF CONTENTS

LIST OF TABLES

LIST OF FIGURES

CHAPTER 1

KINETICS AND THERMODYNAMICS IN IRON OXIDATION: THE TENSION BETWEEN K(RATE) AND K(STABILITY)

Iron is an important transition metal in microbial biotic systems, which is essential for many redox processes such as oxygen transportation, etc. In recent years, it is well established that the biogeochemical cycling of iron is a critical micronutrient in marine ecosystem and higher level of iron is beneficial for phytoplankton fertilization.[1]

As a first row transition element, iron can exist in several different oxidation states with Fe(II) and Fe(III) as the most common oxidation states and Fe(IV) to a lesser extent. The redox chemistry of iron, which is one of the most abundant elements in the earth's crust, dissolved iron in oceans is in a range of 0.1 to 9 nmol/kg.[2] This is due to the lower solubility Fe(III), approximately 10^{-17} M at pH 7 comparing with Fe(II) (10^{-1}M) under the same pH.[3] Inorganic Fe(III) forms precipitates and eventually more stable crystalline minerals and this affects its bioavailability.[4-8]

Although Fe(III) is the thermodynamically stable form over Fe(II), in natural environment, however, both forms occur and they are dynamically cycling between each other.[9-13] Fe(II) is generated from either direct photolysis of complexed or colloidal ferric iron species, indirect processes such as reduction by superoxide or other reductive species, as well as biological processes.[2, 14-19] In oxic zones of water column, Fe(II) is not stable and can be oxidized rapidly by dissolved oxygen (primary oxidation) and the

generated reactive oxygen species (ROS) such as superoxide, peroxide and hydroxyl radical (secondary oxidation), *etc*.

As the mechanism illustrated, in natural environment, when dissolved oxygen is available, Fe(II) is oxidized into Fe(III). During this process, redox cycle between Fe(II) and Fe(III) also occurs, as Figure 1 shows.

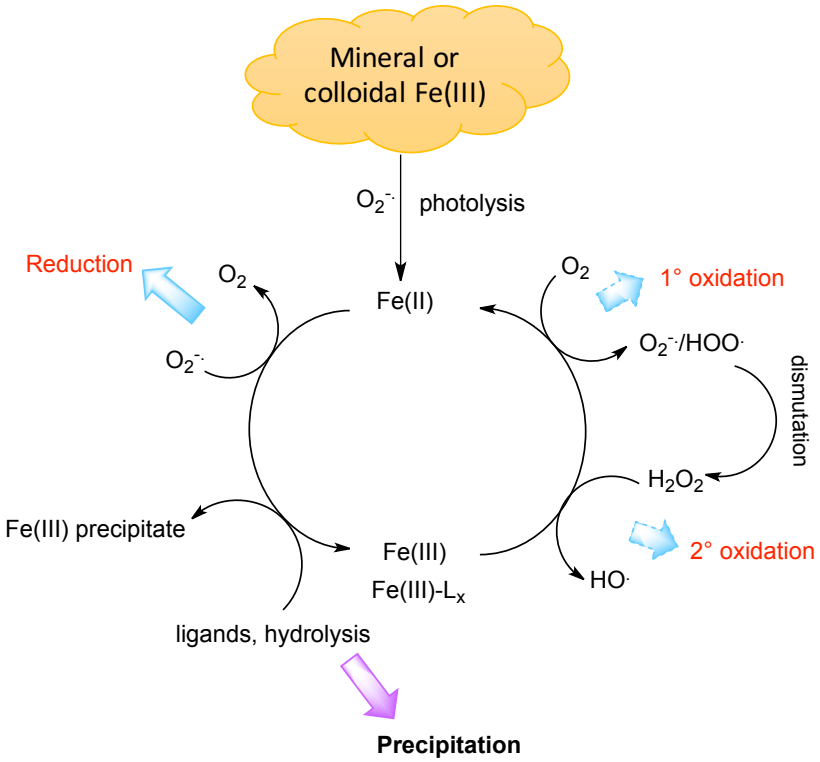

Figure 1.1 The redox cycle between Fe(II) and Fe(III) during the oxidation of Fe(II).

Fe(II) includes dissolved Fe(II) species in all forms including labile and complexed Fe(II). Fe(III) at the bottom refers to dissolved Fe(III), which has two fates: form complexes with natural organic matter (Fe(III)-L_x) and remain dissolved, or bind with precipitating ligands to form insoluble complexes and escape from the redox cycle.

1.1 Thermodynamics of iron in natural waters

The interaction between trace metal cations and anions/ligands as well as the speciation of these metals present in natural waters had received intensive studies in the past several decades.[20-22] The speciation of metals in natural waters is highly dependent on the ionic strength and composition of the system. Different models were proposed based on the studies of speciation in natural waters. The most common models are: (1) ion pairing model proposed by Sillen[23] and Garrel *et al*;[24] (2) the specific ion interaction model proposed by Biedermann;[25] and (3) the Pitzer's model,[21] which was applied in a variety of areas to determine the association between aqeous species,the solubility of minerals, and the solubility of atmospheric gases in natural waters.[26] Millero has used the combination of ion pairing model and Pitzer's model to study the speciation of rare earth's metals in natural waters[22] and the speciation of Fe(II) and Fe(III) in natural waters with organic complexes considered.[26]

Generally, the formation of a complex between metal M and ligand L can be expressed by the following reaction:

$$M^{m+} + L^{n-} \rightarrow ML^{m-n}$$

The stoichiometric stability constant K^*_{ML} for the formation of this complex is given by

$$K^*_{ML} = K_{ML}\gamma_M\gamma_L/\gamma_{ML}$$

where K_{ML} is the thermodynamic constant in pure water, and the γ_i values are the activity coefficients of the ions the the formed complex. The fraction of the free metal ion M is given by

$$[M]_F \Big/ [M]_T = (1 + \Sigma K^*_{MLi}[L_i]_F)^{-1}$$

and the fraction of free ligand L is given by

$$[L]_F \Big/ [L]_T = (1 + \Sigma K^*_{MiL}[M_i]_F)^{-1}$$

Using the equations above, the fraction of a given complex can be determined from

$$[MX] \Big/ [M]_T = \mathrm{K}^*_{ML}[X]_F/(1 + \Sigma K^*_{MLi}[L_i]_F)$$

$$[MX] \Big/ [X]_T = \mathrm{K}^*_{ML}[M]_F/(1 + \Sigma K^*_{MiL}[M_i]_F)$$

When K^*_{ML} is known, the speciation of a given ion can be determined by solving equation (12)-(14).[26]

The kinetics of Fe(II) oxidation is highly dependent on the speciation of iron in both oxidation states since the complexation reaction may be the rate determining step, or the produced iron complex may show different reactivity to dissolved oxygen.

1.2 Fe(II) oxidation

The well-accepted mechanism was proposed by King *et al*, which is known as the Haber-Weiss mechanism,[27] and Fe(II) reacts as follows:

$$\mathrm{Fe(II)} + O_2 \rightarrow Fe(III) + O_2^{-\cdot}$$

$$\mathrm{Fe(II)} + O_2^{-\cdot} + 2H^+ \rightarrow Fe(III) + H_2O_2$$

$$\mathrm{Fe(II)} + H_2O_2 \rightarrow Fe(III) + HO^{\cdot} + OH^-$$

$$\mathrm{Fe(II)} + OH^{\cdot} \rightarrow Fe(III) + OH^-$$

However, the term Fe(II) can refer to both complexed and labile Fe(II). Thermodynamic models have approved the co-existence of various iron complexes based

the the present ligands/anions, and complexed and labile Fe(II) are usually present in either the same or greater concentration levels than labile Fe^{2+}.[2, 28]

1.2.1 Oxidation of the hydrolyzed Fe(II) ---- the pH dependent mechanism

The most basic ligand in aqueous system is hydroxide, which involves the pH dependence mechanism, which has been studied by numerous researchers.[29-30] Under the condition of pH <2, the rate law is given by

$$-\frac{d[Fe(II)]}{dt} = k[Fe(II)][O_2]$$

From a pH of 2 to 5, the rate law becomes

$$-\frac{d[Fe(II)]}{dt} = k[Fe(II)][OH^-][O_2]$$

and while between pH 5 to 8 the rate law is given by

$$-\frac{d[Fe(II)]}{dt} = k[Fe(II)][OH^-]^2[O_2]$$

The reaction scheme involves acid-base equilibria as well as the change in the speciation of Fe(II).[31] The hydrolysis of Fe(II) becomes critical with the pH increases. The hydrolysis of Fe^{2+} is given by

$$Fe^{2+} + H_2O \rightarrow Fe(OH)^+ + H^+$$

$$Fe^{2+} + 2H_2O \rightarrow Fe(OH)_2^0 + 2H^+$$

$$Fe^{2+} + 3H_2O \rightarrow Fe(OH)_2^- + 3H^+$$

If all the hydrolyzed forms of Fe(II) are considered, the oxidation of total Fe(II) species can be expressed as several steps in parallel,

$$Fe^{2+} + O_2 \xrightarrow{k_0} Product$$

$$Fe(OH)^{+} + O_2 \xrightarrow{k_1} Product$$

$$Fe(OH)_2^0 + O_2 \xrightarrow{k_2} Product$$

$$\mathrm{Fe(OH)_3^-} + O_2 \xrightarrow{k_3} Product$$

and the overall reaction rate becomes

$$-\frac{d[Fe(II)]}{dt} = k_{obs}[Fe]_T = k_0[Fe^{2+}] + k_1[Fe(OH)^{+}] +$$

$$k_2[Fe(OH)_2^0] + k_3[\mathrm{Fe(OH)_3^-}]$$

where k_{obs} is the overall pseudo first order rate constant. k_0 is 1.1×10^{-6} sec^{-1},[32] which is quite small comparing with the other rate constants, which k_1 = 1.7 min^{-1} in water and 2.2 min^{-1} in seawater, $k_2 = 3.5\times10^5$ min^{-1} and $k_3 = 1\times10^8$ min^{-1}.[30] The rate determining steps of Fe(II) oxidation are the first three steps (reaction 8-10). When the oxidation of Fe(II) occurs, it is a combined reactions involving the oxidation of all Fe(II) species, and the rate of the oxidation is the sum of the oxidation rates of various Fe(II) species, and the expression of the overall rate constant k_{obs} is

$$k_{obs} = 4(k_1\alpha_{Fe^{2+}} + k_2\alpha_{Fe(OH)^{+}} + k_3\alpha_{Fe(OH)_2^0} + \cdots + k_n\alpha_n) \quad [33]$$

where k_1, k_2, k_3, …, k_n are rate constants for the oxidation reactions of different Fe(II) species by dissolved oxygen, and α is the fraction of each iron species in solution.

1.2.2 The effects of other inorganic and organic ligands

The oxidation of Fe(II) can be greatly affected by various organic and inorganic ligands as well as colloids.[33-40] Sung and Morgan[41] have determined the rate constant k of Fe(II) oxidation given by

$$-\frac{d[Fe^{II}]}{dt} = k[Fe^{II}][OH^-]^2 P_{O_2}$$

in the presence of $NaClO_4$, NaCl and $NaSO_4$ in pH less than 7. Results were indicating that log(k) is showing a linear relationship to ionic strength (adjusted by $NaClO_4$). Meanwhile, their results showed reduced oxidation rates in the presence of NaCl and $NaSO_4$. Their results are indicating the formation of species such as $FeCl^+$, $FeCl_2$ and $FeSO_4^0$ ion pairs. The oxidation of these species must be the rate determining steps. Similar results of the effect a series of anions on the rate of Fe(II) oxidation from Millero are also indicating the formation of complex is competing with the oxidation reaction of labile and hydrolyzed Fe(II). The overall order or the rate constants is HCO_3^- >> Br^- > NO_3^- > ClO_4^- > Cl^- >> SO_4^{2-} >> $B(OH)_4^-$.[29]

According to Millero's results, bicarbonate anion shows the most obvious effect on increasing the oxidation rate, and this was attributed to the formation of $FeCO_3^0$,

$$Fe^{2+} + CO_3^{2-} \rightarrow FeCO_3^0 \qquad (12)$$

and the formed iron carbonate complex has a faster rate of oxidation than $Fe(OH)_2^0$. Bicarbonate anion is an important ligand exists in aqueous phase because of the slightly higher solubility of carbon dioxide and, more importantly, the presence of natural carbon. In attempt to prove the role of bicarbonate anion and provide a consistent model for iron oxidation in natural waters, King investigated Fe(II) oxidation reactions in the presence of carbonate anion and proposed a model for the oxidation of Fe(II) in the presence of carbonate and calculated the oxidation rate constant for each formed Fe(II) species in the presence of bicarbonate ion.[33] The results are showing $FeCO_3^0$ is the dominant species of Fe(II) under circumneutral pH, which may be kinetically reactive to oxygen. A disagreement of this study on the previous hypothesis of Millero[29] is that the oxidation reactions of $Fe(HCO_3)^+$ and $FeCO_3^0$ are both very slow.[33]

Burns *et al*[42] also observed an acceleration of the net oxidation of Fe(II) in the presence of CO_3^{2-} as well as PO_4^{3-} over a pH range of 6.5-8.5. However, this outcome was attributed to the formation Fe(III) precipitates and the removal of the produced Fe(III) species in the iron cycling.[40, 43-44]

Emmenegger *et al* also investigated the effects of bicarbonate anion on Fe(II) oxidation in a pH range of 6.8-8.3. For pH above 7.4, the oxidation rates are in consistent of King's model. However, under lower pH ($6.8 < pH < 7.4$), higher rates were observed, which was not expected. This was attributed to some unknown organic ligands present in lake water, which can form strong complex with Fe(II) and the resulting complex will be oxidized into the corresponding Fe(III) complex so that the cycle between the two

oxidation states continues, and the net oxidation rate of Fe(II) observed may be increased or decreased.[45]

In natural waters, the presence of various types of natural organic matter results in complicated reaction systems as well as difficulties on studies. The existence of strong complex of Fe-organic ligands in natural waters has been demonstrated by previous work.[36, 46-48] Efforts were made in order to fully understand the kinetics of Fe(II) oxidation in the presence of organic ligands and resolve the effects of these ligands.

The formation of Fe(II)-L is an important step and may be the rate limiting step during the oxidation process, and the oxidized Fe (III)-L complex may be reduced to Fe(II) again, in which the cycle continues. The oxidation rate may be accelerated or decelerated depending of the actual properties of the present organic matter. Harris *et al* [45] and Kurimura *et al* [49-50] reported their results of Fe(II) oxidation in the presence of several organic chelating reagents. Both of their results indicated the enhance of Fe(II) oxidation reaction by some chelators.

A strong correlation between the Fe(II) rate constants and the stablility constants of the corresponding Fe(II)-L complex was observed by Kurimura *et al*, [49-50] and they suggested the mechanism may be initiated by the formation of Fe(II)-L followed by the oxidation of these complex.

In Theis' studies[51] on the effect of some reductive naturally occurring organic acids (gallic acid, tannic acid, syringic acid, *etc*), most of them decclerated the oxidation reaction of Fe(II) due to the formation of oxidation resistant complex except for the reductive property of these acids. Acceleration of Fe(II) oxidation in the presence of

fulvic acid and polyglutamate under neutral pH was observed by Liang *et al*,[52] which indicated that the formed Fe(II)-L were more reactive.

Those results confirmed the importance of the formation complex and the creation of two pathways of oxidation in parallel. Detailed kinetic models were developed by Santana-Casiano *et al*[53] who studied the effects of several naturally occurring organic matter including amino acids and aminopolycarboxylic acids on the oxidation of Fe(II).[54] Their model was based on the two parallel pathways involving the oxidation of inorganic Fe(II) (may include hydrolyzed Fe(II) and/or carbonate complex) and organic Fe(II) complex, and the overall rate constant is given by

$$k_{oc} = \alpha_i k_i + \alpha_L k_L$$

where $\alpha_i$and $\alpha_L$are the fraction of Fe(II) in inorganic and organic complex forms, and k_i and $k_L$refer to the rate constants of the oxidation reactions, respectively. According to their results, the term involving the oxidation of chelated Fe(II) is not negligible. Some types of chelators (e.g. EDTA), the oxidation of Fe(II) can be completely inhibited, while other organic matter can enhance the oxidation of Fe(II)-L to Fe(III)-L, which can be reduced by either biological processes or superoxide, and accelerate the cycling of iron between the two oxidation states. They also suggested the formation of intermediates between the chelators and the hydrolyzed Fe(II), $Fe(OH)_xL_n$, which is dependent on pH and concentrations of the chelators.

The model proposed by Rose and Waite accounted for the complexation of Fe(II) and Fe(III) as well as the "back reaction" of Fe(III) reducing by produced superoxide (the back reaction of reaction (1)). When strong Fe(III) binding chelators are present, acceleration of the Fe(II) oxidation was observed, which agrees with the ideas reported

previously. However, except for the formed Fe(II) is acting as a more reactive reagent to dissolved oxygen, Rose et al also attributed the increase on the reaction rate to the consumption of ROS, since some ligands may be very selective and only form stable complex with Fe(III). Their model suggested that, when most of the Fe(III) in the system is stabilized, the produced superoxide from reaction (2) will not be consumed by Fe(III) species any more. Since there is more superoxide available for Fe(II), even not in complex form, an increase net oxidation rate will still be observed.

Table 1.1. Selected thermodynamic constants and oxidation rate constants of some iron complexes in pure water, 25°C

Species	logK	logk(O_2) [a]	Ref.
Fe^{2+}		-0.63	[28]
$Fe^{2+} + HCO_3^- \Leftrightarrow FeHCO_3^-$	1.47	< 0.1	[22]
$Fe^{2+} + CO_3^{2-} \Leftrightarrow FeCO_3^0$	5.69	< -0.4	[28]
$Fe^{2+} + 2CO_3^{2-} \Leftrightarrow Fe(CO_3)^{2-}$	7.45	-4.04	[28]
$Fe^{2+} + CO_3^{2-} + OH^- \Leftrightarrow Fe(CO_3)(OH)^-$	9.97	-2.2	[28]
$Fe^{2+} + H_2O \Leftrightarrow FeOH^+ + H^+$	-9.51	0.84	[26]
$Fe^{2+} + 2H_2O \Leftrightarrow Fe(OH)_2 + 2H^+$	-20.61	5.94	[26]
$Fe^{2+} + Cl^- \Leftrightarrow FeCl^+$	0.30	-4.8	[28]

$Fe^{2+} + SO_4^{2-} \Leftrightarrow FeSO_4^0$	2.42	-4.8	28
$Fe^{3+} + H_2O \Leftrightarrow FeOH^{2+} + H^+$	-2.20		26
$Fe^{3+} + 2H_2O \Leftrightarrow Fe(OH)_2^+ + 2H^+$	-5.54		26
$Fe^{3+} + 3H_2O \Leftrightarrow Fe(OH)_3^0 + 3H^+$	-11.80		26
$Fe^{3+} + 4H_2O \Leftrightarrow Fe(OH)_4^- + 4H^+$	-21.60		26
$Fe^{3+} + Cl^- \Leftrightarrow FeCl^{2+}$	1.28		26
$Fe^{3+} + SO_4^{2-} \Leftrightarrow FeSO_4^+$	4.27		26

[a] The rate constants were calculate by King *et al* [28]

Larger stability constant does not necessarily result in faster oxidation rate. This was discussed by Theis based on their work about the oxidation reaction of Fe(II) complex.[51] The oxidation reaction of Fe(II)L involves the following steps:

$$Fe^{2+} + O_2 \xrightarrow{O_2} Fe^{3+}$$

$$Fe^{2+} + L \underset{k_3}{\overset{k_2}{\rightleftharpoons}} Fe(II)\text{-}L \xrightarrow[k_4]{O_2} Fe(III)$$

k is the rate constant for each step, and the stability constant of the formed Fe(II)-L is given by

$$K = \frac{k_2}{k_3}$$

Based on the rate constant k and stability constant K, there are different combinations which may explain either the enhance or deceleration of Fe(II) oxidation by ligands.

When K is very small and $k_1 >> k_4$, most oxidized ferrous iron should be in the labile form, and the presence of the ligand is not showing any obvious effect. In the opposite situation, when K is large and $k_1 << k_4$, since the oxidation of ferrous ions is slower than complex, most of the ferrous ions are binding with the ligand when being oxidized and the ligand is accelerating the oxidation reaction. Slightly more complicated situations such as that involves a large K and $k_1 >> k_4$ can also occur, which is indicating an inhibited oxidation by the ligand. A special form of this case if that K is moderate which indicates the dissolution and formation of the complex are occurring in very similar rates, with $k_1 >> k_3$ and $k_1 >> k_4$. In this case, the complexed Fe(II) slows down the oxidation while the fast oxidation of ferrous ions occurring at the same time. At the beginning, when most of the Fe (II) are still labile, it will show a fast initial oxidation trend until most of the left over Fe(II) are complexed, when the net oxidation starts to slow down.

The possible reasons for the acceleration/ deceleration effects caused by ligands vary to the types, structures and other properties of the ligands. For example, after forming a complex, the oxygen attack on the Fe(II) center can be hindered and the oxidation reaction is decelerated. Other than the effects on Fe(II), the fate of Fe(III) is also important during the process of oxidation reaction because of the availability of the "back reaction" of Fe(III) reduced by either superoxide or reducing bacteria in natural environment.

1.2.3 The fates of Fe(III)

Ferrous iron is more soluble in water, and more reactive. Recent results have showed that, in seawater, dissolved Fe(II) is present in both labile and complexed forms such as $FeCO_3$, $Fe(CO_3)OH^-$, $FeCl^+$, or Fe-NOM when binding with natural organic matter (NOM). [27, 33, 36] A similar situation applies to the small amount of dissolved Fe(III) is mostly binding with organic matter in natural waters.[1, 55-56]

To keep cycling between the two oxidation states, after Fe(II) is oxidized into Fe(III), the back reaction (reduction of Fe(III)) must occur as a feedback. Regarding to Fe(III) reduction, there are two major pathways: photo-induced Fe(III) reduction, and the "back reaction" of Fe(II) oxidation, which is the reduction of Fe(III) by superoxide.[29] The minerals can undergo this kind of process and therefore they are reduced into Fe(II) which forms soluble species and comes back to the redox cycle. The reduction of Fe(III) by superoxide, on the other hand, must occur in aqueous phase.

It has been demonstrated that Fe(III) is the limiting factor in iron redox cycle due to its low solubility.[57] In aqueous solutions, when dissolved Fe(II) is oxidized, the resulting Fe(III) undergoes pH dependent hydrolysis and produces insoluble solid forms and the mechanism is well-established.[58-60] It is known that $Fe(OH)^{2+}$ and $Fe(OH)_3$ are the dominating species of Fe(III) in seawater under neutral to slight basic pH.[56] Zafiriou *et al*[61] proposed the rate constant of the reaction for formation of $Fe(OH)^{2+}$ from $Fe(OH)_3$ as 3×10^{10} M^{-1} s^{-1}, and Rose *et al* estimated the rate constant for the hydrolysis of Fe(III) as 8×10^{3} M^{-1} s^{-1} based on the assumption that this reaction is the rate-determining step.[2] The produced $Fe(OH)_3$, which is more stable and less reactive, will exist in colloidal form and be removed from the redox cycle. Under the condition of excess amount of Fe(III),

the formed monomeric $Fe(OH)_3$, can aggregate and/or polymerize to form larger particles.[59] Under lower pH (below 3), the polymerization of small monomers are easily reversible.[62] However, once a relatively large chain polymer forms, the bonds between iron atoms are stronger and the resulting polymers are more stable. These results in a much slower depolymerization, and the process of precipitation occurs.[63]

Pham *et al* demonstrated the existence of $Fe(OH)_3^0$ and suggested that it is the dominant precursor in Fe(III) polymerization reactions as well as the subsequent precipitation. They also calculated the rate constant of $Fe(OH)_3^0$ precipitation to be $k_{Fe(OH)_3^0} = 2.0 \times 10^7\ M^{-1}s^{-1}$.[64]

Ligands in which oxygen is the electron donating atom tend to stabilize Fe(III) and decrease the reduction potential of iron. The structure, composition and reactivity of the formed hydrolysis product can be affected when certain oxyanions (e.g. CO_3^{2-}, PO_4^{3-}, etc)[65] or organic matter is present.[59, 66-67] On the other hand, those ligands in which nitrogen or sulfur are the electron donating atoms tend to stabilize Fe(II) and increase the reduction potential of iron.[3] The formed complexes are usually thermodynamically stable with large stability constants. However, the other important factor we need to consider is the rate of the complexity, which is determining the speciation of iron in both oxidation states.

Due to the low solubility of Fe(III) species, there are various types of iron-rich minerals present in natural environments. The combination of dissolved Fe(II) and those minerals received intensive studies. The kinetic and thermodynamic properties of heterogeneous systems will be reviewed in the coming section.

1.3 Heterogeneous systems

In natural environments, soil, sediments, or minerals are wide spread, and they can affect the iron oxidation rate and/or pathways as well as the mechanisms. Therefore, it is important to understand the mechanism(s) of the oxidation reaction on the solid-liquid interface. In this section, the kinetics of the oxidation of ferrous iron minerals in heterogeneous systems and some thermodynamic properties of those iron-rich will be reviewed.

1.3.1 The formation and thermodynamic properties of iron oxides

The formation of iron-rich minerals is a part of the iron cycle. Since Fe(III) species are less soluble, they may form precipitate and iron-bearing minerals when binding with precipitating ligands and/or through polymerization. The formed iron oxides and hydroxides can also affect the kinetics of Fe(II) oxidation. They can be reduced by photoredox reactions and microbial processes so that the cycling continues,[68] or, more commonly, associate with Fe(II) to form Fe(II)-surface species. Studies have agreed that the adsorbed Fe(II) on iron oxide surfaces is more reductive to organic and inorganic contaminants.[69-72]

Thermodynamically speaking, surface complexed Fe(II) is more reductive than aqueous Fe^{2+},[73-74] even though some results reported by Scherer *et al* [12] indicated that it was the coexistence, rather than sorbed Fe(II) only, of sorbed Fe(II) and dissolved Fe(II) making the redox potential lower and sufficient to reduce some organic contaminants in natural waters.

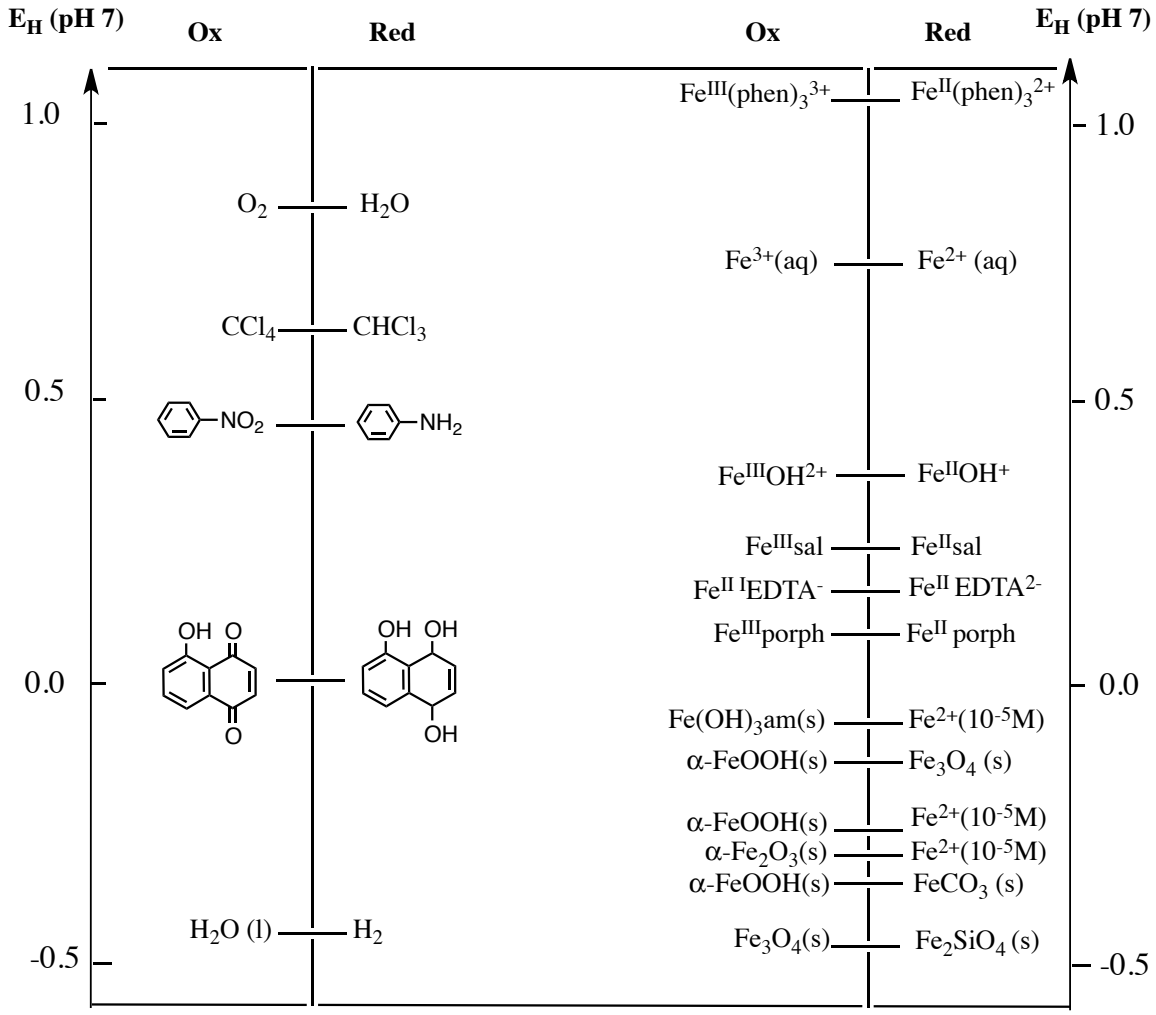

Figure 1.2 Representative redox couples at pH 7.0 (data from Klausen *et al* [75]). phen = phenanthroline, sal = salicylate, porph = porphyrin

Figure 1.2 shows us some redox potentials of various iron species. The iron-bearing minerals associated with dissolved Fe(II) are mostly at the level of -0.5-0.0 V, which is indicating that the oxidation Fe(II) associated with those iron(III) or Fe (II, III) oxides is thermodynamically favored.

1.3.2 The interactions between Fe(II) and mineral surfaces----the formation of surface-cation complexes

In heterogeneous systems, the interactions between solid phase and dissolved ions is quite complicated and not fully understood. It is proved that metal oxide surfaces may undergo a series of processes in the presence of soluble species, which include physical adsorption, surface complexation, hydration of surfaces, adsorption of soluble species, and charge transfer reactions. Oxide particles can be treated as an oxoacid (or base) which has the tendency to undergo proton-transfer reactions and coordination with metal ions. The center ion (e.g. iron, in the cases of iron oxides) in the surface layer can be considered as Lewis acids. The coordinated hydroxyl groups can undergo ligand exchange and be replaced by anions or weak acids.[68, 76]

Many experimental evidences have proved that, in the presence of iron-bearing minerals, the resulting Fe(II) species are more reactive to reduce organic contaminants under anoxic environments, which cannot be done by dissolved Fe(II) in the absence of surfaces.[75] The high reactivity of Fe(II) in the presence of some surfaces was commonly attributed to the adsorption of Fe(II) complexed with hydroxo ligands on those surfaces.[76-77] The reduction rate5 of the oxidant by adsorbed Fe(II) is proportional to the concentration of the adsovrbed Fe(II) in most of the cases. However, except for the adsorbed Fe(II), other factors, such as structure of the surface and Fe(II) surface speciation, must also be taken into account.[78]

Interactions between dissolved Fe(II) and iron-bearing minerals (mostly Fe^{3+} oxides) are complicated, which involves sorption, electron-transfer reactions, atom-exchange, and

sometimes dissolution and the formation of new minerals.[12, 79-81] Generally, the interaction between dissolved ions and surfaces as well as the surface reactivity are both affected by the formed surface functional group.[82] In the cases of hydrous oxides and some silicates, the most important functional groups are surface hydroxyl (–OH) groups. Surface hydroxyl groups, $\equiv \mathrm{Fe^{III}} - \mathrm{OH}$ on iron oxide surfaces are donor ligands, which can increase the electron density of the metal center and form complexes with metal ions. According to the surface complex model proposed by Schindler and Stumm,[82] the iron hydroxide surface binding of metal ions may be given by

$$\equiv \mathrm{Fe^{III}} - \mathrm{O}H^0 + M^{2+} \leftrightarrow Fe - MOH_2^+ + H^+$$

where $\equiv \mathrm{Fe^{III}} - \mathrm{O}H^0$ is the oxide surface, M^{2+} is the dissolved metal ion, and $Fe - MOH_2^+$ is the resulting complex. This surface complex model is indicating the formation of stable complex on the ligand binding sites of the oxide surface. Similarly, the surface can bind with anions or weak acids via ligand exchange:

$$\equiv \mathrm{Fe^{III}} - \mathrm{O}H^0 + X^- \leftrightarrow Fe - OX^- + OH^-$$

As a typical example, the dissolved Fe(II) associated with various surfaces on either iron oxides or other surfaces such as Al_2O_3, silica gel, or TiO_2 has been reported in a number of studies.[12, 71, 75, 83-84]

Larese-Casanova et al reported the first spectroscopic evidence of the sorbed stable Fe(II) species on Fe_2O_3 surface. Their results suggested a quick electron-transfer reaction between Fe(II) and Fe_2O_3 at lower dissolved Fe(II) concentration, while a co-existance of

both stable sorbed Fe(II) on Fe_2O_3 surface and electron-transfer reaction. The sorbed Fe(II) phase include both Fe^{2+} and $Fe(OH)_2$ precipitation.[85]

Electron transfer between dissolved Fe(II) and structural Fe(III) in iron oxides starts from the sorption of dissolved Fe(II) onto the oxide surface, followed by inner- or outer-sphere electron-transfer reactions between sorbed Fe(II) and structural Fe(III) in bulk oxide, which induces a growth of Fe(III) on the solid surface which is similar to the structure of the bulk oxide. Since many of the iron oxides and oxyhydroxides are semiconductors with significant charge carrier mobilities, the electrons injected are in a higher degree of freedom in the bulk oxide.[86] This may be one of the possible reasons that the resulting sorbed Fe(II) is more reactive. For example, many studies have shown that the resulting iron oxides are capable of reducing organic contaminants such as nitrobenzene in faster reaction rates.[79, 87-89] However, this reduction reaction can only occur in the presence of dissolved Fe(II), and this is suggesting a new mechanism which is not completely understood.[12]

Surface precipitation is another result of sorption of metal ions on surfaces. A surface precipitation model based on the surface model proposed by Farley *et al* predicts the surface precipitation resulting from the sorption of metal cations as well as anions, and the sorption isotherm behavior of dissolved metal as a function of metal concentrations is shown in Figure 1.3.[90] In brief, this model is predicting the transition between surface reactions and bulk solution precipitation (the formation of a new phase on the surface) of the sorbate when the dissolved metal concentration increases: when metal concentration is in a lower range ($<10^{-7}$ M), monolayer adsorptive coverage dominates; as the metal concentration increases, both adsorption and solid solution

precipitation become important, and the sorption of dissolved metal follows a Freundlich isotherm; and when the metal concentration reaches a higher level, solid solution precipitate dominates the sorption process.

Surface precipitation/coating is sometimes accompanied with the formation of a secondary mineralization. This occurs when the initial solid is an unstable amorphous iron oxide, such as iron (oxy)hydroxide, ferrihydrite, or lepidocrocite, [80, 91-93] but rarely observed for more stable iron oxides (e.g. goethite, hematite, magnetite, etc.).[12, 83, 94] In all iron oxide minerals, Fe_3O_4, or magnetite, is a special one because of the presence of Fe(II). Fe_3O_4 can reduce $ArNO_2$ even in the absence of dissolved Fe^{2+}, and the rate of this reaction was found to be proportional to the stoichiometry ($x=Fe^{2+}/Fe^{3+}$).[79, 95] Several models were built and studied to explain this heterogeneous redox reaction, and most of the results indicated that the diffusion of Fe2+ from the bulk solid to the surface is playing an important role on determining the rate of the reduction of ArNO2 and other organic contaminants.

Electron-transfer reactions and atom exchange are also proved by experimental results. Electron-transfer reaction occurs when the surface is exposed to the dissolved metal ions. A typical example is when an iron oxide (e.g. hematite, magnetite, goethite, ferryhydrite) is exposed to dissolved Fe(II), a stable Fe(II)-iron oxide complex forms in the first place, followed by the electron-transfer reaction occurring at the interface between the associated Fe(II) and the Fe(III) on the iron oxide surface.[12, 85]

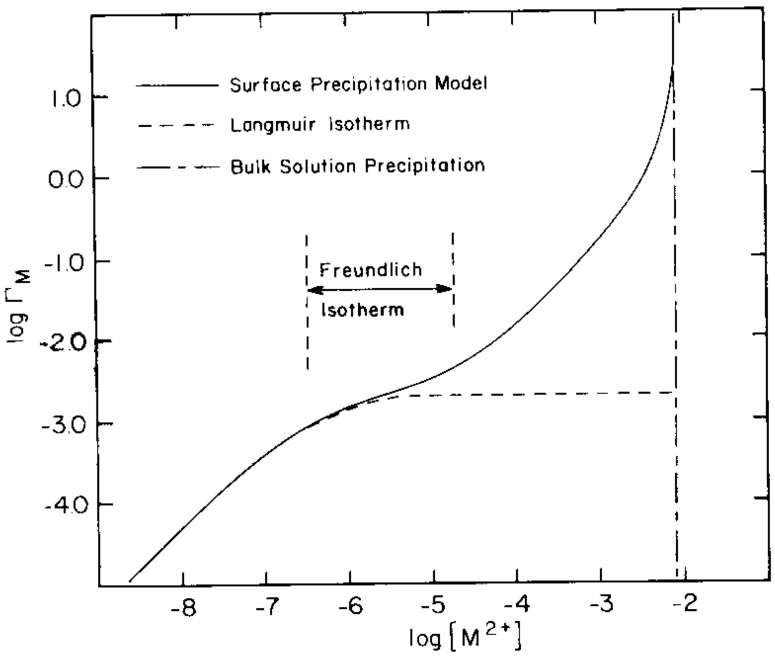

Figure 1.3 Sorption isotherm behavior for the surface precipitation model (data from ref 90)

It is critical to understand that sorption, electron transfer, surface precipitation, atom exchange and dissolution are not independent but occurring sequentially in most of the cases. Handler et al proposed a conceptual model involves all five steps, which is illustrated in Figure 1.4.

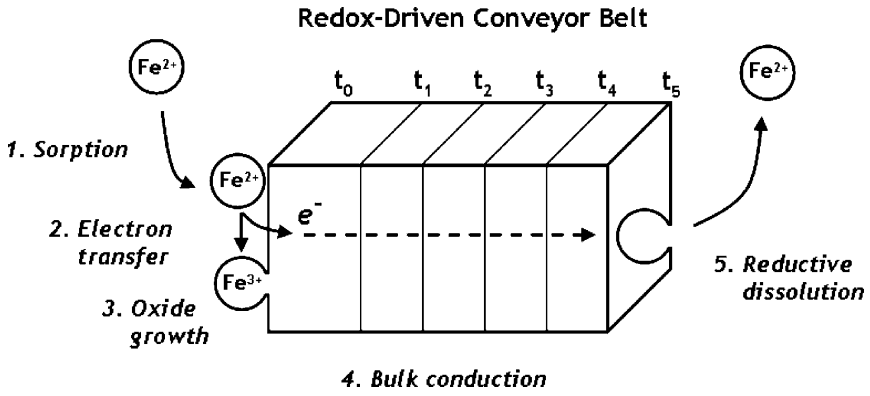

Figure 1.4 Conceptual model for the five steps associated with the redox-driven conveyor belt mechanism proposed by Handler *et al* [80]

1.3.3 Kinetics

Due to the reductive property of the sorbed Fe(II) on surfaces, the reduction of organic contaminants by Fe(II) associated with iron oxides has been studied extensively. Experimental evidences have shown that either the dissolved Fe(II) or the iron oxide (except stoichiometric Fe_3O_4) can barely reduce these contaminants, but the heterogeneous system including both species can dramatically increase the rate of the reduction reaction. It was found that, even though it was agreed that the adsorbed Fe(II) is more reactive and dominants the reduction reaction, the dissolved Fe(II) is still required to reduce some of the contaminants such as $ArNO_2$.[12]

The kinetics of Fe(II) oxidation in heterogeneous systems can be affected by a variety of factors including surface area, structures of solids, pH, present anions, etc.

In surface-controlled reactions, if the reactions upon the surfaces are slower than diffusion or other steps in bulk solutions, the steps occurring on the surfaces would be the rate-determining steps and the concentrations of solutes on surfaces are equal to those in solutions. When the system is dominated by a steady-state on the surface, the kinetics follows a zero-order rate law, and the reaction rate is proportional to the surface area of the solid a (m^2),

$$r = k^0 a$$

where k^0 is the zero-order rate constant, which is sensitive to the concentration of the surface and their structure identity.[68]

Other than the surface area, the formation of iron oxide in the solid phase can also affect the kinetics of the oxidation reaction. Larese-Casanova et al[96] have investigated

the kinetics of the reduction reaction of organic contaminant by Fe(II) associated with aluminum oxide. A slow kinetics was first observed, and, after the formation of a yellow color precipitate (amorphous goethite), the reduction reaction was obviously accelerated.

The present iron oxides can also be a sink of Fe^{3+} by co-precipitating. In this case, the mechanism of the oxidation reaction will barely be affected by the addition of surfaces except that the oxidation rate can be enhanced. In our recent work, the reactive oxygen species (including hydrogen peroxide, superoxide, and hydroxyl radical) generated during the oxidation of Fe(II) in the presence of four different types of iron oxides were monitored and no obvious difference on the detected level of reactive oxygen species was observed. This is indicating that when the sorbed Fe(II) was oxidized by dissolved oxygen, it was going through the same pathway as when the surfaces are absent. However, the observed reaction rate was increased by the addition of surfaces and was not proportional to the surface area. From the mechanism, it is reasonable to conclude that the surfaces are acting as sinks of Fe(III) species, which is similar to the role of those Fe(III) precipitating ligands such as bicarbonate and phosphate.

1.4 Summary

In summary, the ferrous iron oxidation kinetics is highly dependent on the present ligands in homogenous systems as well as the solid phase in heterogeneous systems.

CHAPTER 2

THE YIELD OF THE EFFICIENCY OF HYDROXYL RADICAL PRODUCTION BY FE(II) OXIDATION[1]

Abstract

The oxidation of Fe(II) by dioxygen is known to generate a sequence of reactive oxygen species, including superoxide, hydrogen peroxide and hydroxyl radical. Understanding the stoichiometry of this process at circumneutral conditions should facilitate the development of Fe-based oxidation systems for remediation and lead to a better understanding of the biogeochemical consequences of Fe(II) oxidation in natural waters. In this paper we report the yields of superoxide, hydrogen peroxide and hydroxyl radical observed during the oxidation of Fe(II) by dioxygen in solution and in suspensions of iron oxides (hematite, magnetite, goethite, and ferrihydrite). The addition of anoxic Fe(II) solutions (100 micromolar) to air saturated aqueous solutions at pH 7.5 (bicarbonate buffer) resulted in the immediate formation of superoxide as indicated by flow through

[1]*S. Meng, B. M. Solomon, D. M. Dias, T. J. Shaw and J.L. Ferry,* Department of Chemistry and Biochemistry, University of South Carolina, Columbia, SC 29208. To be submitted to *Environmental Science: Impacts and Processes*

chemiluminometry. Superoxide appeared to reach a stable steady state within approximately 30 seconds after addition that typically varied between 25 and 40 nM and the value of the steady state did not correlate to the presence of a surface. Hydrogen peroxide was generated immediately upon Fe(II) addition and after an initial generation pulse proceeded to decay in a coincident manner with Fe(II), suggesting that on the timescale of the experiments decay through reaction with Fe(II) with a more significant loss route than reaction with or adsorption on iron oxide surfaces. Hydroxyl radical production was monitored through its reaction with terephthalic acid. Measured hydroxyl radical was compared to the theoretical yield based on known rate constants for the Fe(II)/hydrogen peroxide reaction manifold and yields determined. Yields ranged from a low of 30% (based on peroxide consumed) in solution to a high of 150% in magnetite suspension. The latter was interpreted as evidence for direct reaction of peroxide with magnetite.

Introduction

Microbial metabolism in flow-restricted soils and sediments often leads to oxygen depletion and locally high concentrations of reduced transition metals, particularly Mn and Fe.[97-99] When the flow regime is altered, for example by inundation, rhizosphere intrusion or physical perturbation of sediments microbially produced reduced metals re-equilibrate with oxygen in the atmosphere. In the case of ferrous iron oxidation the fundamental reaction between oxygen and ferrous iron is an inner sphere one-electron transfer that results in the formation of superoxide, $O_2^{\cdot-}$ (Eqn 1). [41, 100-101] Superoxide can then react with itself to produce hydrogen peroxide or in the presence of excess Fe(II)

could be reduced again to hydrogen peroxide (Eqn 2, 3).[102] An additional equivalent of ferrous iron can then lead to HO formation (Eqn 4).[103]

$$\mathrm{Fe(II)} + O_2 \rightleftarrows Fe(III) + O_2^{-\cdot} \quad (1)$$

$$O_2^{-\cdot} + O_2^{-\cdot} + 2H^+ \rightleftarrows Fe(III) + H_2O_2 \quad (2)$$

$$\mathrm{Fe(II)} + O_2^{-\cdot} + 2H^+ \rightleftarrows Fe(III) + H_2O_2 \quad (3)$$

$$\mathrm{Fe(II)} + H_2O_2 \rightleftarrows Fe(III) + HO^{\cdot} + OH^- \quad (4)$$

This family of reactions has been shown capable of oxidizing biogenic carbon and also anthropogenic carbon and they are often proposed for remediation of environmental contaminants.[103-108]

The effects of suspended particles on these reactions is not yet quantitatively understood. Generally speaking, suspended particles (particularly Fe oxides) appear to accelerate reaction 1, as indicated by the loss of Fe(II).[84, 109] This outcome appears to be a result Fe(III) scavenging by particles, leading to particle growth and minimizing the back reaction for reaction 1.[110] Superoxide has been qualified in iron oxide suspensions but there is not yet a clear relationship between the rate of Fe(II) oxidation and the quantity or rate of appearance of superoxide.[111-112] Hydrogen peroxide has been quantified in iron oxide suspensions and soils under many different conditions but these studies are typically for added or photochemically generated hydrogen peroxide and are addressing the *in-situ* chemical oxidation process or photo-Fenton process. [88, 113-117] Many of these studies have addressed the rate of peroxide degradation in suspensions and it is analogous the Haber-Weiss process, where the conjugate base of hydrogen peroxide reacts with particle-associated Fe(III) to produce superoxide and Fe(II) (Eqn 5).

Resulting Fe(II), whether free in solution or associated with the surface then reacts with hydrogen peroxide to yield hydroxyl radical and hydroxide ion (Eqn 4).

$$\text{Fe(III)}surf + H_2O_2 \rightleftarrows Fe(II) + O_2^{-\cdot} + 2H^+ \quad (5)$$

Eqn 5 is kinetically slow at most environmentally relevant pHs, probably because of the high pKa for H_2O_2 (11.6) and these reactions are often measured over an hours-days timescale. Hydroxyl radical has been measured in these environments and its yield varies widely, ranging from less than 1% (based on peroxide consumed) to higher than 30% for some soils.[113, 115-116]

In this study we report the simultaneous quantification of Fe(II), superoxide, hydrogen peroxide and hydroxyl radical in solution and in suspensions of several iron oxides (hematite, magnetite, goethite, and ferrihydrite). The primary objective of this work was to test the hypothesis that rapid Fe(III) deposition on particles rendered them essentially equivalent with respect to their ability to support or promote reactive oxygen species formation during the oxidation of Fe(II) by oxygen. Reactions were carried out by adding degassed Fe(II) solutions to aerated receiving solutions in the presence or absence of iron oxide and observing the loss of Fe(II) and growth of reactive oxygen species. The identity of the starting particle had no statistically significant impact on the outcome for every case except magnetite, which showed a strong ability to increase the yield of hydroxyl radicals.

Experimental

Materials and methods

Reagents. All chemicals were uses as purchase without further purification. Diethylenetriaminepentaacetic acid (98+%), teraphthalic acid, iron (III) oxide (gamma

Fe_2O_3) and iron(II) chloride anhydrous (99.5+%) were purchased from Alfa Aesar. Iron(II) chloride was stored in a desiccator and all solutions were kept under nitrogen in a glove box. Catalase (from bovine liver, 11,000 units/mg solid, 14000 units/mg protein), Iron (II, III) oxide (Fe_3O_4, nanopowder, ≥98%), goethite (30-60% Fe), 3-(2-pyridyl)-5,6-diphenyl-1,2,4-triazine-p,p'-disulfonic acid mono sodium salt hydrate (ferrozine), horseradish peroxidase (HRP, 162.9 units/mg) and 2-methyl-6-(*p*-methoxyphenyl)-3,7-dihydroimidazo[1,2-a]pyrazine-3-one (MCLA) were obtained from Sigma Chemical Company. 10-acetyl-3,7-dihydroyphenoxazine (amplex red) was purchased from American Advanced Scientific, and the latter three reagents were stored in a desiccator at -5^{o}C. Dimethyl sulfoxide (DMSO, 99.9%) were purchased from Fisher Scientific. Hydrogen peroxide (30%, w/w), sodium bicarbonate, sodium hydroxide and ammonium acetate were purchased from VWR international company.

All aqueous solutions and suspensions were prepared with Barnstead E-Pure water (18 mΩ) deionized (DI) water, and all the pH values of buffer solutions were adjusted by using sodium hydroxide (0.1 M) and hydrochloric acid (0.1-3 M). The stock solution of and sodium bicarbonate buffer (4 mM, with 1mM terephthalic acid, pH 7.50 ± 0.10) were stored at ~5°C when they are not in use. DTPA solution (0.01 M) was prepared in 0.05 M sodium phosphate buffer (pH 7.50 ± 0.05) in and stored at room temperature. Ferrozine solution (0.01 M, buffered in 0.1 M ammonium acetate without further pH adjustment) was prepared in water and stored at ~5°C.

Stock suspensions of iron (III) oxide, iron (II, III) oxide and goethite (2g/L) were prepared daily by suspending the corresponding solid in 18 mΩ DI water with more than 10 minutes of pre-equilibration. Ferrihydrite suspension was synthesized following the

reported procedure.[118]

Deoxygenated DI water was prepared by boiling 18 mΩ DI water for ~5 minutes on a hot plate to remove most dissolved oxygen and kept deoxygenized by purging with N_2. H_2O_2-free water was prepared by dissolving 3-5 mg of catalase in about 1 L of regular DI water, stirring for 30 minutes followed by boiling for 20 minutes.

Analytical Methods. Spectroscopic measurements for all observations were performed on a Molecular Devices™ SpectraMax M5 Multi-mode Microplate Reader. All samples of suspensions were centrifuged for 30 seconds to isolate the liquid phase at 3075-3375 rpm with a Dade Immufuge™ II centrifuge.

Dissolved Fe (II) concentrations were quantified by using ferrozine method revised by Viollier et al.[119] The produced colorimetric complex absorbs light at 562 nm with an extinction coefficient of 27,900 M^{-1} cm^{-1}. Hydrogen peroxide measurements were performed by using amplex red method as previously reported.[120] In brief, an indicator solution was made by mixing 100 uL of 10 mM amplex red/DMSO solution, 200 uL of 10 U/mL horse radish peroxidase and 9.7 mL of 0.05 M sodium phosphate buffer (pH 7.50± 0.05). 200 uL of sample was transferred into a microplate followed by the addition of 100 uL of the indicator solution to each sample. After 30 minutes of incubation in the dark, samples were excited at 530 nm, and the emissions at 585 nm were measured. Since hydrogen peroxide is known to degrade over time, all samples were centrifuged and analyzed within 10 minutes after generated.

Hydroxyl radical was measured with the hydroxyl terephthalic acid method.[120] Samples were excited at 310 nm and the emissions at 420 nm were measured.

Experimental procedure

All reactions were run at pH 7.5 buffered by 2mM sodium bicarbonate buffer (pH adjusted by sodium hydroxide and hydrochloric acid) at room temperature (25◦C). Solutions and iron oxide suspensions were made up to 50 mL and stirred by magnetic stirring for 15 min to achieve saturation. $FeCl_2$ (5 mM) solutions were prepared by dissolving anhydrous $FeCl_2$ in deoxygenated water, handled under nitrogen and stored in a glove box when not in use. At the beginning of each experiment, an aliquot (1mL) of the 5mM Fe(II) stock solution was injected into 50 mL of the buffered suspension with an Eppendorf pipette and three identical samples were withdrawn immediately by using a multichannel pipette and injected immediately into three 1.5 mL plastic centrifuge tubes containing ferrozine solution, DTPA solution and methanol, respectively. At each following time points samples were collected in the same way. Other analytes were sampled for as indicated above.

Results and Discussion

Results

Fe oxidation in oxygen-saturated solution. Ferrous iron chloride was added to aeriated bicarbonate buffer as well as suspensions of four types of iron oxides buffered at pH 7.5. The systems were monitored for changes in ferrous iron, superoxide, hydrogen peroxide and hydroxyl radical for up to 900 seconds (which allows enough time to consume most of the ferrous iron) upon the addition of ferrous iron. In order to understand the interactions between aqueous Fe(II) and particles, the adsorption experiments in suspensions were performed in the absence of oxygen. Figure 2.1 is showing the consumption of aqueous Fe(II) by the added particles (the Fe(III) loading is 1mM).

Consumption of Fe(II) was observed in all iron oxides suspensions with the same loading of Fe(III), in which Fe2O3 (hematite) consumed the most aqueous Fe(II) while the amorphous ferric oxide consumed the least.

Ferrous iron in oxygen-saturated solution is consumed rapidly by the dissolved oxygen, which follows the profile of a typical first order reaction as Figure 2.2 shows and the half live is about 300 seconds. Reactive oxygen species such as superoxide ($O_2^{-\cdot}$)(Figure 2.3), hydrogen peroxide (H_2O_2) (Figure 2.4) and hydroxyl radical (Figure 2.5) were detected during this process.

Superoxide is showing a steady state during the oxidation of ferrous iron, while hydrogen peroxide is showing a quick initial jump immediately after the addition of ferrous iron into the oxygen-saturated buffer, followed by a decay until all the ferrous iron is consumed.

The hydroxyl radical generation shown in Figure 2.5 is the integrated signal, which is the sum of the total generated hydroxyl radical at each time point. It shows a linear relationship until the last data point, which may be indicating a constant amount of hydroxyl radical was generated until the ferrous iron was completely consumed.

Fe oxidation in suspensions. The added solid accelerated the ferrous iron oxidation rate without changing the order of the oxidation reactions. Figure 2.6 is showing the observed first order oxidation rates in the presence of four types of iron oxides (Fe_2O_3, Fe_3O_4, FeOOH, and ferrihydrite) in different loadings, and ferrihydrite was showing the most obvious effect on the Fe oxidation rate.

Superoxide formations in suspensions (and the maximum yield) is shown in Figure 2.7. The maximum yield of superoxide does not vary to the loadings or types of the

added iron oxide. However, FeOOH (goethite) yields about twice the amount of the other iron oxides, which is shown in the insert plot.

A rapid production of hydrogen peroxide was detected in the presence of all loadings/types of iron oxides, followed by a slow decay, which is shown in Figure 2.8. The decay rate is dependent on the type of the underlined particle. The maximum hydrogen peroxide (the insert plot) was not significantly different between different iron oxides.

Plots of hydrogen peroxide concentration as a function of aqueous Fe(II) (Figure 2.9) are all showing a non-linear relationship. The addition of particles enhanced the generation of hydroxyl radical (Figure 2.10 and Figure 2.11). The yield of hydroxyl radical was enhanced obviously in magnetite suspension (up to ~20 %).

Discussion

The generation of hydrogen peroxide involved the first two steps in the mechanism,

$$Fe^{2+} + O_2 \xrightarrow{k_{O_2^{-\cdot}}} Fe^{3+} + O_2^{-\cdot}$$

$$Fe^{2+} + O_2^{-\cdot} \xrightarrow{2H^+} Fe^{3+} + H_2O_2$$

where k is the second order rate constant for each step, and the theoretical yield of hydrogen peroxide is given by

$$[H_2O_2]_{Theoretical} = {}^1\!/_2\,[Fe^{2+}]_i$$

where $[Fe^{2+}]_i$ is the initial Fe(II) concentration. The factor 1/2 is based on the assumption that two moles of Fe(II) is producing one mole of hydrogen peroxide. In all of our reaction systems, the initial concentration of Fe(II) was 100 μM. Therefore the

theoretical yield of hydrogen peroxide should be 50 μM. However, no more than 3.5 μM of hydrogen peroxide was detected from all reaction systems. This is indicating a fast consumption rate of hydrogen peroxide competing with the production. Here we set up a simple kinetic model for estimating the net reaction rate of hydrogen peroxide.

The production rate of hydrogen peroxide is given by

$$\frac{d[H_2O_2]}{dt} = k_{O_2^{-}\cdot}[Fe^{2+}][O_2^{-}\cdot]\alpha$$

where $k_{O_2^{-}\cdot}$ is the rate constant for the reaction between Fe(II) and superoxide, and α is the fraction of superoxide reacted with Fe(II), and α can be calculated as

$$\alpha = \frac{k_{O_2^{-}\cdot}[[Fe^{2+}][O_2^{-}\cdot]}{k_{O_2^{-}\cdot}[[Fe^{2+}][O_2^{-}\cdot] + k_{Fe(III)-O_2^{-}\cdot}[[Fe^{3+}][O_2^{-}\cdot]}$$

where $k_{Fe(III)\text{-}O2\text{-}\cdot}$ is the rate constant for the back reaction of Fe(III) and superoxide, and the consumption rate is given by

$$-\frac{d[H_2O_2]}{dt} = k_{H_2O_2}[Fe^{2+}][H_2O_2]$$

where $k_{H_2O_2}$ is the rate constant for Fenton reaction. The net rate of hydrogen peroxide can be estimated by (production rate – consumption rate). All the rate constants are listed in Table 2.1.

Since the superoxide dismutation rate is fairly slow under the current pH (< 0.3 $M^{-1}s^{-1}$), the dimutation of superoxide was not considered in this model. The speciation of Fe(II) and Fe(III) are also important for this estimation. Due to the limited availability of

the rate constants for the complexation of Fe(II)/Fe(III) with bicarbonate anion, we also assumed these reactions are much slower than the reactions between those with superoxide, thus the complexation reactions are not considered.

Figure 2.12 is a typical plot with the calculated net reaction rate of hydrogen peroxide as a function of time in the absence of any particles. According to this model, the net reaction rate is possitive in the earlier period of the oxidation reaction, and becomes negative at around 200 seconds after the reaction started.

However, our actual hydrogen peroxide data showed a sudden jump after the Fe(II) spike in about 5 seconds. There are two possible reasons for this sudden jump: (1) from the physical equilibrium at the initial mixing of the stock solution, or (2) a hydrogen peroxide contamination in the stock solution. The background hydrogen peroxide level was tested in an anoxic glovebox and no higher than 0.5 uM of hydrogen peroxide was tested. Therefore, we can conclude that the hydrogen peroxide jump should be from initial dilution of the much more concentrated Fe(II) stock solution. In order to calculate the net generation of hydrogen peroxide, we modeled the consumption of hydrogen peroxide based on the initial hydrogen peroxide by treating the first hydrogen peroxide datapoint seprately. The integrated second order rate law for Fenton reaction, is given by

$$\frac{1}{[H_2O_2]_0 - [Fe(II)]_0} ln \frac{[H_2O_2]_t [Fe(II)]_0}{[Fe(II)]_t [H_2O_2]_0} = kt$$

Rearrage this equation, and the final concentration of H_2O_2, $[H_2O_2]_t$ is given by

$$\ln[H_2O_2]_t = kt([H_2O_2]_0 - [Fe(II)]_0) + ln[Fe(II)]_t + ln[H_2O_2]_0 - ln[Fe(II)]_0$$

The modeled hydrogen peroxide at each time point can be calculated by the equation above, and the "net generation" of hydrogen peroxide was calculated by subtracting the modeled hydrogen peroxide from the actual data at each time point. A typical modeled dataset of hydrogen peroxide is shown in Figure 2-6. The production of hydrogen peroxide is showing two phases: the formation is dominant until 250 seconds, and a consumption-dominating phase after 250 seconds.

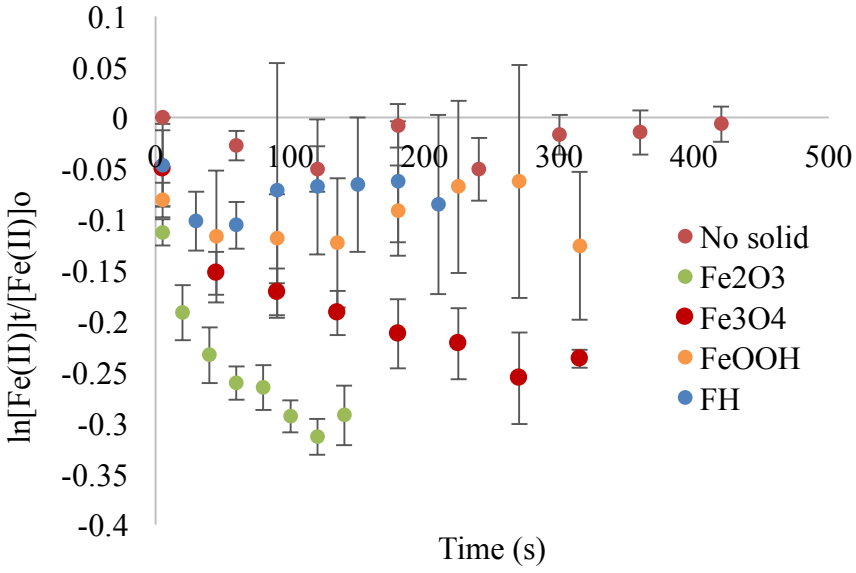

Figure 2.1 The consumption of aqueous Fe(II) by particles in the absence of oxygen (Fe(III) loading = 0.98+/-0.16 mol/L)

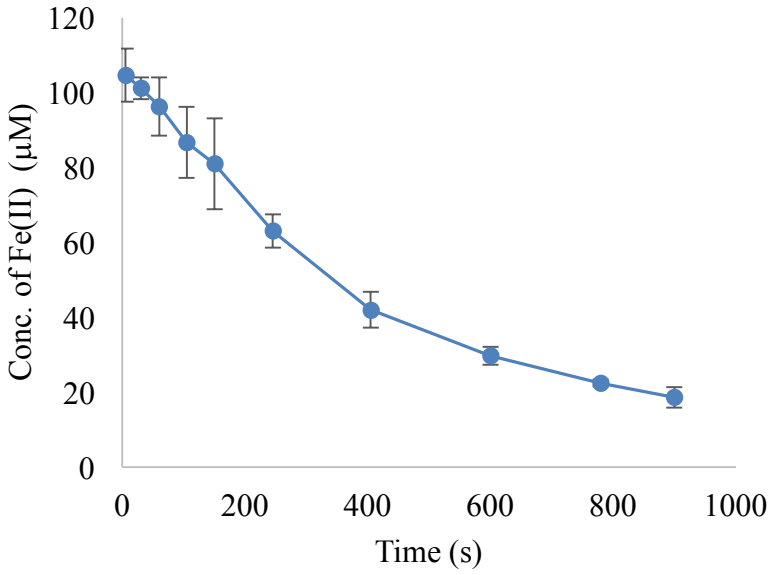

Figure 2.2 Fe(II) autoxidation in oxygen saturated solution

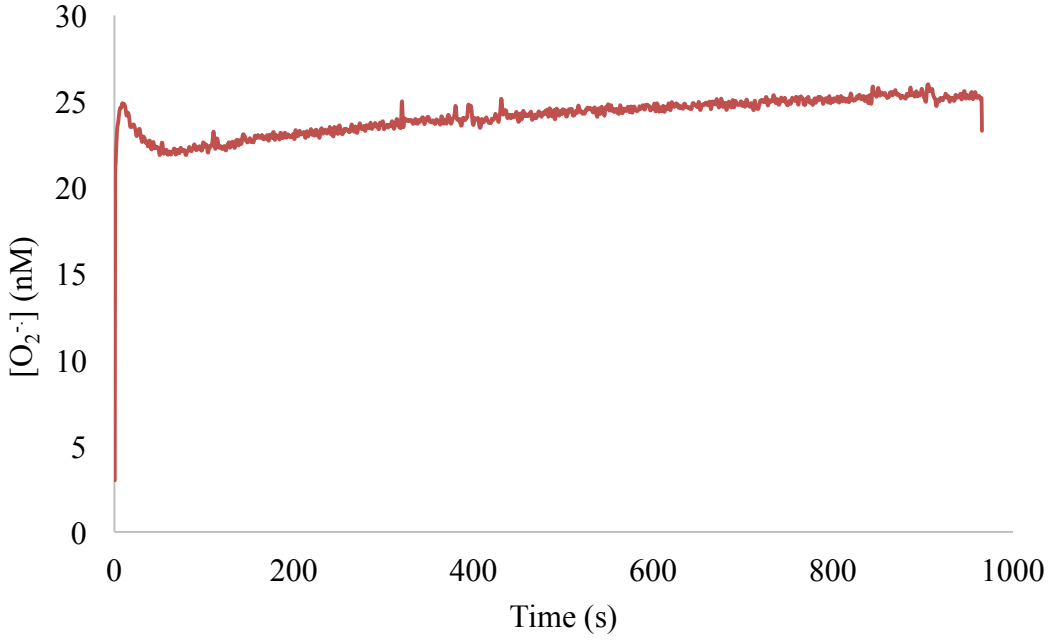

Figure 2.3 Superoxide formation during the oxidation of ferrous iron in solution

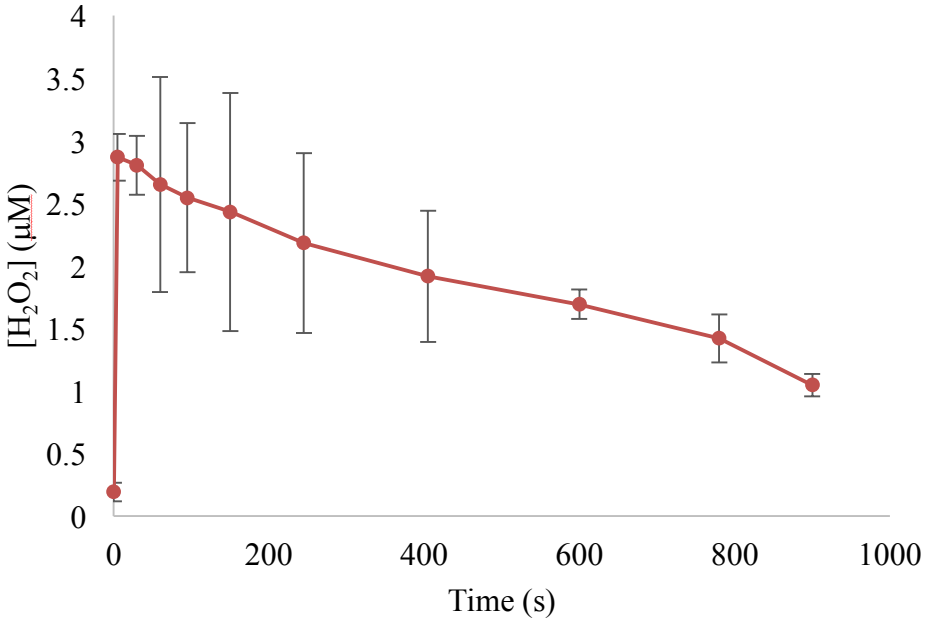

Figure 2.4 Hydrogen peroxide formation during the oxidation of ferrous iron in solution

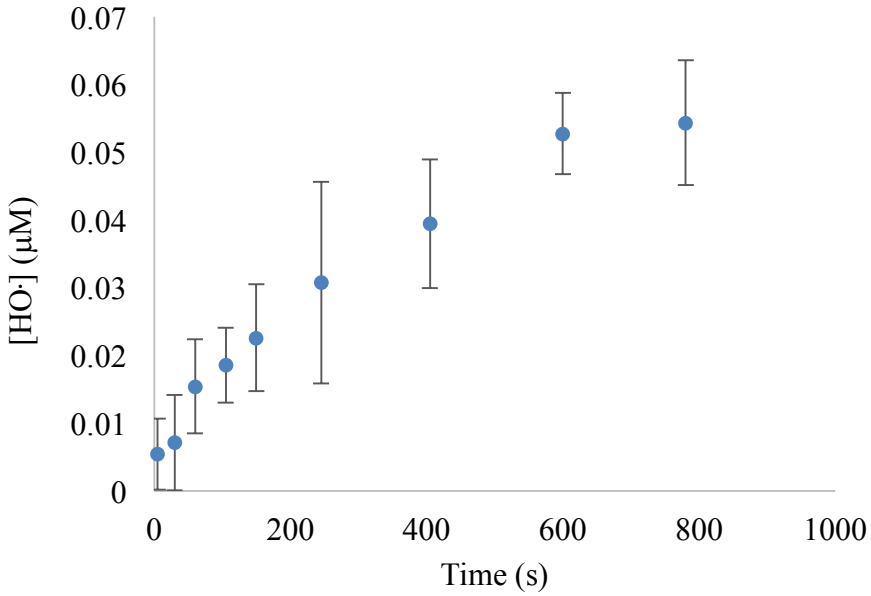

Figure 2.5 Integrated hydroxyl radical generated during the ferrous iron oxidation

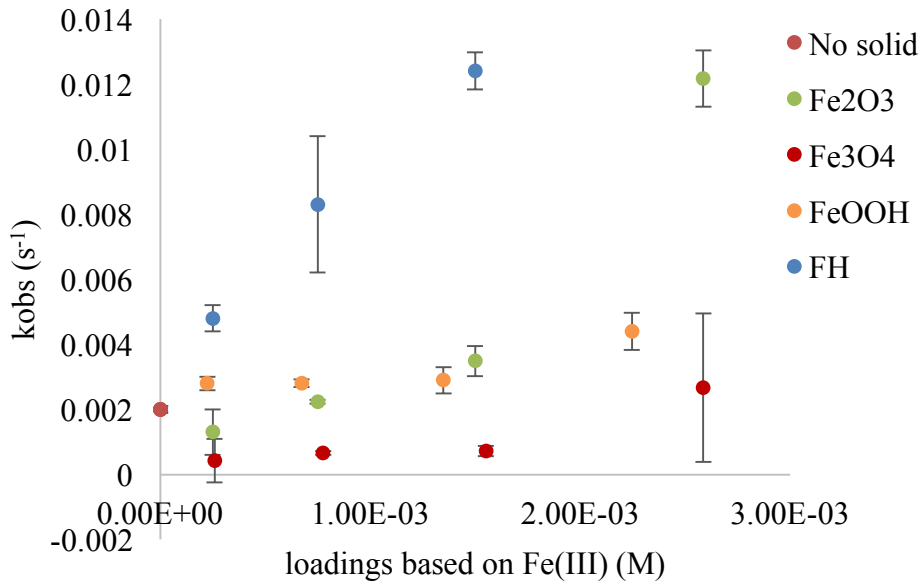

Figure 2.6 Rates of ferrous iron oxidation as a function of the added Fe(III) loadings

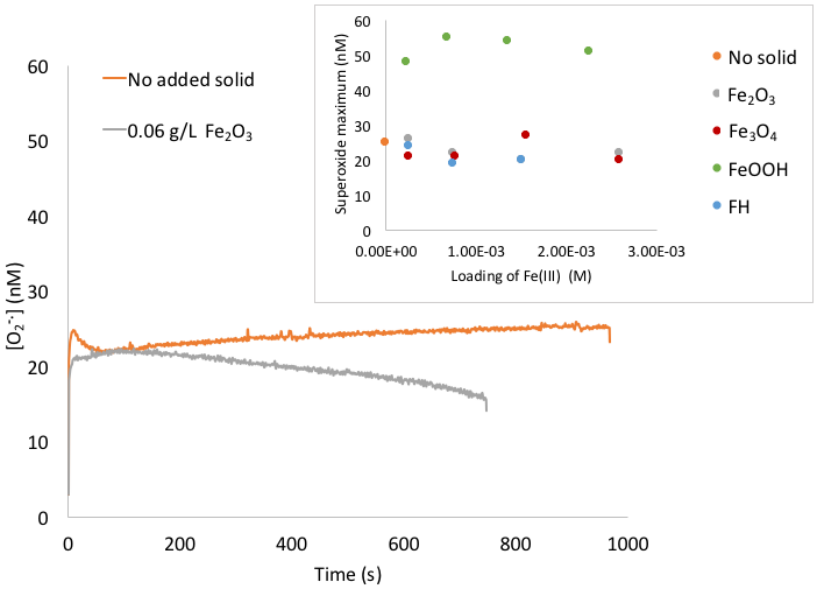

Figure 2.7 The measurement of superoxide in real time in the absence and presence of iron oxide (shown as Fe_2O_3, the gray line). Same levels of superoxide (~25 nM) were detected in every iron oxide except goethite (~50 nM)

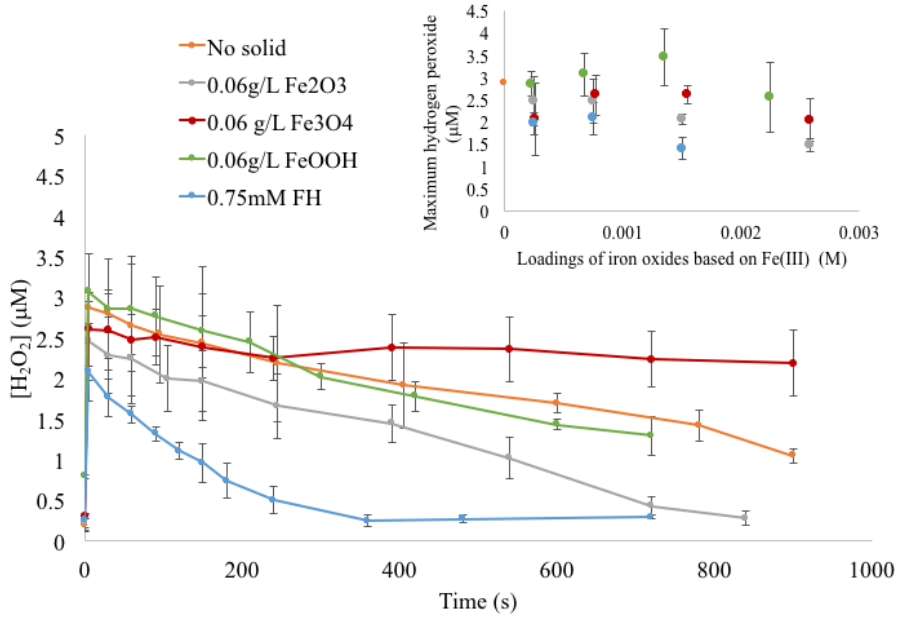

Figure 2.8 Hydrogen peroxide was detected in all conditions showing a quick increase at the beginning followed by a decay. The maximum hydrogen peroxide concentrations in the presence of particles are shown in the insert

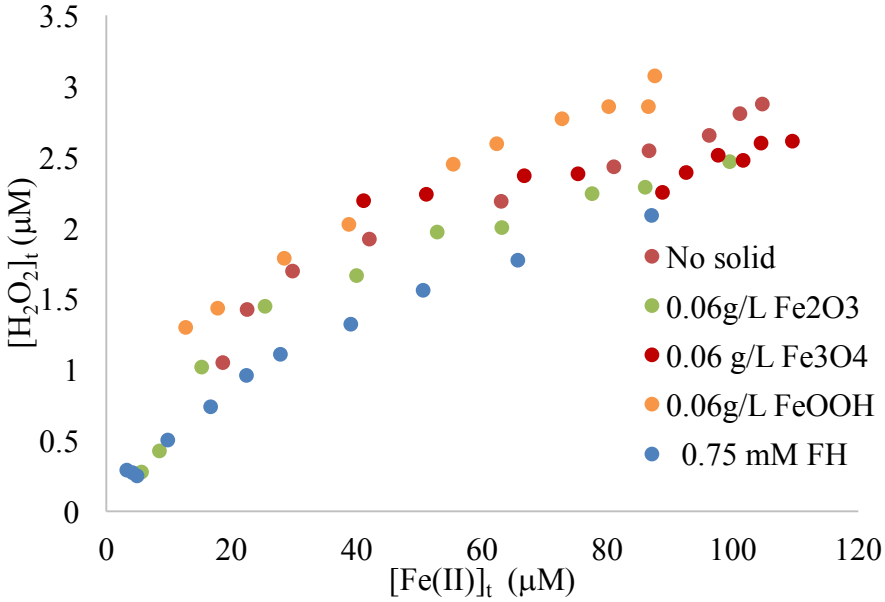

Figure 2.9 Hydrogen peroxide concentrations plotted as a function of the corresponding ferrous iron in the presence of iron oxides

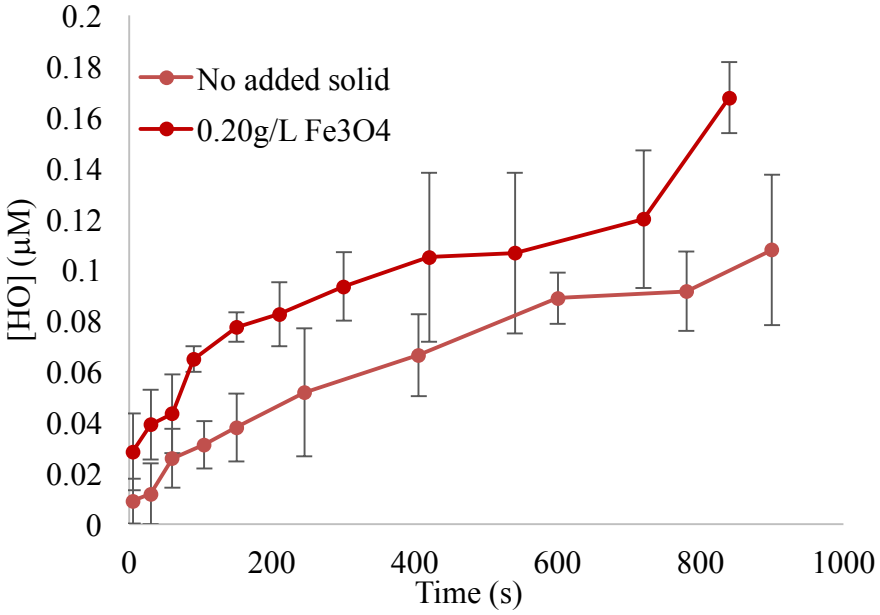

Figure 2.10 Hydroxyl radical generation in solution and 0.20g/L Fe_3O_4 suspension

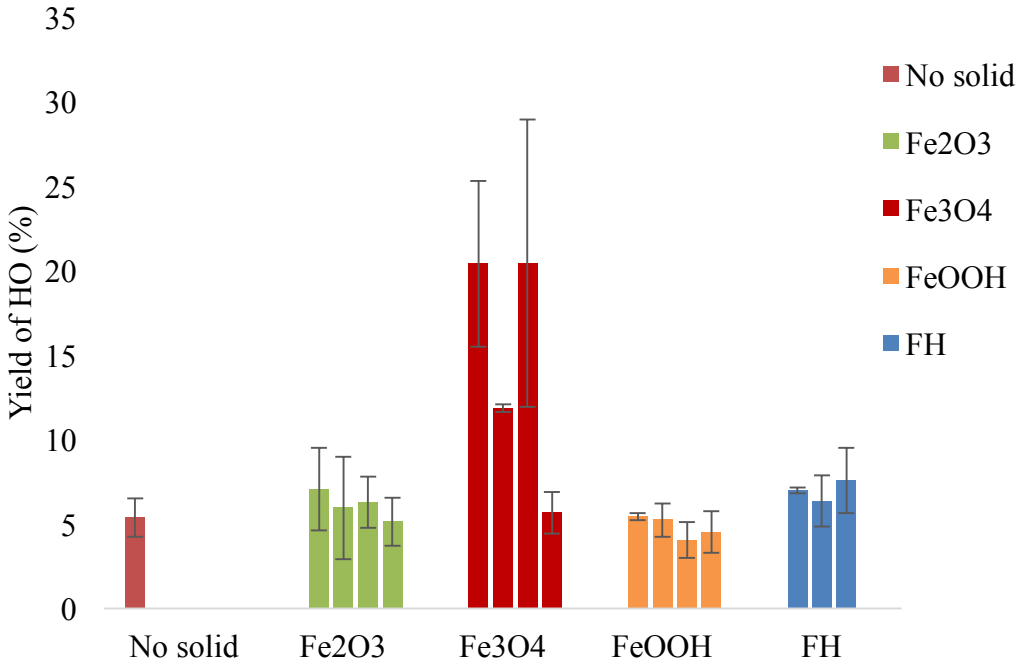

Figure 2.11 The yield of HO in the presence of all solids. Magnetite system is showing the highest level of HO return

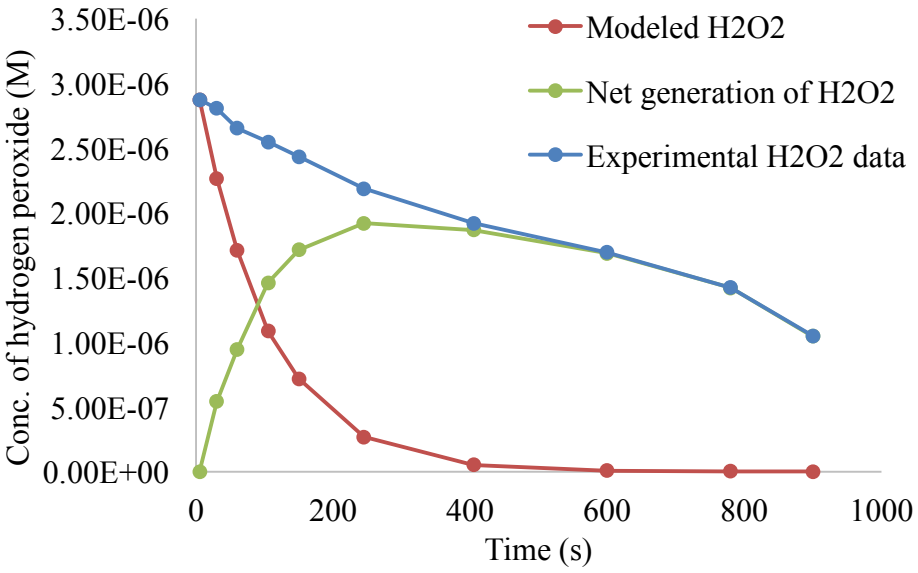

Figure 2.12 A typical plot with the calculated net reaction rate of hydrogen peroxide as a function of time in solution phase

Table 2.1 Reactions and rate constants

#	Reactions	Rate Constants ($M^{-1}s^{-1}$)	Ref.
1	$Fe^{2+} + O_2 \xrightarrow{k_{O_2^{-}\cdot}} Fe^{3+} + O_2^{-}\cdot$	1.0×10^{7}	121
2	$Fe^{3+} + O_2^{-}\cdot \xrightarrow{k_{Fe(III)-O_2^{-}\cdot}} Fe^{2+} + O_2^{-}\cdot$	1.5×10^{8}	122
3	$Fe(II) + H_2O_2 \xrightarrow{k_{H_2O_2}} Fe(III) + OH^{-} + HO\cdot$	63	53

CHAPTER 3

HYDROUS FERRIC OXIDES IN SEDIMENT CATALYZE FORMATION OF REACTIVE OXYGEN SPECIES DURING SULFIDE OXIDATION[2]

Abstract: The formation of reactive oxygen species is reported as a result of the oxidation of dissolved sulfide by Fe(III)-containing sediments suspended in oxygenated seawater over the pH range 7.00 and 8.25. Sediment samples were obtained from across the coastal littoral zone in South Carolina, US, at locations from the beach edge to the forested edge of a *Spartina* dominated estuarine salt marsh and suspended in aerated seawater. Reactive oxygen species production was initiated by the addition of sodium

---

[2] *Sarah A. Murphy, [1] Shengnan Meng, [1] Benson A. Solomon,[1] Dewamunnage M. C. Dias,[1] Timothy J. Shaw, [1,2] John L. Ferry*[1,2]* (**AUTHOR ADDRESS:** 1. Department of Chemistry and Biochemistry, University of South Carolina, Columbia SC 29208. 2. Nanocenter at the University of South Carolina, Columbia SC 29208, *indicates corresponding author); submitted to *Frontiers in Marine Science* on 6/15/2016.

bisulfide and the subsequent loss of HS-, formation of Fe(II) (as indicated by Ferrozine), superoxide and hydrogen peroxide were monitored over time. After an initial increase above baseline superoxide persisted at an apparent steady state concentration ofapproximately 500 nM at pH 8.25 and 200 nM at pH 7.00 respectively until >97% hydrogen sulfide was consumed. Measured superoxide was used to predict hydrogen peroxide yield based on superoxide dismutation and observed to over predict the measured peroxide yield by a factor of 2-134 respectively. Experiments conducted with episodic spikes of added hydrogen peroxide indicated rapid peroxide consumption could account for its apparent low instantaneous yield, presumably from Fe(II) species, polysulfides or bisulfite. All sediment samples were characterized for total Fe, Cu, Mn, Ni, Co and hydrous ferric oxide. The salt marsh sediment and intracoastal waterway sediment, the two with the highest loadings of hydrous ferric oxide, were the only sediments that produced significant dissolved Fe(II) species or ROS as a result of sulfide exposure.

KEYWORDS nanomaterial, ISCO, hydroxyl radical, mineralization, catalytic

Introduction: Reactive oxygen species (ROS, including superoxide, hydrogen peroxide and hydroxyl radical) are critical for enabling abiotic reaction paths between organic carbon and atmospheric oxygen in surface waters. Abiotic ROS production in seawater is usually attributed to photoprocesses involving the direct reduction of oxygen by photoexcited natural organic matter or by Fe(II) generated from photoinduced ligand to metal charge transfer.[123-124] In the latter case oxidizable ligands can include a wide variety of organic molecules and some ligands that are not ordinarily considered reductants, including water and chloride.[114, 125-126] However there are other abiotic

sources of reductive equivalents that can reduce Fe(III) to Fe(II) without the need for sunlight; including hydrogen sulfide, polysulfides, some forms of organic carbon (e.g. polyhydroxylated phenols, organothiols etc.) and superoxide.[127-140] Our own interest in Fe(II) is associated with the tidally driven efflux of anoxic porewater and this has led us to investigate the potential for ROS formation as a consequence of the thermal reduction of Fe(III) by sulfide and other reduced sulfur species (Figure 3.1).

The thermal (i.e. aphotic) interaction between the carbon, oxygen and sulfur cycles as ROS sources is interesting because the potential ROS generation capacity is so large, as (***very* speculatively!**) indicated by the number of moles of Fe(II) produced/yr globally by the reoxidation of microbially reduced sulfate. The oxic portion of the biosphere is a metastable mixture of different oxidation states of carbon, sulfur and oxygen energetically poised from equilibrium by the net rate differentials between photosynthetic carbon fixation and its metabolic or abiotic oxidation.[141] Sedimentary carbon burial widens this gap by imposing a significant mass transfer limitation on the rate of carbon transport between the lithosphere, atmosphere and hydrosphere. It also restricts oxygen transport, forcing microbial metabolism of buried material to rely on alternative electron acceptors such as sulfate or carbon dioxide. The anaerobic microbial metabolism of buried carbon results in the reduction of approximately $11.3x10^{12}$-$75x10^{12}$ moles of sulfate to sulfide per year in marine sediments and coastal marshes.[142-144] This range is compiled from recent efforts to reconcile older sulfate reduction estimates based on spatial averaging to more recent measurements correlating the global carbon flux to sediment with sulfate reduction (see the recent work by Bowles and co-workers and references therein).[142] Based on the more conservative estimate of $11.3x10^{12}$ moles of

microbially produced sulfide/yr, and applying accepted percentage outcomes for the fate of sulfur in the sulfur cycle, approximately $2.3x10^{12}$ moles of this is immobilized annually in the process of pyrite burial. The remaining $9.0x10^{12}$ moles sulfide is reoxidized and returned to the water column (primarily as sulfate). The direct oxidation of sulfide by dioxygen is kinetically unfavorable and requires the intercession of a catalyst such as sedimentary Fe(III) or Mn(IV) (Eqns 1-9).[133, 139, 142-150] Here we consider the ferric/ferrous iron system given its relative geographical importance and kinetic facility. The initial oxidation of sulfide and bisulfide by $Fe(III)_{aq}$ or hydrous ferric oxides (represented collectively $Fe(III)OH_x$ in the following equations) results in a mixture of Fe(II)-containing species as summarized in Eqn 1-6.[135, 140, 151-155] These may undergo rapid oxidation by dissolved O_2, generating the reactive oxygen species superoxide ($O_2\cdot^-$) and hydrogen peroxide (H_2O_2) while regenerating $Fe(III)OH_x$ to continue sulfide oxidation (Eqns 5,6). The self-reaction of superoxide with its conjugate acid HOO· (Eqn 8) is the kinetically favored outcome for superoxide at typical seawater pH unless there is a significant quantity of Fe(II) present, in which case superoxide may be reduced directly by Fe(II) to yield Fe(III) and hydrogen peroxide (Eqn 9).[102, 156]

$$Fe(III)OH_x + HS^- \rightleftarrows Fe(III)S^- + H_2O \quad (1)$$

$$Fe(III)S^- \rightleftarrows Fe(II)S\cdot \quad (2)$$

$$Fe(II)S\cdot + H_2O \rightleftarrows Fe(II) + HS\cdot + HO^- \quad (3)$$

$$Fe(II) + HS^- \rightleftarrows [Fe(II)SH]^+ \quad (4)$$

$$Fe(II) + O_2 \rightleftarrows Fe(III)(OH)_x + O_2\cdot^- \quad (5)$$

$$[Fe(II)SH]^+ + O_2 \rightleftarrows Fe(III)(OH)_x + O_2\cdot^- + S_{oxidized} \quad (6)$$

$$O_2\cdot^- + H_2O \rightleftarrows HOO\cdot + HO\text{-} \ (pKa = 4.83) \quad (7)$$

$$O_2\cdot^- + HOO\cdot + H_2O \rightleftarrows H_2O_2 + HO^- \quad (8)$$

$$O_2\cdot^-/\ HOO\cdot + Fe(II) + H_2O \rightleftarrows H_2O_2 + HO^- + Fe(III) \quad (9)$$

If one conservatively assumes a 1:1 stoichiometry between Fe(III) and HS^- this implies a 1:1 conversion of the reductive equivalents in sulfide to superoxide. Given the most significant loss of superoxide is through formation of hydrogen peroxide (Eqns 7-9) this implies an annual global sulfide-driven ROS formation potential of 9.0×10^{12} moles - 4.5×10^{12} moles, depending on whether the terminal ROS is superoxide or hydrogen peroxide. There are relatively few estimates of annual photochemical ROS production in surface waters to compare this to, but recent work by Powers and Miller suggests the marine average is between of 2.9×10^{12} - 10.9×10^{12} moles ROS in the top meter of the oceans/yr.[124] There are other sources of sulfide not considered in this estimate such as volcanic and hydrothermal vents so the overlap between potential sulfide-driven ROS production and the estimated photochemical ROS production demonstrated here is not quantitative.[134, 157-159] There are also other sources of Fe(II), such as the direct reduction of Fe(III) by facultative anaerobes.[105, 160-162] Nonetheless, the estimated values are intriguingly close, certainly within the same order of magnitude, and that serves as justification for studying potential mechanisms for sulfide-driven ROS generation.

Here we report an investigation of the sources and mechanisms of ROS formation in sediment suspensions containing dissolved hydrogen sulfide (and bisulfide) and oxygen. These conditions are rarely observed in the open water column but are often encountered at the sediment/water interface. Specific examples include conditions associated with bioturbation, undersea mudflow, dredging, wave-driven mixing and the trailing edges of the tidal prism.[135, 147, 163-169] This work is a continuation of an investigation of ROS

generation associated with the oxidation of reduced transition metals at sediment surfaces.[42, 65, 149, 170] It reports a test of the hypothesis that the conditions of frequent episodic anoxia set the stage for pulsed ROS production in marine littoral zones, focusing on the roles of hydrogen sulfide, ferric oxides and pH on superoxide and hydrogen peroxide production (Figure 3.1). The oxidation of reduced sulfur species by dissolved Fe(III) and hydrous ferric oxides is much more rapid than by more crystalline iron oxides such as goethite, lepidocrite or magnetite, and a central hypothesis tested by this work was that hydrous ferric oxides would play a correspondingly more important role in ROS formation than other ferric iron sources.[9, 135, 137, 140, 144, 171-172] Sediments were collected from across the marine littoral zone in South Carolina, from the beach face to the forested inland edge of a saline *Spartina alterniflora*-dominated estuary. The addition of pulses of HS^- to aerated suspensions of collected sediments resulted in rapid Fe(II) production with concomitant superoxide and hydrogen peroxide formation. After a brief initiation phase superoxide was essentially steady state in the tested systems while hydrogen peroxide was more dynamic and sensitive to instantaneous concentration of Fe(II). This pump-and-probe experimental strategy of interrogating sediments for ROS production capacity was applied to all sediments tested and marsh sediments were additionally exposed to multiple sequential pulses of HS^- and hydrogen peroxide. All sediments tested consumed HS- but only marsh sediments produced significant ROS.

Materials and Methods: *Reagents* Iron(III) chloride hexahydrate (99+%) and sodium sulfide nonahydrate (99.99+% trace metal free), potassium superoxide (98%) and chromatographic sand were purchased from Aldrich and used without further purification. Hydrochloric acid (ACS grade) was obtained from BDH. Horseradish

peroxidase and 2-methyl-6-(*p*-methoxyphenyl)-3,7-dihydroimidazo[1,2-a]pyrazine-3-one (MCLA) were obtained from Sigma-Aldrich. 10-Acetyl-3,7-dihydroxyphenoxazine (Amplex Red, 97%) was purchased from American Advanced Scientific and the latter three reagents were stored in a desiccator at -5°C. Diethylenetriaminepentaacetic acid (98+%) and iron(II) chloride anhydrous (99.5+%) were purchased from Alfa Aesar. Iron(II) chloride was stored in a desiccator and all solutions were kept under nitrogen in a glove box. Ferrozine iron reagent (98%) was purchased from VWR. All other salts used as purchased from (Fisher, 99%).

Sediment Characterization Sediment samples were obtained from the top 2 cm of material at five locations (Figure 2) across the marine littoral zone of coastal South Carolina, including (progressing toward the ocean) the landward forested edge of a *Spartina alterniflora* dominated salt marsh (33°20'24.36"N; 79°12'9.23"W) the bank of a dredged canal between the marsh and a barrier island (33°42'51.22"N; 78°55'17.79"W), the sand dunes on the same barrier island (33°42'0.74"N; 78°52'10.77"W), the swash zone at the surf's edge (33°42'0.69"N; 78°52'8.54"W) and at a depth of 1 m below the surf edge at low tide (33°42'0.11"N; 78°52'7.28"W). A control sample was prepared from commercially available sand (Sigma Aldrich) that was triple washed with aqua regia (60 min exposure/wash) followed by a triple rinse with 18 MΩ deionized water to purify the sample of solution accessible acid soluble metals. Samples were sieved, dried and analyzed for metal content using inductively coupled plasma mass spectrometry. Fe was the dominant transition metal in all samples. Acid digestion of sediments showed 25% of the total Fe in sample A from the forested marsh edge was hydrous ferric oxides, all other samples were less than 10% hydrous ferric oxides (Figure 3.2).[173]

Experimental procedure Sediment samples were suspended in 500 mL pH-adjusted seawater (adjusted by dropwise addition of HCl).[149, 172] After a thirty minute equilibration period aqueous hydrogen sulfide was added to the suspension sufficient to yield a concentration of 300 x 10^{-6} M and aliquots of known volume were periodically withdrawn for analysis of sulfide accessible Fe, HS^- and H_2O_2 over time.[174-176] Aqueous sediment loading was 10.00 g L^{-1} of air dried, sieved sediment, consistent with the low range of solid/liquid ratio (99% porosity) observed in the top layers of many coastal surface sediments.[168] Samples were removed from the reactors and centrifuged on a Baxter Dade Immufuge II centrifuge at 3225 rpm for 30 seconds to remove suspended solids before subsequent spectroscopic assays. This basic experimental design was varied by adding replicates that included episodically spiked "refreshers" of hydrogen sulfide or hydrogen peroxide to determine the effect of rapidly resupplying or depleting Fe(II) on the system.

Analytical Iron(II) and sulfide measurement. $Fe(II)_{aq}$ and hydrogen sulfide were monitored colorimetrically using the Ferrozine and methylene blue methods respectively as previously reported.[42, 65, 175, 177] Samples were withdrawn from the reactors and added directly to developing solutions (varied by analyte). Particulates were removed by immediate centrifugation (3225 rpm; Dade Immufuge II). Supernatant was removed by pipetting and transferred to a 96-well glass microplate. Absorption spectra were recorded on a Spectramax M5 plate reader.

Hydrogen peroxide measurements were episodic. Slurry samples were withdrawn from reactors and dispensed into precharged vials containing 0.01M Diethylenetriaminepentaacetic acid adjusted to pH 7.4. Particles were removed by

immediate centrifugation and an aliquot of the supernatant was transferred to a 96 well plate before subsequent derivatization and spectroscopic analysis using the Amplex Red technique.[176] Horseradish peroxidase was dissolved in a 0.05 M sodium phosphate buffer at pH = 7.4 and a 100 μL aliquot was added to each sample, followed by 100 μL of 10 mM 10-acetyl-3,7-dihydroxyphenoxazine prepared in dimethyl sulfoxide. The samples were incubated at room temperature for 30 minutes and then analyzed for development of the indicator resorufin by fluorescence and absorbance spectroscopy.[176] At least one full calibration curve was run with each plate, for a minimum of 5 replicate calibration curves per day of analysis. All glassware was cleaned in a muffle furnace and acid washed in a 10% HCl/1 M oxalic acid mixture. After rinsing with 18MΩ deionized water glassware was handled and stored as trace metal clean glassware to prevent inadvertent oxidation of sulfide in the absence of added metals. Superoxide was continuously measured by flow injection analysis (Waterville Analytical) with the MCLA chemiluminescence technique.[178-179] All initial flow rates (sample and MCLA) were 2.5 mL/min. The flow cell volume was 2.0 mL and the PMT integration time set to 0.200 s. Calibration was performed daily against spectroscopically verified superoxide stock solutions (UV absorbance at 240 nm) made up at pH 10 (NaOH) or higher.

Quality Assurance/Quality Control Replicate blanks (n=3) were obtained for all reagents. Blanks were updated with preparation of fresh reagent solutions. Reference standards were interrogated for peroxide analysis at a frequency of 1 reference check/5 unknown determinations. Peroxide reference standards were externally calibrated against the optical absorbance of the concentrated stock at 254 nm. The detection limit for each method was defined by the linear dynamic range of the calibration curves.

Results and Discussion: Hydrogen sulfide was added to separate, aerated suspensions of all sediments studied or a sediment-free control at pH 7.00, 7.50, 8.00 and 8.25. The systems were monitored for changes in sulfide, Fe(II), superoxide and hydrogen peroxide for 120 min following sulfide addition. Sulfide consumption followed two profiles; an extremely rapid decay (95+%) in the first 30 seconds with a slow decay thereafter or an overall slow decay that in many cases was not statistically different than the control (Figure 3.3). Sediments from the marsh fell in the former category at all pHs studied, whereas the sediments from the intracoastal waterway, dune or beach swash zone displayed the latter. Marsh sediments were also the only samples to experience significant increases in Fe(II) (as indicated by Ferrozine) over the timescale of the experiments (Figure 3.4), obtaining a maximum Fe(II) of 45.0×10^{-6} M very rapidly (less than 60 sec) at pH 8.25. In contrast intracoastal waterway sediment yielded the second highest apparent Fe(II) concentration of 7.3×10^{-6} M at approximately 600 sec. These results justified focusing primarily on the marsh system. For marsh sediments the instantaneous concentration of Fe(II) at a given time never exceeded an amount corresponding to an Fe(II) yield above 15% of HS^- consumed at the same time. The apparent half-life for Fe(II) was also considerably slower than would be expected based on existing Fe(II) oxidation models.[27, 42, 65, 180-181] These results can be explained by two exclusive models of the system; one where Fe(II) oxidation was slowed by the presence of a stabilizing ligand or one where Fe(II) oxidation was kinetically facile and the measured concentration was actually the product of simultaneous Fe(III) reduction and Fe(II) oxidation. The two models were resolved by examination of the concentration vs time profiles for superoxide (Figure 5) in marsh sediments. Both pH conditions

experienced a sudden increase in superoxide upon the addition of hydrogen sulfide, indicating at least some of the total Fe(II) was available for oxidation by dioxygen (Eqn 5). The half-lives for superoxide were calculated at the maximum superoxide concentration obtained from the data based on loss through dismutation (Eqn 10):

$$t_{½} = \frac{1}{k[O_2^-]_0} \qquad (10)$$

where at pH 7.00 $k = 5.01\text{x}10^5$ $M^{-1}s^{-1}$ and superoxide = $204\text{x}10^{-9}$ M and at pH 8.25 $k = 1.78\text{x}10^4$ $M^{-1}s^{-1}$ and superoxide = $514\text{x}10^{-9}$ M (conditional k values obtained from a comprehensive review by Bielski and colleagues).[156] Under these conditions $t_{½}$ was 9.8 sec and 109.0 sec at pH 7.00 and 8.25 respectively. Given the apparent stability of superoxide in the experiments (Figure 3.5) and the truism that dismutation sets the *minimum* rate of superoxide decay in aqueous systems we concluded that superoxide was continually replenished by the oxidation of Fe(II) in both cases; i.e. the kinetically facile model was correct.

The stoichiometry of the process was investigated by considering the total quantity of ROS produced. The production of superoxide between any two time points (time *a* and *b*) can be estimated by calculating the loss from time *a* to time *b* from dismutation and adding the difference between the new concentration and that observed (Eqn 11):

$$O_{2\ produced\ net}^- = ([O_2^-]_b - [O_2^-]_a) + ([O_2^-]_a - \frac{1}{kt + \frac{1}{[O_2^-]_a}}) \qquad (11)$$

where k = the conditional pH dependent dismutation value, t = the elapsed time between times *a* and *b* (0.5 s in this study) and assuming measurement times were close enough so

not all superoxide was consumed between times *a* and *b*. The accumulated superoxide was summed over the duration of the experiment (7200 seconds) and plotted against time to obtain a nearly linear net increase in superoxide (r^2 = 0.998 and 0.991 for pH 7.00 and 8.25 respectively, Figure 3.6). Given that superoxide production came at the cost of Fe(II) oxidation, the negatives of the slopes in Figure 3.6 were the rate of Fe(II) oxidation at the two pHs and the reaction was zero order in Fe(II). This was consistent with the model of ferric and ferrous iron playing the role of a kinetically saturated catalyst for HS^- oxidation. The stoichiometry of the process was investigated by assuming all superoxide produced was consumed by dismutation and comparing the measured hydrogen peroxide yield to that predicted from dismutation (Figures 3.7 and 3.8 for pH 7.00 and 8.25 respectively). At pH 7.00 superoxide was consumed very rapidly with little hydrogen peroxide production and at pH 8.25 superoxide was converted nearly quantitatively to hydrogen peroxide. The insert plot of hydrogen peroxide predicted vs measured in Figure 2.8 is notable for a slope of nearly 1. However this model was inadequate for predicting hydrogen peroxide yield at pH 7 (Figure 3.7 and insert). Presumably this was a result of a pH dependent reaction (or reactions) that consumed either superoxide or hydrogen peroxide more effectively at the lower pH, such as the reaction of hydrogen peroxide with bisulfite or Fe(II), or more likely their reaction with an FeS species.[127, 132, 182-185] It was also possible that at the lower pH some hydrogen peroxide or superoxide was consumed by reactions involving natural carbon in the sediments.[102, 156, 183]

The effects of sequential reductant and oxidant additions were measured in marsh sediments at pH 8.25. Additional hydrogen sulfide or hydrogen peroxide additions occurred at time = 1800, 3000 and 4500 seconds after the initiating hydrogen sulfide

pulse, with each addition sufficient to bring the system to a nominal concentration of $300x10^{-6}$ M HS^- or experience a net increase of $10x10^{-6}$ M hydrogen peroxide. Each additional HS^- spike oxidized rapidly and the nominal concentrations were only directly observed in blanks. In sediment suspensions measured sulfide fell typically by 95% within the first 30 sec after addition. The concentration of Fe(II) roughly followed the time profile of HS^- over multiple additions, indicating the sediments sustained their ability to oxidize sulfide with very short reoxidation times (Figure 3.9). The ROS response of this system was also monitored. The sequential addition of HS^- spikes to these samples resulted in an apparent decrease in superoxide immediately after each addition, however hydrogen peroxide tended to increase in concentration after the pulse while superoxide fell or plateaued (Figure 3.10). Peroxide did not rise to higher levels than previously observed, indicating that consumption was occurring simultaneously with production. Regardless of brief changes in the relative slope of the time profile of superoxide or hydrogen peroxide, the introduction of multiple HS^- pulses reduced the apparent plateau concentrations of superoxide by approximately 25% and hydrogen peroxide by approximately 50%. It is possible these reductions were an outcome of the accumulation of partially oxidized S species in the system such as S_8, which coat sediment surfaces and inhibit their ability to act as catalysts or directly scavenge oxidants.[135, 152]

In contrast added hydrogen peroxide pulses did not have a statistically significant effect on measured HS^- or Fe(II) under these conditions (Figure 3.11). However superoxide appeared to experience a $(50\text{-}100)x10^{-9}$ M increase after each addition (Figure 12). The most interesting result from this experiment was the changing slope of

hydrogen peroxide post-spike; it was evident that the initial spike was consumed rapidly while the latter two appeared to demonstrate more of a step function-like increase. Presumably this was due to consumption of oxidizable sulfur species, at least on the time scale of this study, so that later additions were more stable.

Conclusions:

This work demonstrated the potential for the global sulfide reoxidation flux to participate in ROS production in parallel to more recognized photoproduction of ROS. Specifically addition of hydrogen sulfide to oxic muds resulted in the rapid production of Fe(II) species, superoxide and hydrogen peroxide. The production of ROS was not stoichiometric and less than 20% of the sulfide consumed appeared to contribute to ROS production in this system. Hydrous ferric oxides played the most significant role in promoting ROS formation over short time scales. The time scale of the experiments shown corresponds to previously measured efflux of the anoxic portion tidal prism through estuarine muds during the falling tide, suggesting that hydrous ferric oxides will be important sources of ROS in those ecosystems. They are also likely to be influential for ROS production in other episodic events, such as bioturbation, storm-driven agitation, dredging etc. It is notable that elevated levels of antioxidant enzymes are frequently observed in biota at environmental compartments that fall in this category, including hydrothermal vents,[186-188] cold seeps[189] and the surface sediments of many coastal salt marshes.[190-192] These observations range from single-celled (planktonic) to complex multicellular organisms (limpets, worms) and suggest ROS may have an unexpected ecological importance even in niches that are reliably aphotic because of depth.

Acknowledgements: The work was supported by the United States National Science Foundation, Grant CHE-1308801. The authors are grateful to Prof. Bill Miller for helpful comments during the preparation of the paper.

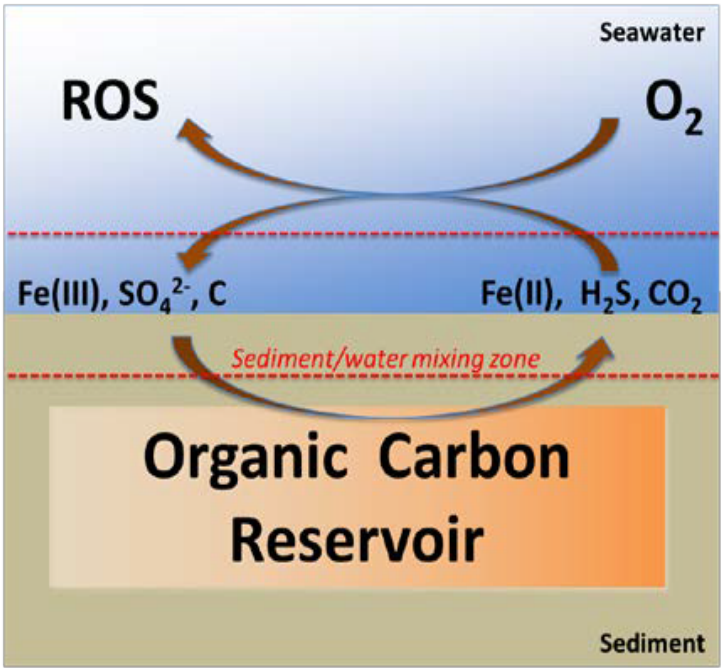

Figure 3.1 Microbial oxidation of buried carbon results in the production of Fe(II) and HS^-. At the oxic/anoxic interface these equilibrate with dissolved O_2 to yield ROS and regenerate Fe(III) and eventually sulfate.

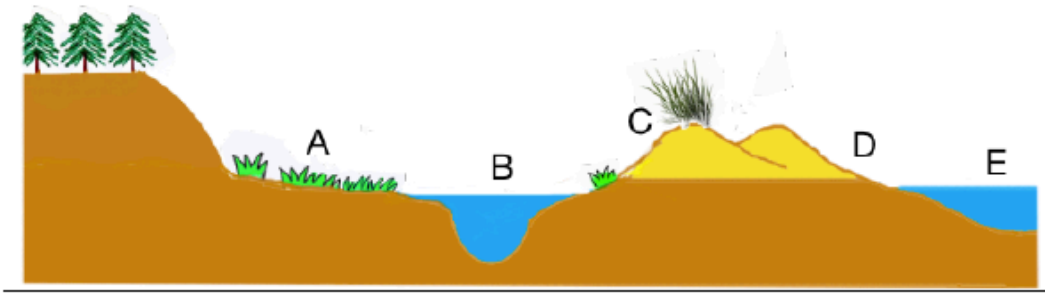

Metal (+/- 0.05mg kg^{-1})	Control	Marsh (A)	Intracoastal waterway (B)	Dune (C)	Beach Face (D)	Low Tide Line (E)
Total Fe	353	38876	3830	1653	63085	3382
Hydrous ferric oxide	-	9838	387	59	61	286
Cu (ppm)	24	27	47	4.0	4.7	2.7
Co (ppm)	0.2	8.5	10	0.4	0.8	0.9
Ni (ppm)	2.0	25	4.7	1.7	2.2	2.9
Mn (ppm)	12	257	126	65	5773	49

Figure 3.2 Sediment collection points and metal content (dry weight). 214 Sediment surface samples were collected from several points across the South Carolina marine littoral zone, including a coastal marsh (A), manmade intracoastal water way (B), a barrier island dune crest (C), the beach face or swash zone (D) and at a depth of 1 m below the low tide line (E). Samples were sieved (4 mm) and air dried before analysis for metals or use in experiments. Characterization was achievedby acid extraction followed by inductively coupled plasma mass spectrometry or ascorbate/HCl extraction with Ferrozine (amorphous Fe only).

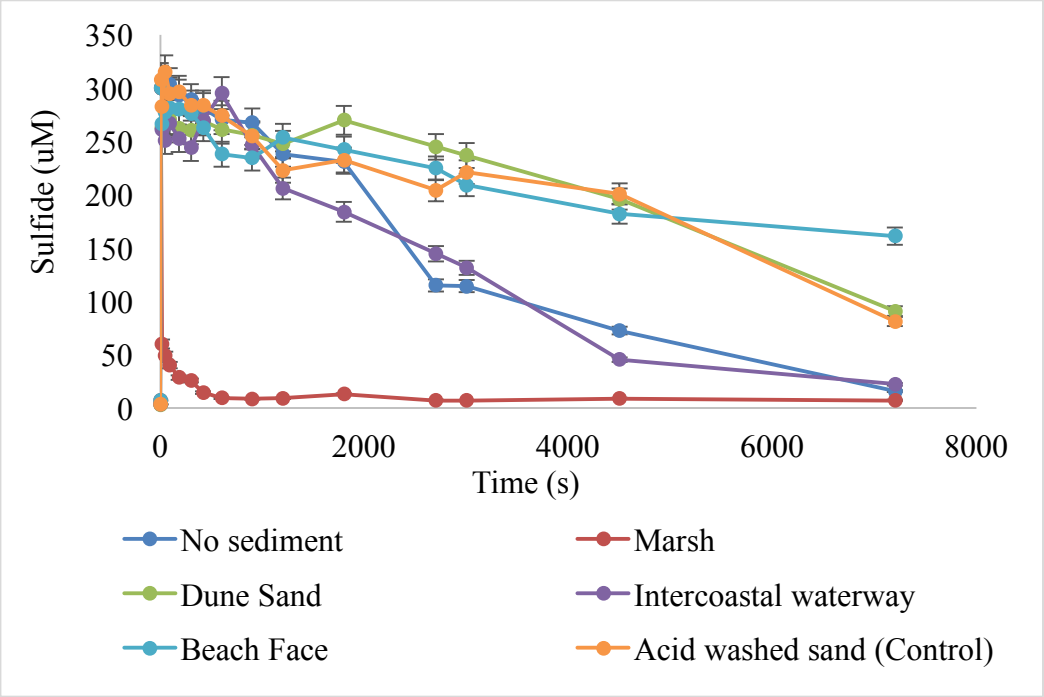

Figure 3.3 The effect of sediment slurries on sulfide oxidation. Sediment suspensions (1.00 wt%) were made up in pH adjusted seawater. Suspension were maintained and aerated through rapid mixing. At time = 0 sec $H_2S_{(aq)}$ was added to bring its solution concentration $300x10^{-6}$ M. HS^- was monitored for a minimum of 7200 seconds from zero. Results from pH 8.25 shown.

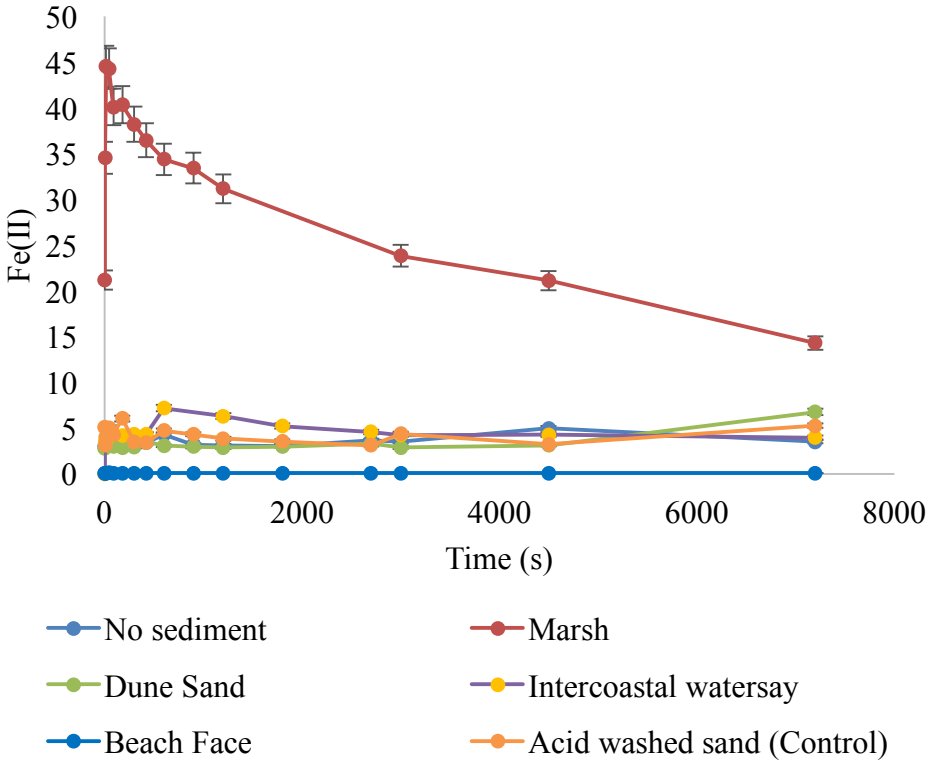

Figure 3.4 Fe(II) evolution after HS^- addition. The introduction of $H_2S_{(aq)}$ to aerated sediment suspensions (1.00 wt%) seawater resulted in the formation of Ferrozine-responsive Fe(II). The highest yields of Fe(II) were obtained from sediments with high concentration of hydrous ferric oxides. Results from pH 8.25 shown.

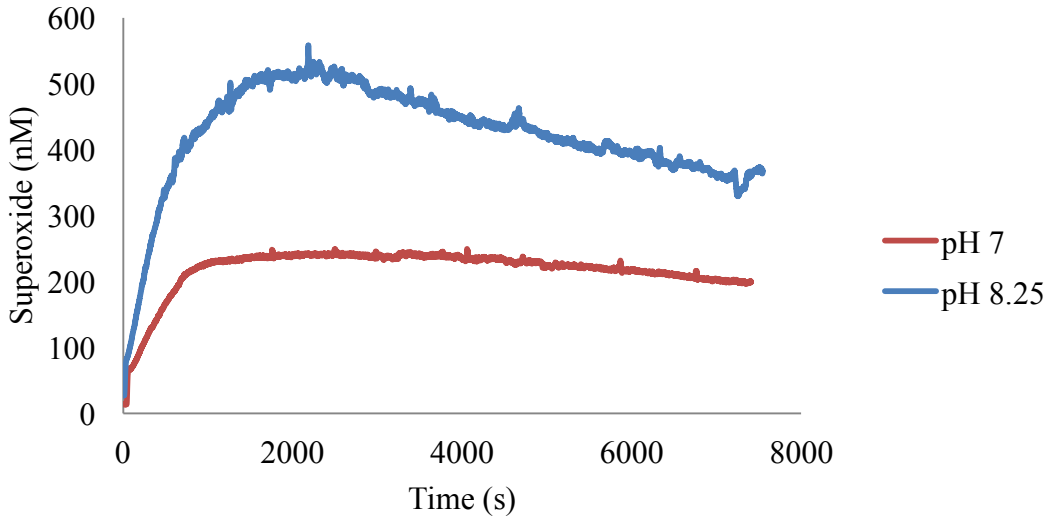

Figure 3.5 Superoxide formation followed HS^- addition. Fe(II) generated from the interaction of sediments and added HS- oxidized in suspension and generated superoxide at pH 7.00 and pH 8.25 (0.1 wt% sediments in pH adjusted seawater).

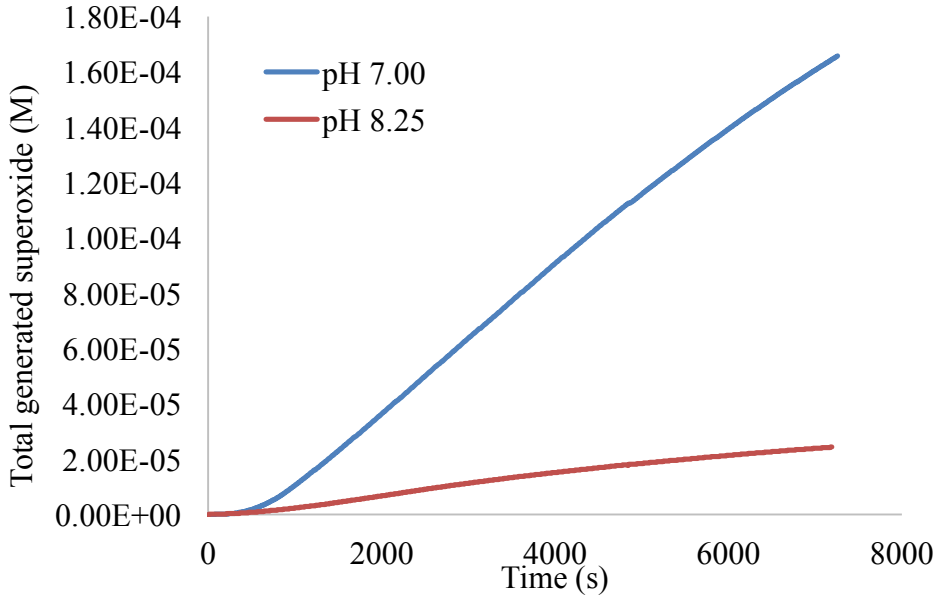

Figure 3.6 Modeled superoxide production. Instantaneous superoxide concentrations were used with Eqn 11 solve for the total number of moles of superoxide generated over the course of the experiment at pH 7.00 and pH 8.25. The higher yield of superoxide estimated at pH 7 was a function of its more rapid dismutation at the lower pH.

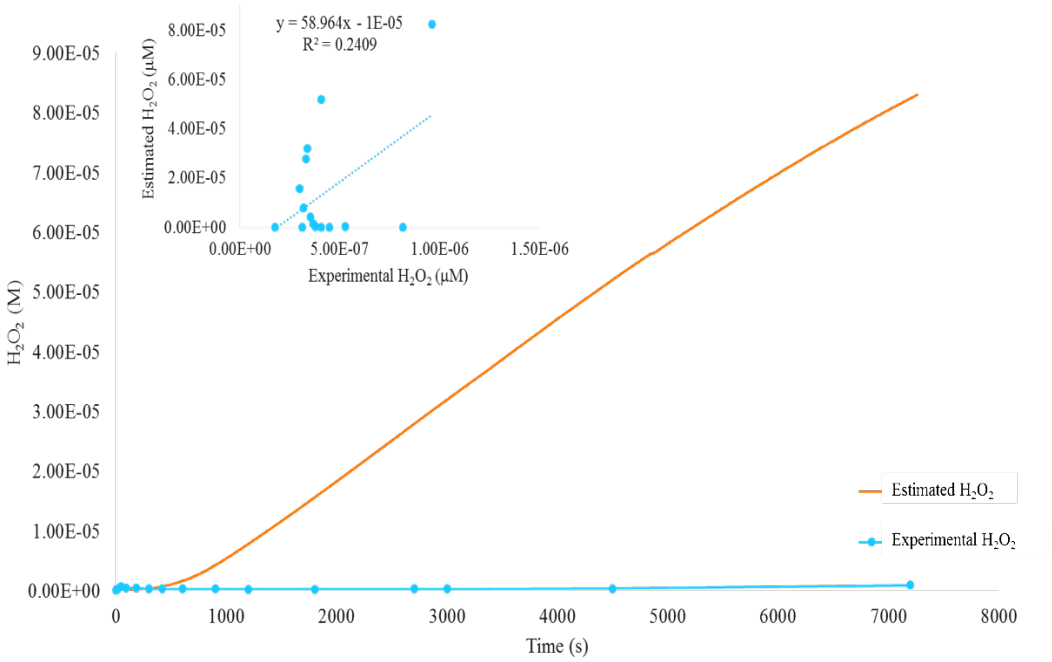

Figure 3.7 Modeled vs predicted hydrogen peroxide, pH 7.00. Modeled superoxide was used to predict hydrogen peroxide observed in sediment suspensions. In marsh sediment suspensions at pH 7.00 the model overpredicted hydrogen peroxide by approximately a factor of 100, indicating the presence of an unknown hydrogen peroxide sink. Poor correlation between model and data shown in the insert.

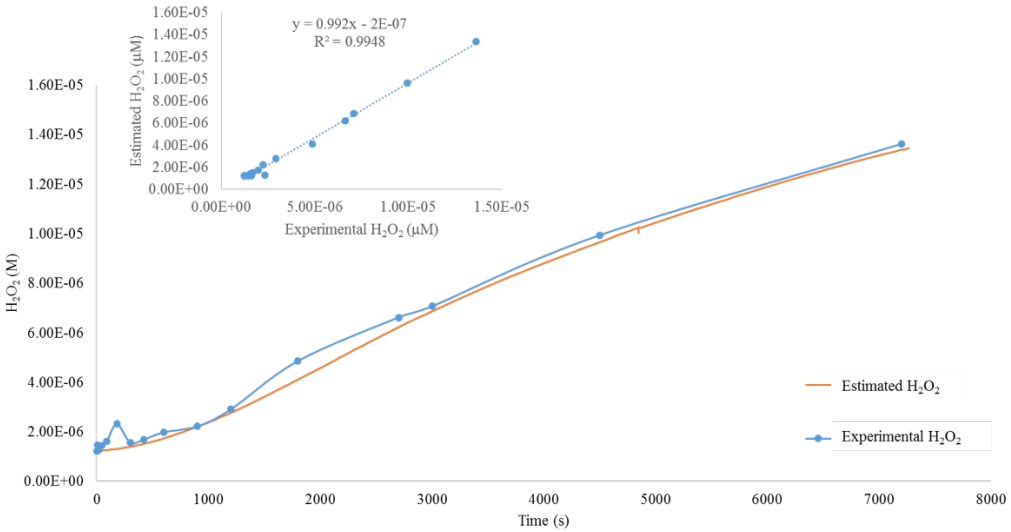

Figure 3.8 Modeled vs predicted hydrogen peroxide, pH 8.25. Modeled superoxide was used to predict hydrogen peroxide observed in sediment suspensions. In marsh sediment suspensions at pH 8.25 the model predicted hydrogen peroxide with an r^2 = 0.992, indicating dismutation was the sink for superoxide.

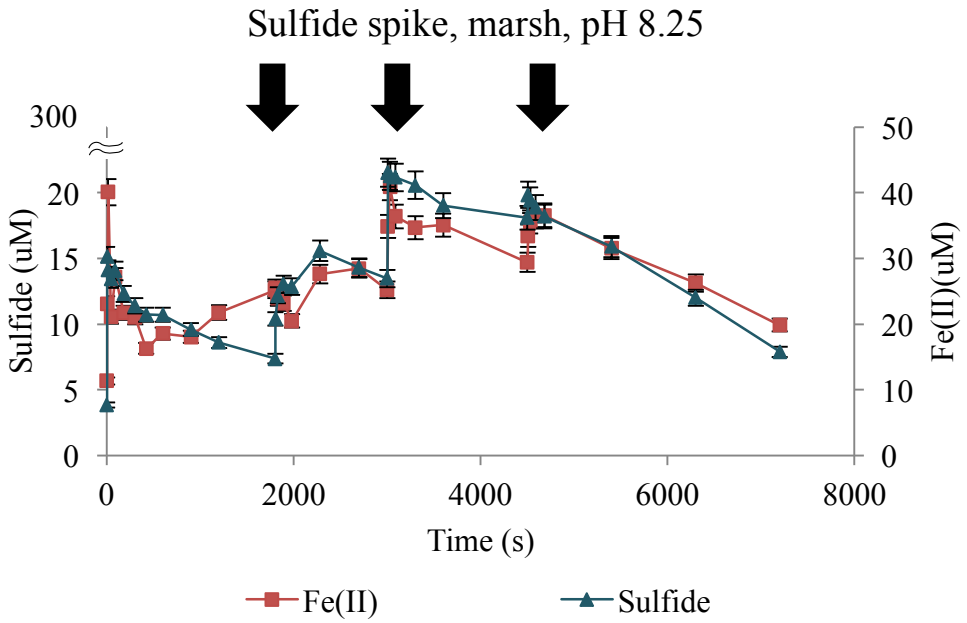

Figure 3.9 Sulfide spiked into sediments correlated with brief reappearances of Fe(II). Multiple aliquots of sulfide were added to sediments in the presence of oxygen. Sulfide was consumed rapidly in all cases with the nominal concentration of $300x10^{-6}$ M at each spike not detected. Dissolved Fe(II) increased slightly corresponding with each addition but was reoxidized on a similar timescale to that of the initiating pulse (⬇ indicates time of sulfide addition, pH 8.25, 1.00 wt% marsh mud shown)

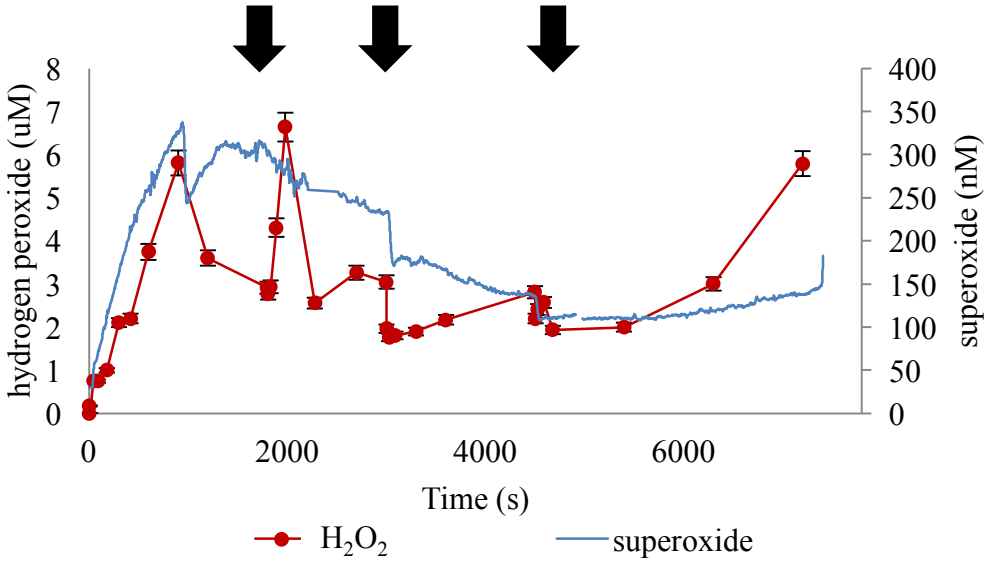

Figure 3.10 Hydrogen sulfide addition decreased instantaneous ROS concentrations. The repeated addition of separate aliquots of hydrogen sulfide resulted in initial declines in ROS followed by slow recovery to pre-spike level. However the system was robustly catalytic for ROS production overall and the variance between the highest and lowest ROS concentrations was generally less than a factor of 2 (⬇ indicates time of sulfide addition, pH 8.25, 1.00 wt% marsh mud shown, each addition sufficient for a net 300×10^{-6} M increase in sulfide).

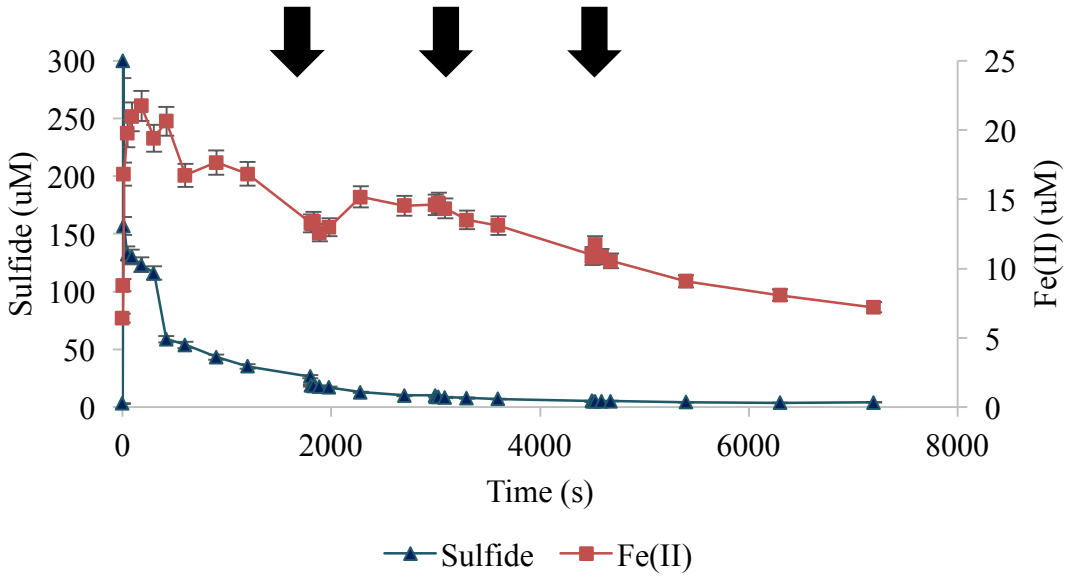

Figure 3.11 Contrasting sequential additions of hydrogen peroxide had no statistically significant effect of Fe(II) and HS^-. Hydrogen peroxide was not a source of feedback or reductive equivalents that affected Fe(II) or the rate of HS^- oxidation (⬇ indicates time of peroxide addition pH, 8.25, 1.00 wt% marsh mud shown, each addition sufficient for a net $10x10^{-6}$ M increase in peroxide).

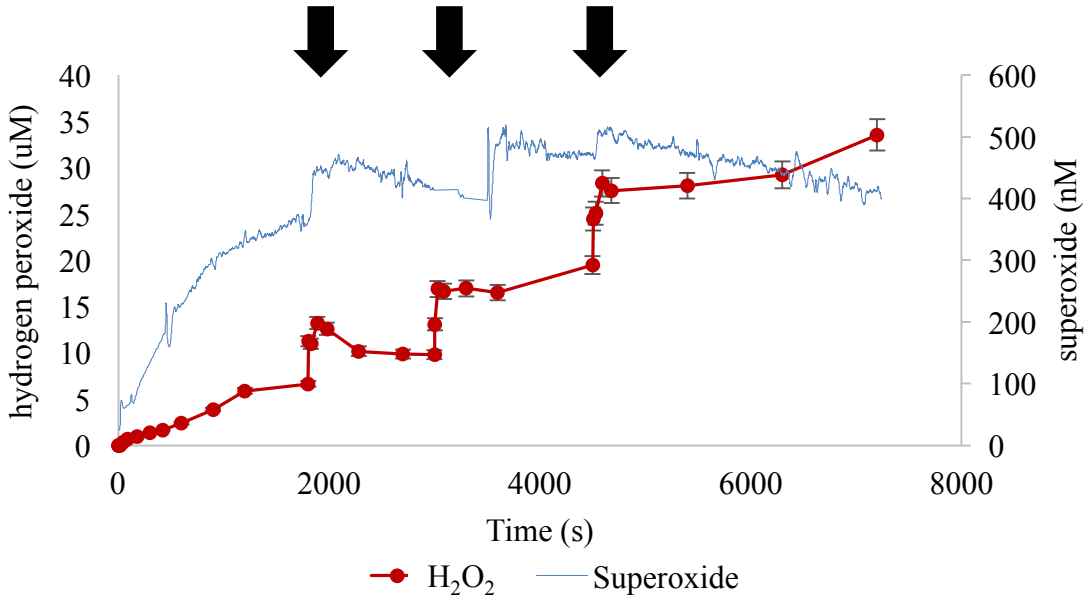

Figure 3.12 Sequential sulfide spikes were increasingly stable. The initial hydrogen peroxide addition decayed rapidly while the latter two were essentially stable additions; indicating that peroxide-consuming reactions were still taking place at the time of first addition. (⬇ indicates time of peroxide addition pH, 8.25, 1.00 wt% marsh mud shown, each addition sufficient for a net $10x10^{-6}$ M increase in peroxide).

CHAPTER 4

THE PRELIMINARY INVESTIGATION OF ANTIOXIDANT ENZYMES IN COASTAL MARSH

Abstract

High concentrations of hydrogen peroxide in cells can cause great damage due to its high capacity of unrestricted oxidation. To maintain homeostasis, antioxidant enzymes like catalase, peroxidase and reductase are important in the processes of degrading hydrogen peroxide. Results from previous studies indicated an obvious difference on the capacity of generating hydrogen peroxide in sterile and non-sterile sediment samples. This chapter focuses on the preliminary investigation of peroxidase in non-sterile sediment samples. The results are showing that peroxidase ranged from 0.001% (1 ppm) to 0.004% (4 ppm) in coastal marsh samples.

4.1 Introduction

The antioxidant enzymes are critical in processes such as cell detoxification during oxidative stress, which is caused by the accumulation of reactive oxygen species (ROS). As one of those reactive oxygen species, high concentration of hydrogen peroxide in cells is toxic due to the high reactivity of this species. Antioxidant enzymes which help to degrade hydrogen peroxides are important in the mechanisms in cells to maintain homeostasis.[193] Previous studies on the ROS generation with sterile and non-sterile mud samples are showing obvious difference are showing obvious difference on the hydrogen

peroxide levels. In the presence of sterile samples, 20-25 μM of hydrogen peroxide was detected,[194] while ~2 μM as a maximum H_2O_2 concentration was detected in non-sterile pore waters.[195]

4.2. Field study

Sediment samples were collected from Folly Beach, SC every hour from 12: 00 pm to 5 pm on Aug. 28th, 2015. At each time point, three samples from different locations were collected from the ~ 3 cm top layer of the sediment, as Figure 5.1 shows. Samples were put into 50 mL centrifuge tubes, frozen by liquid nitrogen immediately. Frozen samples were kept in dry ice during transportation and transferred to a -70-degree freezer. Foranalysis, each sample was allowed a slow thawing in a fridge at 5 degrees.

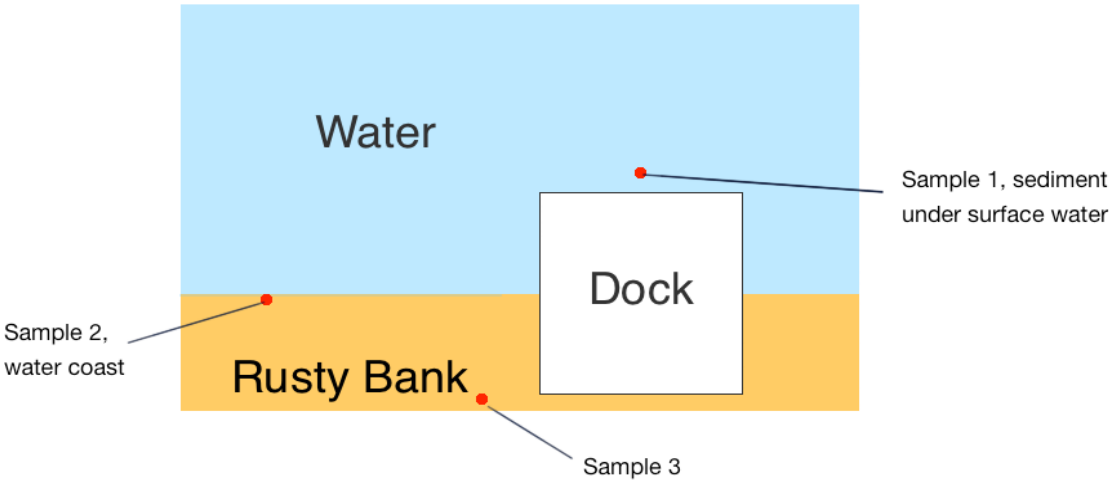

Figure 4.1 Locations of sample collection. Sample 1 was collected from the sediment under the surface water; sample 2 and 3 were collected from the riverband. All samples were collected in 50 mL plastic centrifuge tubes

4.3 Materials and Methods

BurBuster HT protein extraction reagent was purchased from Novagen. Coomassie Brilliant Blue G250 (CBB) was purchased from Sigma.

Each thawed sample was taken out from the fridge and treated by using 5 mL of 0.05 M phosphate buffer (pH 7.5) and 500 uL of BugBuster protein extraction reagent. The resulting sample was vortexed for about 2 minutes followed by 5 minutes' centrifuge. The pellet was treated again in the same way to ensure the complete extraction of proteins in the sample. 200 uL of each supernatant was transferred into a quartz plate, and treated by CBB solution (Bradford assay) or amplex red/ H_2O_2 indicator solution for total proteins and peroxidase detection.

Total protein was detected by using Bradford assay as reported.[196] In brief, CBB (100 mg) was dissolved in 100 mL 95% methanol. 100 mL of 85% (w/v) phosphoric acid was then added to this solution. The resulting solution was diluted to 1 L by ozonated DI water. To detect the total protein in a sample, 10 uL sample was transferred to a quartz plate, and 300 uL of the CBB solution was added to the sample. After ~15 min of incubation, the absorbance at 595 nm was measured by microplate reader.

The peroxidase was detected by using amplex red method reported by Gorris *et al.*[197] A indicator solution was made by mixing 50 uL of 10 mM amplex red (dissolved in DMSO) solution, 0.5 mL of 20 mM hydrogen peroxide solution and 4.45 mL of phosphate buffer (pH 7.5). 200 uL of each sample was transferred into a quartz plate and treated with 100 uL of the indicator solution, incubated for 30 minutes. The resulting samples were excited at 530 nm and the emission at 585 nm was measured.

4.4 Results and discussion

Peroxidase was detected in most of the sediment samples. Results of the detected total proteins and peroxidase are listed in Table 5.1.

Table 4.1 The detected total proteins and peroxidase in the sediment samples

Sample number	Peroxidase (ug/g wet sample)	Total protein (ug/g wet sample)	% peroxidase
12pm-1	0.00436	-	
12pm-2	0.0053	419.71	0.001262777
12pm-3	0.00286	216.05	0.001323768
1pm-1	0.00209	263.08	0.000794435
1pm-2	0.012	159.29	0.00753343
1pm-3	0.00753	191.2	0.003938285
2pm-1	Below detection limit	-	
2pm-2	0.00812	190.61	0.004260007
2pm-3	0.073	-	
3pm-1	0.00389	212.4	0.00183145
3pm-2	0.00526	140.66	0.003739514
3pm-3	0.00353	219.19	0.001610475
4pm-1	0.0039	-	
4pm-3	1.12	-	
5pm-1	0.0043	299.73	0.001434624
5mp-3	0.0131	-	

The results showed that the peroxidase weight percent ranged from 0.001-0.004% (1ppm - 4 ppm). Since peroxidase is an efficient and highly selective enzyme, even at the percentage of 0.001% can degrade hydrogen peroxide very efficiently. This can be one

possible reason for the low detected hydrogen peroxide level from pore water samples collected over non-sterile mud. On the other hand, the treatments for sterile sediment sample deactivated most of the enzymes, and the resulting sediment samples cannot degrade hydrogen peroxide any more.

CHAPTER 5

CONCLUSIONS

In chapter 1, the thermodynamics and kinetics of iron species in homogeneous and heterogeneous systems were reviewed. Focusing on the oxidation of Fe(II) binding with various ligands as well as ferric oxides. Oxitation of associated ferrous iron species (Fe(II)-L) with a range of stability constants (K) have been studied by researchers, and the resulting rate constants for are not showing a correspondingly proportionality with the known stability constants. This is indicating the effects of the ligands are not limited to Fe(II) but sometimes Fe(III) and the generated ROS.

Chapter 2 discussed the generation of ROS during the autoxidation of Fe(II) in heterogeneous systems and the effects of the added ferric oxides. The yields of ROS under all conditions in the presence of iron oxides are much lower than the theoretical yields, which is indicating some process occurring which are not generating ROS.

Chapter 3 demonstrated a potential pathway of ROS generation, the reoxidation of sulfide catalyzed by iron-containing sediments, which is in parallel of the well-known photo-induced process. Among the sediment samples under investigation, significant aqueous Fe(II) as well as ROS were only produced in the presence of those contain the highest loadings of hydrous ferric oxide, which is indicating the important role of hydrous ferric oxide as a catalyst in the process of sulfide reoxidation.

In chapter 4, a preliminary investigation on the detection of anti-oxidant enzymes in sediment samples was introduced. An assay was developed for extracting horseradish peroxidase from samples. Future work needs to focus on improving the techniques of sample handling and the extraction process.

REFERENCES

1. Nolting, R. F.; Gerringa, L. J. A.; Swagerman, M. J. W.; Timmermans, K. R.; de Baar, H. J. W., Fe (III) speciation in the high nutrient, low chlorophyll Pacific region of the Southern Ocean. *Marine Chemistry* **1998,** *62* (3-4), 335-352.

2. Rose, A. L.; Waite, T. D., Kinetic model for Fe(II) oxidation in seawater in the absence and presence of natural organic matter. *Environmental Science & Technology* **2002,** *36* (3), 433-444.

3. Welch, K. D.; Davis, T. Z.; Aust, S. D., Iron autoxidation and free radical generation: Effects of buffers, ligands, and chelators. *Archives of Biochemistry and Biophysics* **2002,** *397* (2), 360-369.

4. Hynes, M. J.; Ó Coinceanainn, M. n., The kinetics and mechanisms of the reaction of iron(III) with gallic acid, gallic acid methyl ester and catechin. *J Inorg Biochem* **2001,** *85*, 131-142.

5. Emmenegger, L.; Schonenberger, R. R.; Sigg, L.; Sulzberger, B., Light-induced redox cycling of iron in circumneutral lakes. *Limnology and Oceanography* **2001,** *46* (1), 49-61.

6. Chever, F.; Rouxel, O. J.; Croot, P. L.; Ponzevera, E.; Wuttig, K.; Auro, M., Total dissolvable and dissolved iron isotopes in the water column of the Peru upwelling regime. *Geochimica et Cosmochimica Acta* **2015,** *162*, 66-82.

7. Rose, A. L.; Waite, T. D., Kinetics of iron complexation by dissolved natural organic matter in coastal waters. *Marine Chemistry* **2003,** *84* (1-2), 85-103.

8. Ryan, P.; Hynes, M. J., The kinetics and mechanisms of the complex formation and antioxidant behaviour of the polyphenols EGCg and ECG with iron(III). *J Inorg Biochem* **2007,** *101*, 585-93.

9. Kostka, J. E.; Luther, G. W., Seasonal Cycling of Fe in Salt-Marsh Sediments. *Biogeochemistry* **1995,** *29* (2), 159-181.

10. Stumm, W.; Sulzberger, B., The cycling of iron in natural environments: Considerations based on laboratory studies of heterogeneous redox processes. *Geochimica et Cosmochimica Acta* **1992,** *56*, 3233-3257.

11. Fortin, D.; Langley, S., Formation and occurrence of biogenic iron-rich minerals. *Earth-Sci Rev* **2005,** *72* (1-2), 1-19.

12. Williams, A. G. B.; Scherer, M. M., Spectroscopic evidence for Fe(II)-Fe(III) electron transfer at the iron oxide-water interface. *Environmental Science & Technology* **2004,** *38* (18), 4782-4790.

13. Cwiertny, D. M.; Handler, R. M.; Schaefer, M. V.; Grassian, V. H.; Scherer, M. M., Interpreting nanoscale size-effects in aggregated Fe-oxide suspensions: Reaction of Fe(II) with Goethite. *Geochimica et Cosmochimica Acta* **2008,** *72*, 1365-1380.

14. Barbeau, K.; Rue, E. L.; Bruland, K. W.; Butler, A., Photochemical cycling of iron in the surface ocean mediated by microbial iron(III)-binding ligands. *Nature* **2001,** *413* (6854), 409-413.

15. Bauer, I.; Kappler, A., Rates and Extent of Reduction of Fe(III) Compounds and O-2 by Humic Substances. *Environmental Science & Technology* **2009,** *43* (13), 4902-4908.

16. Bligh, M. W.; Waite, T. D., Formation, reactivity, and aging of ferric oxide particles formed from Fe(II) and Fe(III) sources: Implications for iron bioavailability in the marine environment. *Geochimica Et Cosmochimica Acta* **2011,** *75* (24), 7741-7758.

17. Borer, P.; Sulzberger, B.; Hug, S. J.; Kraemer, S. M.; Kretzschmar, R., Photoreductive dissolution of lepidocrocite and other iron (hydr) oxides in the absence of organic ligands : experimental studies and kinetic modeling. *Environmental Science and Technology* **2008,** *43*, 1864-1870.

18. Rose, A. L.; Waite, T. D., Reduction of organically complexed ferric iron by superoxide in a simulated natural water. *Environmental Science & Technology* **2005,** *39* (8), 2645-2650.

19. Fujii, M.; Ito, H.; Rose, A. L.; Waite, T. D.; Omura, T., Superoxide-mediated Fe(II) formation from organically complexed Fe(III) in coastal waters. *Geochimica Et Cosmochimica Acta* **2008,** *72* (24), 6079-6089.

20. Bradley, D. J.; Pitzer, K. S., Thermodynamics of Electrolytes. 12. Dielectric Properties of Water and Debye-Huckel Parameters to 350 "C and 1 kbar. *Journal of Physical Chemistry* **1979,** *83* (12), 1599-1603.

21. Pitzer, K. S., Thermodytriarnicsof Electrolytes. I. Theoretical Basis and General Equations. *Journal of Physical Chemistry* **1973,** *77* (2), 268-277.

22. Millero, F. J.; Hawke, D. J., Ionic interactions of divalent metals in natural-waters. *Marine Chemistry* **1992,** *40* (1-2), 19-48.

23. Sillen, L. G., *The physical chemistry of sea water*. AAAS: Washington, DC, 1961.

24. Garrels, R. M.; Thompson, M. E., Chemical model for seawater at 25 degrees C and one atmosphere total pressure. *American Journal of Science* **1962,** *260* (1), 57-66.

25. Crea, F.; Giacalone, A.; Gianguzza, A.; Piazzese, D.; Sammartano, S., Modelling of natural and synthetic polyelectrolyte interactions in natural waters by using SIT, Pitzer and Ion Pairing approaches. *Marine Chemistry* **2006,** *99* (1-4), 93-105.

26. Millero, F. J.; Yao, W. S.; Aicher, J., The speciation of Fe(II) and Fe(III) in natural-waters. *Marine Chemistry* **1995,** *50* (1-4), 21-39.

27. King, D. W.; Lounsbury, H. A.; Millero, F. J., Rates and mechanism of Fe(II) oxidation at nanomolar total iron concentrations. *Environmental Science & Technology* **1995,** *29* (3), 818-824.

28. King, D. W.; Farlow, R., Role of carbonate speciation on the oxidation of Fe(II) by H_2O_2. *Marine Chemistry* **2000,** *70* (1-3), 201-209.

29. Millero, F. J., Effect of ionic interactions on the oxidation of Fe(II) and Cu(I) in natural waters. *Marine Chemistry* **1989,** *28*, 1-18.

30. Millero, F. J., The effect of ionic interactions on the oxidation of metals in natural-waters. *Geochimica Et Cosmochimica Acta* **1985,** *49* (2), 547-553.

31. Wilkins, R. G., *The study of kinetics and mechanism of reactions of transition metal complexes*. Allyn and Bacon, Inc., Boston: 1974.

32. Lowson, R. T., Aqueous oxidation of pyrite by molecular oxygen. *Chemical Reviews* **1982,** *82* (5), 461-497.

33. King, D. W., Role of carbonate speciation on the oxidation rate of Fe(II) in aquatic systems. *Environmental Science & Technology* **1998,** *32* (19), 2997-3003.

34. Rose, A. L.; Waite, T. D., Effect of dissolved natural organic matter on the kinetics of ferrous iron oxygenation in seawater. *Environmental Science & Technology* **2003,** *37* (21), 4877-4886.

35. Voelker, B. M.; Sulzberger, B., Effects of fulvic acid on Fe(II) oxidation by hydrogen peroxide. *Environmental Science & Technology* **1996,** *30* (4), 1106-1114.

36. Roy, E. G.; Wells, M. L., Evidence for regulation of Fe(II) oxidation by organic complexing ligands in the Eastern Subarctic Pacific. *Marine Chemistry* **2011,** *127*, 115-122.

37. Pullin, M. J.; Cabaniss, S. E., The effects of pH, ionic strength, and iron-fulvic acid interactions on the kinetics of nonphotochemical iron transformations. I. Iron(II) oxidation and iron(III) colloid formation. *Geochimica Et Cosmochimica Acta* **2003,** *67* (21), 4067-4077.

38. Park, B.; Dempsey, B. A., Heterogeneous Oxidation of Fe(II)

on Ferric Oxide at Neutral pH and a

Low Partial Pressure of O2. *Environ. Sci. Techol.* **2005,** *39*, 7.

39. Pham, A. N.; Waite, T. D., Modeling the kinetics of Fe(II) oxidation in the presence of citrate and salicylate in aqueous solutions at pH 6.0-8.0 and 25 degrees C. *Journal of Physical Chemistry A* **2008,** *112* (24), 5395-5405.

40. Burns, J. M.; Craig, P. S.; Shaw, T. J.; Ferry, J. L., Short-Term Fe Cycling during Fe(II) Oxidation: Exploring Joint Oxidation and Precipitation with a Combinatorial System. *Environ. Sci. Techol.* **2011,** *45*, 7.

41. Sung, W.; Morgan, J. J., Kinetics and product of ferrous iron oxygenation in aqueous systems. *Environmental Science & Technology* **1980,** *14* (5), 561-568.

42. Burns, J. M.; Craig, P. S.; Shaw, T. J.; Ferry, J. L., Combinatorial Parameter Space As an Empirical Tool for Predicting Water Chemistry: Fe(II) Oxidation Across a Watershed. *Environmental Science & Technology* **2011,** *45* (9), 4023-4029.

43. Burns, J. M.; Craig, P. S.; Shaw, T. J.; Ferry, J. L., Multivariate Examination of Fe(II)/Fe(III) Cycling and Consequent Hydroxyl Radical Generation. *Environ. Sci. Techol.* **2010,** *44* (19), 6.

44. Benitez-Nelson, C. R.; Sekula-Wood, E.; Schnetzer, A.; Anderson, C.; Berelson, W. M.; Brzezinski, M. A.; Burns, J. M.; Caron, D. A.; Cetinic, I.; Ferry, J. L.; Fitzpatrick, E.; Jones, B. H.; Miller, P. E.; Morton, S. L.; Schaffner, R. A.; Siegel, D. A.; Thunell, R., Rapid downward transport of the neurotoxin domoic acid in coastal waters. *Nat Geosci* **2009,** *2* (4), 272-275.

45. Emmenegger, L.; King, D. W.; Sigg, L.; Sulzberger, B., Oxidation kinetics of Fe(II) in a eutrophic Swiss lake. *Environmental Science & Technology* **1998,** *32* (19), 2990-2996.

46. Rue, E. L.; Bruland, K. W., Complexatio of iron (III) by natural organic-ligands in the central north pacific as determined by a new competitive ligand equilibration adsorptive cathodic stripping voltammetric method. *Marine Chemistry* **1995,** *50* (1-4), 117-138.

47. Luther, G. W.; Shellenbarger, P. A.; Brendel, P. J., Dissolved organic Fe(III) and Fe(II) complexes in salt marsh porewaters. *Geochimica Et Cosmochimica Acta* **1996,** *60* (6), 951-960.

48. Carey, E.; Burns, J.; DiChristina, T. J.; Taillefert, M., Formation of soluble organic-Fe(III) complexes during microbial iron reduction. *Geochimica Et Cosmochimica Acta* **2005,** *69* (10), A225-A225.

49. Kurimura, Y.; Ochiai, R.; Matsuura, N., Oxygen oxidation of ferrous ions induced by chelation. *B Chem Soc Jpn* **1968,** *41* (10), 2234-+.

50. Harris, D. C.; Aisen, P., Facilitation of Fe(II) autoxidation by Fe(III) complexing agents. *Biochimica Et Biophysica Acta* **1973,** *329* (1), 156-158.

51. Theis, T. L.; Singer, P. C., Complexation of iron(II) by organic-matter and its effect on iron(II) oxygenation. *Environmental Science & Technology* **1974,** *8* (6), 569-573.

52. Liang, L. Y.; Mcnabb, J. A.; Paulk, J. M.; Gu, B. H.; Mccarthy, J. F., Kinetics of Fe(II) oxygenation at low partial-pressure of oxygen in the presence of natural organic-matter. *Environmental Science & Technology* **1993,** *27* (9), 1864-1870.

53. De Laat, J.; Gallard, H., Catalytic decomposition of hydrogen peroxide by Fe(III) in homogeneous aqueous solution: Mechanism and kinetic modeling. *Environmental Science & Technology* **1999,** *33* (16), 2726-2732.

54. Santana-Casiano, J. M.; Gonzalez-Davila, M.; Rodriguez, M. J.; Millero, F. J., The effect of organic compounds in the oxidation kinetics of Fe(II). *Marine Chemistry* **2000,** *70* (1-3), 211-222.

55. Volker, C.; Wolf-Gladrow, D. A., Physical limits on iron uptake mediated by siderophores or surface reductases. *Marine Chemistry* **1999,** *65* (3-4), 227-244.

56. Millero, F. J., Solubility of Fe(III) in seawater. *Earth Planet Sc Lett* **1998,** *154* (1-4), 323-329.

57. Burns, J. M.; Craig, P. S.; Shaw, T. J.; Ferry, J. L., Short-term Fe cycling during Fe(II) oxidation: Exploring joint oxidation and precipitation with a combinatorial system. *Environmental Science and Technology* **2011,** *45*, 2663-2669.

58. Rose, A. L.; Waite, T. D., Reconciling kinetic and equilibrium observations of iron(III) solubility in aqueous solutions with a polymer-based model. *Geochimica Et Cosmochimica Acta* **2007,** *71* (23), 5605-5619.

59. Gunnars, A.; Blomqvist, S.; Johansson, P.; Andersson, C., Formation of Fe(III) oxyhydroxide colloids in freshwater and brackish seawater, with incorporation of phosphate and calcium. *Geochimica Et Cosmochimica Acta* **2002,** *66* (5), 745-758.

60. Davison, W.; Seed, G., The kinetics of the oxidation of ferrous iron in synthetic and natural-waters. *Geochimica Et Cosmochimica Acta* **1983,** *47* (1), 67-79.

61. Zafiriou, O. C.; True, M. B., INTERCONVERSION OF IRON(III) HYDROXY COMPLEXES IN SEAWATER. *Marine Chemistry* **1980,** *8* (4), 281-288.

62. Dousma, J.; Debruyn, P. L., Hydrolysis-precipitation studies of iron solutions. I. Model for hydrolysis and precipitation from Fe(III) nitraite solutions. *J Colloid Interf Sci* **1976,** *56* (3), 527-539.

63. Dousma, J.; Ottelander, D. D.; Bruyn, P. L. D., Influence of Sulfate-ions on the formation of iorn(III) oxides. *J Inorg Nucl Chem* **1979,** *41* (11), 1565-1568.

64. Pham, A. N.; Rose, A. L.; Feitz, A. J.; Waite, T. D., Kinetics of Fe(III) precipitation in aqueous solutions at pH 6.0-9.5 and 25 degrees C. *Geochimica Et Cosmochimica Acta* **2006,** *70* (3), 640-650.

65. Burns, J. M.; Craig, P. S.; Shaw, T. J.; Ferry, J. L., Short-Term Fe Cycling during Fe(II) Oxidation: Exploring Joint Oxidation and Precipitation with a Combinatorial System. *Environmental Science & Technology* **2011,** *45* (7), 2663-2669.

66. He, Q. H.; Leppard, G. G.; Paige, C. R.; Snodgrass, W. J., Transmission electron microscopy of a phosphate effect on the colloid structure of iron hydroxide. *Water Research* **1996,** *30* (6), 1345-1352.

67. Mayer, T. D.; Jarrell, W. M., Phosphorus sorption during iron(II) oxidation in the presence of dissolved silica. *Water Research* **2000,** *34* (16), 3949-3956.

68. Stumm, W.; Sulzberger, B., The cycling of iron in natural environments - considerations based on laboratory studies of heterogeneous redox processes. *Geochimica Et Cosmochimica Acta* **1992,** *56* (8), 3233-3257.

69. Gregory, K. B.; Larese-Casanova, P.; Parkin, G. F.; Scherer, M. M., Abiotic transformation of hexahydro-1,3,5-trinitro-1,3,5-triazine by fell bound to magnetite. *Environmental Science & Technology* **2004,** *38* (5), 1408-1414.

70. Elsner, M.; Schwarzenbach, R. P.; Haderlein, S. B., Reactivity of Fe(II)-bearing minerals toward reductive transformation of organic contaminants. *Environmental Science & Technology* **2004,** *38* (3), 799-807.

71. Jeon, B. H.; Dempsey, B. A.; Burgos, W. D., Kinetics and mechanisms for reactions of Fe(II) with iron(III) oxides. *Environmental Science & Technology* **2003,** *37* (15), 3309-3315.

72. Charlet, L.; Silvester, E.; Liger, E., N-compound reduction and actinide immobilisation in surficial fluids by Fe(II): the surface Fe(III)OFe(II)OH degrees species, as major reductant. *Chemical Geology* **1998,** *151* (1-4), 85-93.

73. Park, B.; Dempsey, B. a., Heterogeneous Oxidation of Fe(II) on Ferric Oxide at Neutral pH and a Low Partial Pressure of O2. *Environmental Science and Technology* **2005,** *39*, 6494-6500.

74. Tamura, H.; Goto, K.; Nagayama, M., Effect of anions on oxygenation of ferrous ion in neutral solutions. *J Inorg Nucl Chem* **1976,** *38* (1), 113-117.

75. Klausen, J.; Trober, S. P.; Haderlein, S. B.; Schwarzenbach, R. P., Reduction of substituted nitrobenzenes by Fe(II) in aquoues mineral suspensions. *Environ. Sci. Technol.* **1995,** *29* (9), 2396-2404.

76. Stumm, W.; Sulzberger, B.; Sinniger, J., The coordination chemistry of the oxide-electrolyte interface: the dependence of surface reactivity (dissolution, redox reactions) on surface structure. *Croat. Chem. Acta* **1990,** *63* (3), 277-312.

77. Stumm, W., Catalysis of redox processes by hydrous oxide surfaces. *Croat. Chem. Acta* **1997,** *70* (1), 71-93.

78. Strathmann, T. J.; Stone, A. T., Mineral surface catalysis of reactions between Fe-II and oxime carbamate pesticides. *Geochimica Et Cosmochimica Acta* **2003,** *67* (15), 2775-2791.

79. Gorski, C. A.; Scherer, M. M., Influence of magnetite stoichiometry on FeII uptake and nitrobenzene reduction. *Environmental Science and Technology* **2009,** *43*, 3675-3680.

80. Handler, R. M.; Beard, B. L.; Johnson, C. M.; Scherer, M. M., Atom Exchange between Aqueous Fe(II) and Goethite: An Fe Isotope Tracer Study. *Environmental Science & Technology* **2009,** *43* (4), 1102-1107.

81. Crosby, H. A.; Johnson, C. M.; Roden, E. E.; Beard, B. L., Coupled Fe(II)-Fe(III) electron and atom exchange as a mechanism for Fe isotope fractionation during dissimilatory iron oxide reduction. *Environmental Science & Technology* **2005,** *39* (17), 6698-6704.

82. Schindler, P. W.; Stumm, W., *The surface chemistry of oxides, hydroxides, and oxide minerals*. Wiley-Interscience: 1987.

83. Larese-Casanova, P.; Scherer, M. M., Fe(II) sorption on hematite: New insights based on spectroscopic measurements. *Environ. Sci. Techol.* **2007,** *41*, 7.

84. Larese-Casanova, P.; Kappler, A.; Haderlein, S. B., Heterogeneous oxidation of Fe(II) on iron oxides in aqueous systems: Identification and controls of Fe(III) product formation. *Geochimica Et Cosmochimica Acta* **2012,** *91*, 171-186.

85. Larese-Casanova, P.; Scherer, M. M., Fe(II) Sorption on Hematite: New Insights Based on Spectroscopic Measurements. *Environmental Science & Technology* **2007,** *41*, 471-477.

86. Rosso, K. M.; Yanina, S. V.; Gorski, C. A.; Larese-Casanova, P.; Scherer, M. M., Connecting Observations of Hematite (alpha-Fe2O3) Growth Catalyzed by Fe(II). *Environmental Science & Technology* **2010,** *44* (1), 61-67.

87. Klupinski, T. P.; Chin, Y. P.; Traina, S. J., Abiotic degradation of pentachloronitrobenzene by Fe(II): Reactions on goethite and iron oxide nanoparticles. *Environmental Science & Technology* **2004,** *38* (16), 4353-4360.

88. Kwan, W. P.; Voelker, B. M., Influence of electrostatics on the oxidation rates of organic compounds in heterogeneous Fenton systems. *Environmental Science & Technology* **2004,** *38* (12), 3425-3431.

89. Chun, C. L.; Penn, R. L.; Arnold, W. a., Kinetic and microscopic studies of reductive transformations of organic contaminants on goethite. *Environmental Science and Technology* **2006,** *40*, 3299-3304.

90. Farley, K. J.; Dzombak, D. A.; Morel, F. M. M., A surface precipitation model for the sorption of cations on metal-oxides. *J Colloid Interf Sci* **1985,** *106* (1), 226-242.

91. Gorski, C. a.; Handler, R. M.; Beard, B. L.; Pasakarnis, T.; Johnson, C. M.; Scherer, M. M., Fe atom exchange between aqueous Fe2+ and magnetite. *Environmental Science and Technology* **2012,** *46*, 12399-12407.

92. Hansel, C. M.; Benner, S. G.; Fendorf, S., Competing Fe(II)-induced mineralization pathways of ferrihydrite. *Environmental Science & Technology* **2005,** *39* (18), 7147-7153.

93. Yang, L.; Steefel, C. I.; Marcus, M. A.; Bargar, J. R., Kinetics of Fe(II)-Catalyzed Transformation of 6-line Ferrihydrite under Anaerobic Flow Conditions. *Environmental Science & Technology* **2010,** *44* (14), 5469-5475.

94. Gorski, C. A.; Scherer, M. M., Fe2+ sorption at the Fe oxide-water interface: a revised conceptual framework. In *Aquatic Redox Chemistry*, 2011 American Chemistry Society: 2011; pp 315-343.

95. Gorski, C. A.; Nurmi, J. T.; Tratnyek, P. G.; Hofstetter, T. B.; Scherer, M. M., Redox Behavior of Magnetite: Implications for Contaminant Reduction. *Environmental Science & Technology* **2010,** *44* (1), 55-60.

96. Larese-Casanova, P.; Cwiertny, D. M.; Scherer, M. M., Nanogoethite Formation from Oxidation of Fe(II) Sorbed on Aluminum Oxide: Implications for Contaminant Reduction. *Environmental Science & Technology* **2010,** *44* (10), 3765-3771.

97. Beck, M.; Dellwig, L.; Schnetger, B.; Brumsack, H. J., Cycling of trace metals (Mn, Fe, Mo, U, V, Cr) in deep pore waters of intertidal flat sediments. *Geochimica Et Cosmochimica Acta* **2008,** *72* (12), 2822-2840.

98. Moore, W. S., The subterranean estuary: a reaction zone of ground water and sea water. *Marine Chemistry* **1999,** *65* (1-2), 111-125.

99. Hartnett, H. E.; Keil, R. G.; Hedges, J. I.; Devol, A. H., Influence of oxygen exposure time on organic carbon preservation in continental margin sediments. *Nature* **1998,** *391* (6667), 572-574.

100. Cai, W. J.; Wang, Y. C.; Krest, J.; Moore, W. S., The geochemistry of dissolved inorganic carbon in a surficial groundwater aquifer in North Inlet, South Carolina, and the carbon fluxes to the coastal ocean. *Geochimica Et Cosmochimica Acta* **2003,** *67* (4), 631-639.

101. Wardman, P.; Candeias, L. P., Fenton chemistry: An introduction. *Radiat Res* **1996,** *145* (5), 523-531.

102. Bielski, B. H. J., Reevaluation of spectral and kinetic-properties of HO_2 and $O_2^{-\cdot}$ free radicals. *Photochemistry and Photobiology* **1978,** *28* (4-5), 645-649.

103. Zepp, R. G.; Faust, B. C.; Hoigne, J., Hydroxyl radical formation in aqueous reaction (pH 3-8) of iron (II) with hydrogen peroxide: the photo-Fenton reaction. *Environmental Science & Technology* **1992,** *26*, 313-319.

104. Comba, P.; Kerscher, M.; Krause, T.; Scholer, H. F., Iron-catalysed oxidation and halogenation of organic matter in nature. *Environmental Chemistry* **2015,** *12* (4), 381-395.

105. Sekar, R.; DiChristina, T. J., Microbially Driven Fenton Reaction for Degradation of the Widespread Environmental Contaminant 1,4-Dioxane. *Environmental Science & Technology* **2014,** *48* (21), 12858-12867.

106. Innocenti, I.; Verginelli, I.; Massetti, F.; Piscitelli, D.; Gavasci, R.; Baciocchi, R., Pilot-scale ISCO treatment of a MtBE contaminated site using a Fenton-like process. *Science of the Total Environment* **2014,** *485*, 726-738.

107. Wink, D. A.; Nims, R. W.; Saavedra, J. E.; Utermahlen, W. E.; Ford, P. C., THE FENTON OXIDATION MECHANISM - REACTIVITIES OF BIOLOGICALLY RELEVANT SUBSTRATES WITH 2 OXIDIZING INTERMEDIATES DIFFER FROM THOSE PREDICTED FOR THE HYDROXYL RADICAL. *P Natl Acad Sci USA* **1994,** *91* (14), 6604-6608.

108. Ito, S.; Ueno, K.; Mitarai, A.; Sasaki, K., Evidence for hydroxyl radicals as an active species generated from Udenfriends reagent. *Journal of the Chemical Society-Perkin Transactions 2* **1993,** (2), 255-259.

109. Shi, Z. Q.; Nurmi, J. T.; Tratnyek, P. G., Effects of Nano Zero-Valent Iron on Oxidation-Reduction Potential. *Environmental Science & Technology* **2011,** *45* (4), 1586-1592.

110. Gorski, C. A. E., R.; Sander, M.; Hofstetter, T.B.; Sterwart, S.M., Thermodynamic Characterization of Iron Oxide−Aqueous Fe2+ Redox Couples. *Environmental Science & Technology* **2016**.

111. Fang, G. D.; Zhou, D. M.; Dionysiou, D. D., Superoxide mediated production of hydroxyl radicals by magnetite nanoparticles: Demonstration in the degradation of 2-chlorobiphenyl. *Journal of Hazardous Materials* **2013,** *250*, 68-75.

112. Fang, G. D.; Dionysiou, D. D.; Al-Abed, S. R.; Zhou, D. M., Superoxide radical driving the activation of persulfate by magnetite nanoparticles: Implications for the degradation of PCBs. *Applied Catalysis B-Environmental* **2013,** *129*, 325-332.

113. Petigara, B. R.; Blough, N. V.; Mignerey, A. C., Mechanisms of hydrogen peroxide decomposition in soils. *Environmental Science & Technology* **2002,** *36* (4), 639-645.

114. Voelker, B. M.; Morel, F. M. M.; Sulzberger, B., Iron redox cycling in surface waters: Effects of humic substances and light. *Environmental Science & Technology* **1997,** *31* (4), 1004-1011.

115. Liu, H. Z.; Bruton, T. A.; Doyle, F. M.; Sedlak, D. L., In Situ Chemical Oxidation of Contaminated Groundwater by Persulfate: Decomposition by Fe(III)- and Mn(IV)-Containing Oxides and Aquifer Materials. *Environmental Science & Technology* **2014,** *48* (17), 10330-10336.

116. Pham, A. L. T.; Doyle, F. M.; Sedlak, D. L., Inhibitory Effect of Dissolved Silica on H2O2 Decomposition by Iron(III) and Manganese(IV) Oxides: Implications for H2O2-Based In Situ Chemical Oxidation. *Environmental Science & Technology* **2012,** *46* (2), 1055-1062.

117. Pham, A. L. T.; Lee, C.; Doyle, F. M.; Sedlak, D. L., A Silica-Supported Iron Oxide Catalyst Capable of Activating Hydrogen Peroxide at Neutral pH Values. *Environmental Science & Technology* **2009,** *43* (23), 8930-8935.

118. Mazzetti, L.; Thistlethwaite, P. J., Raman spectra and thermal transformations offerrihydrite and schwertmannite. *J. Raman Spectrosc.* **2002,** *33*, 8.

119. Viollier, E.; Inglett, P. W.; Hunter, K.; Roychoudhury, A. N.; Van Cappellen, P., The ferrozine method revisited: Fe(II)/Fe(III) determination in natural waters. *Applied Geochemistry* **2000,** *15* (6), 785-790.

120. Gomes, A.; Fernandes, E.; Lima, J. L. F. C., Fluoresence probes used for detection of reactive. *J. Biochem. Biophys. Methods* **2005,** *65*, 36.

121. Rush, J. D.; Bielski, B. H. J., Pulse Radiolytic Studies of the Reactions of HO2/O2- with Fe(II)/Fe(III) Ions. The Reactivity of HO2/O2- with Ferric Ions and Its Irnpllcation on the Occurrence of the Haber-Weiss Reaction. *J. Phys. Chem.* **1985,** *89*, 5.

122. Rush, J. D.; Bielski, B. H. J., Pulse radiolytic studies of the reaction of perhydroxyl/superoxide O2- with iron(II)/iron(III) ions. The reactivity of HO2/O2- with ferric ions and its implication on the occurrence of the Haber-Weiss reaction. *The Journal of Physical Chemistry* **1985,** *89*, 5062-5066.

123. Zepp, R. G.; Callaghan, T. V.; Erickson, D. J., Effects of enhanced solar ultraviolet radiation on biogeochemical cycles. *Journal of Photochemistry and Photobiology B-Biology* **1998,** *46* (1-3), 69-82.

124. Powers, L. C.; Miller, W. L., Blending remote sensing data products to estimate photochemical production of hydrogen peroxide and superoxide in the surface ocean. *Environ. Sci.-Process Impacts* **2014,** *16* (4), 792-806.

125. Sulzberger, B.; Laubscher, H., Reactivity of various types of iron(III) (hydr)oxides towards light-induced dissolution. *Marine Chemistry* **1995,** *50* (1-4), 103-115.

126. Sima, J.; Makanova, J., Photochemistry of iron(III) complexes. *Coordination Chemistry Reviews* **1997,** *160*, 161-189.

127. Duinea, M. I.; Costas, A.; Baibarac, M.; Chirita, P., Mechanism of the cathodic process coupled to the oxidation of iron monosulfide by dissolved oxygen. *J Colloid Interf Sci* **2016,** *467*, 51-59.

128. Peiffer, S.; Behrends, T.; Hellige, K.; Larese-Casanova, P.; Wan, M.; Pollok, K., Pyrite formation and mineral transformation pathways upon sulfidation of ferric hydroxides depend on mineral type and sulfide concentration. *Chemical Geology* **2015,** *400*, 44-55.

129. Havig, J. R.; McCormick, M. L.; Hamilton, T. L.; Kump, L. R., The behavior of biologically important trace elements across the oxic/euxinic transition of meromictic Fayetteville Green Lake, New York, USA. *Geochimica Et Cosmochimica Acta* **2015,** *165*, 389-406.

130. Chirita, P.; Schlegel, M. L., Oxidative dissolution of iron monosulfide (FeS) in acidic conditions: The effect of solid pretreatment. *Int. J. Miner. Process.* **2015,** *135*, 57-64.

131. Wan, M. L.; Shchukarev, A.; Lohmayer, R.; Planer-Friedrich, B.; Peiffer, S., Occurrence of Surface Polysulfides during the Interaction between Ferric (Hydr)Oxides and Aqueous Sulfide. *Environmental Science & Technology* **2014,** *48* (9), 5076-5084.

132. Chirita, P.; Schlegel, M. L., Reaction of FeS with Fe(III)-bearing acidic solutions. *Chemical Geology* **2012,** *334*, 131-138.

133. Johnston, S. G.; Keene, A. F.; Bush, R. T.; Burton, E. D.; Sullivan, L. A.; Isaacson, L.; McElnea, A. E.; Ahern, C. R.; Smith, C. D.; Powell, B., Iron geochemical zonation in a tidally inundated acid sulfate soil wetland. *Chemical Geology* **2011,** *280* (3-4), 257-270.

134. Gartman, A.; Yucel, M.; Madison, A. S.; Chu, D. W.; Ma, S. F.; Janzen, C. P.; Becker, E. L.; Beinart, R. A.; Girguis, P. R.; Luther, G. W., Sulfide Oxidation across

Diffuse Flow Zones of Hydrothermal Vents. *Aquatic Geochemistry* **2011,** *17* (4-5), 583-601.

135. Rickard, D.; Luther, G. W., Chemistry of iron sulfides. *Chemical Reviews* **2007,** *107* (2), 514-562.

136. Konovalov, S. K.; Luther, G. W.; Yucel, M., Porewater redox species and processes in the Black Sea sediments. *Chemical Geology* **2007,** *245* (3-4), 254-274.

137. Ma, S. F.; Noble, A.; Butcher, D.; Trouwborst, R. E.; Luther, G. W., Removal of H2S via an iron catalytic cycle and iron sulfide precipitation in the water column of dead end tributaries. *Estuar Coast Shelf S* **2006,** *70* (3), 461-472.

138. Larsen, O.; Postma, D.; Jakobsen, R., The reactivity of iron oxides towards reductive dissolution with ascorbic acid in a shallow sandy aquifer - (Romo, Denmark). *Geochimica Et Cosmochimica Acta* **2006,** *70* (19), 4827-4835.

139. Carey, E.; Taillefert, M., The role of soluble Fe(III) in the cycling of iron and sulfur in coastal marine sediments. *Limnology and Oceanography* **2005,** *50* (4), 1129-1141.

140. Poulton, S. W.; Krom, M. D.; Raiswell, R., A revised scheme for the reactivity of iron (oxyhydr)oxide minerals towards dissolved sulfide. *Geochimica Et Cosmochimica Acta* **2004,** *68* (18), 3703-3715.

141. Watson, A.; Lovelock, J. E.; Margulis, L., Methanogenesis, fires and the regulation of atmospheric oxygen. *Biosystems* **1978,** *10* (4), 293-298.

142. Bowles, M. W.; Mogollon, J. M.; Kasten, S.; Zabel, M.; Hinrichs, K. U., Global rates of marine sulfate reduction and implications for sub-sea-floor metabolic activities. *Science* **2014,** *344* (6186), 889-891.

143. Bottrell, S. H.; Newton, R. J., Reconstruction of changes in global sulfur cycling from marine sulfate isotopes. *Earth-Sci Rev* **2006,** *75* (1-4), 59-83.

144. Luther, G. W.; Findlay, A. J.; MacDonald, D. J.; Owings, S. M.; Hanson, T. E.; Beinart, R. A.; Girguis, P. R., Thermodynamics and kinetics of sulfide oxidation by oxygen: a look at inorganically controlled reactions and biologically mediated processes in the environment. *Front. Microbiol.* **2011,** *2*, 9.

145. Lin, C.; Larsen, E. I.; Larsen, G. R.; Cox, M. E.; Smith, J. J., Bacterially mediated iron cycling and associated biogeochemical processes in a subtropical shallow coastal aquifer: implications for groundwater quality. *Hydrobiologia* **2012,** *696* (1), 63-76.

146. Kubo, K.; Knittel, K.; Amann, R.; Fukui, M.; Matsuura, K., Sulfur-metabolizing bacterial populations in microbial mats of the Nakabusa hot spring, Japan. *Systematic and Applied Microbiology* **2011,** *34* (4), 293-302.

147. Aller, R. C.; Madrid, V.; Chistoserdov, A.; Aller, J. Y.; Heilbrun, C., Unsteady diagenetic processes and sulfur biogeochemistry in tropical deltaic muds: Implications for oceanic isotope cycles and the sedimentary record. *Geochimica Et Cosmochimica Acta* **2010,** *74* (16), 4671-4692.

148. Roden, E. E.; Sobolev, D.; Glazer, B.; Luther, G. W., Potential for microscale bacterial Fe redox cycling at the aerobic-anaerobic interface. *Geomicrobiol J* **2004,** *21* (6), 379-391.

149. Murphy, S. A.; Solomon, B. M.; Meng, S. N.; Copeland, J. M.; Shaw, T. J.; Ferry, J. L., Geochemical Production of Reactive Oxygen Species From Biogeochemically Reduced Fe. *Environmental Science & Technology* **2014,** *48* (7), 3815-3821.

150. Vazquez, F.; Zhang, J. Z.; Millero, F. J., Effect of metals on the rate of the oxidation of H_2S in seawater. *Geophysical Research Letters* **1989,** *16* (12), 1363-1366.

151. Rickard, D. T., Kinetics and mechanism of pyrite formation at low-temperatures. *American Journal of Science* **1975,** *275* (6), 636-652.

152. Rickard, D.; Schoonen, M. A. A.; Luther, G. W., Chemistry of iron sulfides in sedimentary environments. *Acs Sym Ser* **1995,** *612*, 168-193.

153. Luther, G. W.; Rickard, D. T.; Theberge, S.; Olroyd, A., Determination of metal (Bi)Sulfide stability constants of Mn2+, Fe2+, Co2+, Ni2+, Cu2+, and Zn2+ by voltammetric methods. *Environmental Science & Technology* **1996,** *30* (2), 671-679.

154. Rickard, D.; Luther, G. W., Kinetics of pyrite formation by the H2S oxidation of iron(II) monosulfide in aqueous solutions between 25 and 125 degrees C: The mechanism. *Geochimica Et Cosmochimica Acta* **1997,** *61* (1), 135-147.

155. Afonso, M. D.; Stumm, W., Reductive dissolution of Iron(III) (Hydr)oxides by Hydrogen-Sulfide. *Langmuir* **1992,** *8* (6), 1671-1675.

156. Bielski, B. H. J.; Cabelli, D. E.; Arudi, R. L.; Ross, A. B., Reactivity of HO_2/O_2^- radicals in aqueous solution. *Journal of Physical and Chemical Reference Data* **1985,** *14* (4), 1041-1100.

157. Moore, T. S.; Shank, T. M.; Nuzzio, D. B.; Luther, G. W., Time-series chemical and temperature habitat characterization of diffuse flow hydrothermal sites at 9 degrees 50 ' N East Pacific Rise. *Deep-Sea Res Pt Ii* **2009,** *56* (19-20), 1616-1621.

158. Field, M. P.; Sherrell, R. M., Dissolved and particulate Fe in a hydrothermal plume at 9 degrees 45 ' N, East Pacific Rise: Slow Fe (II) oxidation kinetics in Pacific plumes. *Geochimica Et Cosmochimica Acta* **2000,** *64* (4), 619-628.

159. Yucel, M.; Mullaugh, K. M.; Luther, G. W., Post-eruption sulfide and iron content of hydrothermal vent fluids from East Pacific Rise, 9 degrees 50 ' N. *Geochimica Et Cosmochimica Acta* **2009,** *73* (13), A1492-A1492.

160. Coates, J. D.; Councell, T.; Ellis, D. J.; Lovley, D. R., Carbohydrate oxidation coupled to Fe(III) reduction, a novel form of anaerobic metabolism. *Anaerobe* **1998,** *4* (6), 277-282.

161. Dollhopf, M. E.; Nealson, K. H.; Simon, D. M.; Luther, G. W., Kinetics of Fe(III) and Mn(IV) reduction by the Black Sea strain of Shewanella putrefaciens using in situ solid state voltammetric Au/Hg electrodes. *Marine Chemistry* **2000,** *70* (1-3), 171-180.

162. Perry, K. A.; Kostka, J. E.; Luther, G. W.; Nealson, K. H., Mediation of Sulfur Speciation by a Black-Sea Facultative Anaerobe. *Science* **1993,** *259* (5096), 801-803.

163. Luther, G. W.; Ferdelman, T. G.; Kostka, J. E.; Tsamakis, E. J.; Church, T. M., Temporal and Spatial Variability of Reduced Sulfur Species (Fes2,S2o32-) and Porewater Parameters in Salt-Marsh Sediments. *Biogeochemistry* **1991,** *14* (1), 57-88.

164. Michaud, E.; Aller, R. C.; Stora, G., Sedimentary organic matter distributions, burrowing activity, and biogeochemical cycling: Natural patterns and experimental artifacts. *Estuar Coast Shelf S* **2010,** *90* (1), 21-34.

165. Santos, I. R.; Eyre, B. D.; Huettel, M., The driving forces of porewater and groundwater flow in permeable coastal sediments: A review. *Estuar Coast Shelf S* **2012,** *98*, 1-15.

166. Precht, E.; Franke, U.; Polerecky, L.; Huettel, M., Oxygen dynamics in permeable sediments with wave-driven pore water exchange. *Limnology and Oceanography* **2004,** *49* (3), 693-705.

167. Aller, R. C.; Blair, N. E., Carbon remineralization in the Amazon-Guianas tropical mobile mudbelt: A sedimentary incinerator. *Cont Shelf Res* **2006,** *26* (17-18), 2241-2259.

168. Aller, J. Y.; Aller, R. C.; Kemp, P. F.; Chistoserdov, A. Y.; Madrid, V. M., Fluidized muds: a novel setting for the generation of biosphere diversity through geologic time*. *Geobiology* **2010,** *8* (3), 169-178.

169. Moore, T. S.; Nuzzio, D. B.; Di Toro, D. M.; Luther, G. W., Oxygen dynamics in a well mixed estuary, the lower Delaware Bay, USA. *Marine Chemistry* **2009,** *117* (1-4), 11-20.

170. Burns, J. M.; Craig, P. S.; Shaw, T. J.; Ferry, J. L., Multivariate Examination of Fe(II)/Fe(III) Cycling and Consequent Hydroxyl Radical Generation. *Environmental Science & Technology* **2010,** *44* (19), 7226–7231.

171. Cai, W. J.; Luther, G. W.; Cornwell, J. C.; Giblin, A. E., Carbon Cycling and the Coupling Between Proton and Electron Transfer Reactions in Aquatic Sediments in Lake Champlain. *Aquatic Geochemistry* **2010,** *16* (3), 421-446.

172. Luther, G. W., The Role of One- and Two-Electron Transfer Reactions in Forming Thermodynamically Unstable Intermediates as Barriers in Multi-Electron Redox Reactions. *Aquatic Geochemistry* **2010,** *16* (3), 395-420.

173. Kostka, J. E.; Luther, G. W., Partitioning and Speciation of Solid-Phase Iron in Salt-Marsh Sediments. *Geochimica Et Cosmochimica Acta* **1994,** *58* (7), 1701-1710.

174. Simpson, S. L., A rapid screening method for acid-volatile sulfide in sediments. *Environmental Toxicology and Chemistry* **2001,** *20* (12), 2657-2661.

175. Stookey, L. L., Ferrozine - a new spectrophotometric reagent for iron. *Analytical Chemistry* **1970,** *42* (7), 779-781.

176. Zhou, M. J.; Diwu, Z. J.; PanchukVoloshina, N.; Haugland, R. P., A stable nonfluorescent derivative of resorufin for the fluorometric determination of trace hydrogen peroxide: Applications in detecting the activity of phagocyte NADPH oxidase and other oxidases. *Analytical Biochemistry* **1997,** *253* (2), 162-168.

177. Cline, J. D., Spectrophotometric Determination of Hydrogen Sulfide in Natural Waters. *Limnol Oceanogr* **1969,** *14* (3), 454-&.

178. Rose, A. L.; Moffett, J. W.; Waite, T. D., Determination of superoxide in seawater using 2-methyl-6-(4-methoxyphenyl)-3,7-dihydroimidazo[1,2-a]pyrazin-3(7H)-one chemiluminescence. *Analytical Chemistry* **2008,** *80* (4), 1215-1227.

179. Godrant, A.; Rose, A. L.; Sarthou, G.; Waite, T. D., New method for the determination of extracellular production of superoxide by marine phytoplankton using the chemiluminescence probes MCLA and red-CLA. *Limnol Oceanogr-Meth* **2009,** *7*, 682-692.

180. Trapp, J. M.; Millero, F. J., The oxidation of iron(II) with oxygen in NaCl brines. *Journal of Solution Chemistry* **2007,** *36* (11-12), 1479-1493.

181. Santana-Casiano, J. M.; Gonzaalez-Davila, M.; Millero, F. J., Oxidation of nanomolar levels of Fe(II) with oxygen in natural waters. *Environmental Science & Technology* **2005,** *39* (7), 2073-2079.

182. Warneck, P.; Ziajka, J., Reaction mechnanism of the iron(III) catalyzed autoxidation of bisulfite in aqueous solution - steady state description for benzene as radicl scavenger. *Ber. Bunsen-Ges. Phys. Chem. Chem. Phys.* **1995,** *99* (1), 59-65.

183. Rush, J. D.; Bielski, B. H. J., Pulse radiolytic studies of the reactions of HO_2/O_2^- with Fe(II)/Fe(III) ions - the reactivity of HO_2/O_2^- with ferric ions and its implication on the occurrence of the Haber-Weiss reaction. *Journal of Physical Chemistry* **1985,** *89* (23), 5062-5066.

184. Giel, J. L.; Nesbit, A. D.; Mettert, E. L.; Fleischhacker, A. S.; Wanta, B. T.; Kiley, P. J., Regulation of iron-sulphur cluster homeostasis through transcriptional control of the Isc pathway by 2Fe-2S -IscR in Escherichia coli. *Molecular Microbiology* **2013,** *87* (3), 478-492.

185. Theil, E. C.; Behera, R. K.; Tosha, T., Ferritins for chemistry and for life. *Coordination Chemistry Reviews* **2013,** *257* (2), 579-586.

186. Genard, B.; Marie, B.; Loumaye, E.; Knoops, B.; Legendre, P.; Zal, F.; Rees, J. F., Living in a hot redox soup: antioxidant defences of the hydrothermal worm Alvinella pompejana. *Aquatic Biology* **2013,** *18* (3), 217-228.

187. Bebianno, M. J.; Company, R.; Serafim, A.; Camus, L.; Cosson, R. P.; Fiala-Medoni, A., Antioxidant systems and lipid peroxidation in Bathymodiolus azoricus from Mid-Atlantic Ridge hydrothermal vent fields. *Aquatic Toxicology* **2005,** *75* (4), 354-373.

188. Geszvain, K.; Butterfield, C.; Davis, R. E.; Madison, A. S.; Lee, S. W.; Parker, D. L.; Soldatova, A.; Spiro, T. G.; Luther, G. W.; Tebo, B. M., The molecular biogeochemistry of manganese(II) oxidation. *Biochem Soc T* **2012,** *40*, 1244-1248.

189. Bernhard, J. M.; Bowser, S. S., Peroxisome proliferation in foraminifera inhabiting the chemocline: An adaptation to reactive oxygen species exposure? *Journal of Eukaryotic Microbiology* **2008,** *55* (3), 135-144.

190. Company, R.; Serafim, A.; Cosson, R.; Fiala-Medioni, A.; Dixon, D.; Bebianno, M. J., Temporal variation in the antioxidant defence system and lipid peroxidation in the gills and mantle of hydrothermal vent mussel Bathymodiolus azoricus. *Deep-Sea Research Part I-Oceanographic Research Papers* **2006,** *53* (7), 1101-1116.

191. Abele, D.; Burlando, B.; Viarengo, A.; Portner, H. O., Exposure to elevated temperatures and hydrogen peroxide elicits oxidative stress and antioxidant response in the Antarctic intertidal limpet Nacella concinna. *Comparative Biochemistry and Physiology B-Biochemistry & Molecular Biology* **1998,** *120* (2), 425-435.

192. Abele, D.; Grosspietsch, H.; Portner, H. O., Temporal fluctuations and spatial gradients of environmental P-O_2, temperature, H_2O_2 and H_2S in its intertidal habitat trigger enzymatic antioxidant protection in the capitellid worm *Heteromastus filiformis*. *Marine Ecology Progress Series* **1998,** *163*, 179-191.

193. Bonnineau, C.; Bonet, B.; Corcoll, N., Catalase in fluvial biofilms: a comparison between different extraction methods and example of application in a metal-polluted river. *Ecotoxicology* **2011,** *20*, 293-303.

194. Murphy, S. A.; Solomon, B. M.; Meng, S.; Copeland, J. M.; Shaw, T. J.; Ferry, J. L., Geochemical production of reactive oxygen species from biogeochemically reduced Fe. *Environ. Sci. Techol.* **2014,** *48*, 7.

195. Copeland, J. M.; Dias, D.-M.; Lively, R. P.; Ihekweazu, J.; Ferry, J. L.; Shaw, T. J., Field Measurements of Biogeochemically Produced Hydrogen Peroxide in Estuarine Sediments. Work in progress, 2016.

196. Sedmak, J. J.; Grossberg, S. E., A rapid, sensitive, and versatile assay for protein using coomassie brilliant blue G250. *Analytical Biochemistry* **1977,** *79* (1-2), 544-552.

197. Gorris, H. H.; Walt, D. R., Mechanistic Aspects of Horseradish Peroxidase Elucidated through Single-Molecule Studies. *Journal of the American Chemical Society* **2009,** *131* (17), 6277-6282.

APPENDIX A – GEOCHEMICAL PRODUCTION OF REACTIVE OXYGEN SPECIES FROM BIOGEOCHEMICALLY REDUCED FE (THE SUBMITTED VERSION)[1]

ABSTRACT

The photochemical reduction of Fe(III) complexes to Fe(II) is a well-known initiation step for the production of reactive oxygen species (ROS) in sunlit waters. Here we show a geochemical mechanism for the same in dark environments based on the tidally driven, episodic movement of anoxic groundwaters through oxidized, Fe(III) rich sediments. Sediment samples were collected from the top 5 cm of sediment in a saline tidal creek in the estuary at Murrell's Inlet, South Carolina and characterized with respect to total Fe, acid volatile sulfides and organic carbon content. These sediments were air dried, resuspended in aerated solution, then exposed to aqueous sulfide at a range of concentrations chosen to replicate the conditions characteristic of a tidal cycle, beginning

[1] Sarah A. Murphy, Benson M. Solomon, Shengnan Meng, Justin M. Copeland, Timothy J. Shaw, and John L. Ferry. 2014. Department of Chemistry and Biochemistry, University of South Carolina, Columbia, South Carolina 29208, United States, *Environmental Science and Technology*. 48 (7): 3815-3821. Reprinted with permission from Environmental Science and Technology. Copyright 2014 American Chemical Society.

with low tide. No detectable ROS production occurred from this process in the dark until sulfide was added. Sulfide addition resulted in the rapid production of hydrogen peroxide, with maximum concentrations of 3.85 micromolar. The mechanism of hydrogen peroxide production was tested using a simplified three factor representation of the system based on hydrogen sulfide, Fe(II) and Fe(III). The resulting predictive model for maximum hydrogen peroxide agreed with measured hydrogen peroxide in field-derived samples at the 95% level of confidence, although with a persistent negative bias suggesting a minor undiscovered peroxide source in sediments.

KEYWORDS submarine groundwater, reactive membrane, remediation, transient oxidants

Introduction

The cycling of Fe between ferrous and ferric oxidation states constitutes a catalytic mechanism of electron transport in aqueous environments ranging from sediments to surface waters.[1-4] This cycle is coupled to atmospheric oxygen through the reduction of O_2 by ferrous iron. In the photic zone, ferrous iron formation is generally photoinduced through the photolysis of Fe(III)-ligand (L) complexes, particularly when L = carboxylic acids (eq 1).[5-7] The resultant $Fe(II)_{aq}$ is thermodynamically unstable in the presence of dissolved oxygen and its oxidation leads to the production of the superoxide anion radical (eq 2). The superoxide anion radical is the conjugate base of the hydroperoxyl radical (pKa 4.8). This radical can react with a second $Fe(II)_{aq}$ or disproportionate to generate hydrogen peroxide (eqs 3, 4).[8-10] Hydrogen peroxide in turn can react with reduced transition metals (M^{x+}) to yield the hydroxyl radical (eq 5).[11, 12] In sediments, aquifers,

and anoxic porewaters microbial respiration can replace photons as the source of reductive equivalents to drive $Fe(II)_{aq}$ production. This is accomplished through a combination of direct microbial reduction and indirect reduction by microbially produced agents such as hydrogen sulfide (eq 6).[13, 14] Reduced sulfur species, derived from anaerobic microbial reduction of sulfate, can occur in groundwaters at concentrations as high as millimolar.[15]

Reaction	**Eq #**	**Ref. #**
$Fe(III)L \xrightarrow{h\nu, LMCT} Fe(II)_{aq} + L_{ox}$	(1)	
$Fe(II)_{aq} + O_2 \rightleftarrows Fe(III) + O_2^{-}\cdot$	(2)	[16]
$Fe(II) + HO_2\cdot \underset{\rightleftarrows}{H^+} H_2O_2$	(3)	[17]
$O_2\cdot + HO_2\cdot \underset{\rightleftarrows}{H^+} H_2O_2 + O_2$	(4)	[17]
$M^{x+}_{aq} + H_2O_2 \rightleftarrows M^{(x+1)+} + HO\cdot + HO^-$	(5)	[18]
$Fe(III) + HS^- \rightleftarrows Fe(II)_{aq} + HS\cdot$	(6)	[19]

Reactions 1-5 suggest microbially generated $Fe(II)_{aq}$ can have the same impact on ROS production as photochemical sources of ROS, but with magnitude mediated by mass transport rather than light intensity.[20-22] Major sources of $Fe(II)_{aq}$ and hydrogen sulfide-rich waters include the outflow of subterranean estuaries,[23] the release of sediment-associated porewater during low tide,[24] mine drainage[25] and the emissions of some hydrothermal vents.[26] Subterranean estuaries and tidally driven mixing are particularly significant among these sources because their releases are in close proximity to high human population densities near coastal regions.[27-29] Recent studies indicate the volume of groundwater associated with subterranean estuary emission represents a major,

continuous flux of $Fe(II)_{aq}$ to the groundwater/seawater mixing zone.[30-32] Estimates based on Ra isotope inventories suggest that on the order of 30 kg water $m^{-2}day^{-1}$ is circulated through the shallow aquifer in the South Carolina salt marsh system alone.[33] This yields an estimate for the entire South Carolina coastline (est. 2000 km^2 salt marsh) of approximately 6.0 $x10^{10}$ kg of water exchanged between the oxic and anoxic conditions per day.[34] The implication is this ecosystem has a potential daily abiotic ROS flux of up to 1.5 $x10^7$ moles day^{-1} (based on the accompanying dissolved oxygen flux). This number is comparable to photochemical sources of ROS, based on measured steady state concentrations of reactive oxygen species in near shore environments.[8, 35, 36] These numbers are rough estimates yet still suggest an important hypothesis: the number of moles of reactive oxygen species derived from $Fe(II)_{aq}$ rich groundwater is potentially on par with that obtained from photochemical processes, with biogeochemical reductants (e.g. sulfide) acting as initiators in a manner analogous to photons.

Direct measurement of the ROS production capacity of a given environmental compartment is a difficult challenge because of the transient nature of the analytes involved. There is a long tradition in aqueous ROS chemistry of addressing that problem by removing a representative fraction of the system in question from the field and initiating ROS production in a laboratory setting.[7, 37, 38] This work reports application of that strategy to test the hypothesis expressed in the preceding paragraph. This was done by infusing oxic sediment samples from a protected coastal marsh with sulfidic solutions (the initiation step) and monitoring subsequent ROS formation. Sediment samples were obtained from the surface of a pristine saline tidal creek at low tide (i.e. top five cm of exposed creek bottom, flooded with seawater at high tide, pH 8.0, salinity of 28 ppt).

Varying concentrations of hydrogen sulfide were spiked into sediments and hydrogen peroxide generation was measured as a function of added sulfide and time. The duration of peroxide generation increased with increasing sulfide but the maximum concentration was constant, consistent with catalytic Fe oxidation/reduction cycles that continued until the sulfide was depleted. The mechanism of peroxide production was tested by comparing these outcomes to those obtained from a trifactorial experiment based on the cooxidation of $Fe(II)_{aq}$ and sulfide in solution in the presence of Fe(III) (central composite design, 15 conditions interrogated, *vide infra*).

Experimental Methods

Materials: Iron(III) chloride hexahydrate and sodium sulfide nonahydrate (99.99+% trace metal free) were purchased from Aldrich. Hydrochloric acid (ACS grade) was obtained from BDH. *N,N*-dimethyl-p-phenylenediamine sulfate salt was acquired from Acros Organics. Diethylenetriaminepentaacetic acid (98+%) and iron(II) chloride anhydrous (99.5+%) were purchased from Alfa Aesar. Iron(II) chloride was stored in a desiccator. FerroZine iron reagent (98%) was purchased from VWR. All other salts (99%) were obtained from Fisher Scientific. All chemicals were used as received. Solutions were made in Barnstead E-pure (18 MΩ cm^{-1}) water which had been distilled under nitrogen to remove trace H_2O_2.

Analytical Methods:

Iron(II) and Sulfide Measurement. $Fe(II)_{aq}$ and hydrogen sulfide were monitored colorimetrically using the ferrozine and methylene blue methods respectively.[39-42] Samples were withdrawn from the reactor and added directly to developing solutions (varied by analyte). Absorption spectra were recorded on a Spectramax M5 plate reader.

Hydrogen Peroxide. Hydrogen peroxide was measured by the acridinium ester chemiluminescence technique utilizing a flow injection analysis instrument with a chemiluminescence detector (Waterville Analytical, Waterville, ME).[43, 44] Chemiluminescence from the reaction between the hydroperoxyl anion and acridinium ester at pH 11.4 was monitored in a flow through cell by a photon multiplier (PMT). All initial flow rates (sample, carrier, acridinium ester, and buffer) were set at a constant 1.5 mL/min. The flow cell volume was 2 mL, with a PMT integration time of 0.200 s and a constant voltage for every experiment set. Daily calibration was achieved by the use of independently verified (UV absorbance at 2.54 $x10^{-7}$ m) peroxide solutions, with hourly drift checks based on standard comparison. New calibrations were performed at least twice/measurement period or when instrument drift exceeded 10%.

All glassware used was cleaned in a muffle furnace and acid washed. After rinsing with 18MΩ deionized water, glassware was handled and stored as trace metal clean glassware to prevent trace metal catalytic oxidation of sulfide in the absence of added metals (S1-S61).

Sediment Experiments. Sediment samples were collected from a tidal creek (Bread and Butter Creek) in North Inlet, part of the Baruch Institute reserve near the town of Murrell's Inlet, South Carolina (S1-S4). Collected sediments included both oxic and anoxic layers. Anoxic portions were sulfidic with a loading of 26.5µmol/g acid volatile sulfides based on dry weight. Aqueous sediment loading was 10.00 g L^{-1} of air dried, sieved sediment, consistent with the low range of solid/liquid ratio (99% porosity) observed in the top layers of many coastal surface sediments.[45] Sediments were stirred for 20 minutes prior to the addition of sulfide and buffered to pH 8.28 with $NaHCO_3$

(0.050 M). Samples were removed from the reactors and spun down on a Baxter Dade Immufuge II centrifuge at 3225 rpm for 30 seconds to remove suspended solids before subsequent spectroscopic assays.

Quality Assurance/Quality Control. Replicate blanks (n=3) were obtained for all reagents. Blanks were updated with preparation of fresh reagent solutions. Reference standards were interrogated for peroxide analysis at a frequency of 1 reference check/5 unknown determinations. Peroxide reference standards were externally calibrated against their optical absorbance at 254 nm. The detection limit for each method was defined by the linear dynamic range of the calibration curves.

Experimental Design

The multifactorial experiments were designed to interrogate the relationship between peroxide yield and the initial concentrations of $Fe(II)_{aq}$, total Fe(III), and hydrogen sulfide. Specific conditions for each experiment were determined by processing the conditional ranges for each variable through the central composite design algorithm, which solved for specific points in parameter space that required experimentation. This design was chosen to allow an estimate of feedback terms, a necessary experimental componenet for systems based on free radical reactions that may involve self-disproportionation in the final observables. This method of interrogation allowed development of models based on the correlation of experimental outcomes with initial conditions without exhaustive understanding of the fundamental equilibria and kinetic constants for every step of the system.

The concentration ranges for each factor were chosen based on reported field measurements to ensure environmental relevance.[15, 46-48] Similar models have previously

been shown competent for accurately predicting net oxidation rates in complex multistep reaction systems.[41, 42, 49]

The pH of each reaction was monitored to ensure consistency. A pH probe (Cole Palmer pH electrode, general purpose, combination, refillable, glass body, BNC) was calibrated at the appropriate ionic strength condition and used to monitor pH throughout. Mean pH for the experimental array was = 8.28 ± 0.07 reported as one standard deviation. The ionic strength of the solutions was established by the buffer; the sum of all other ionic species added contributed less than 2% to the total. All measurements were performed in triplicate, except the midpoint (initial conditions 1.50 x10^{-4} M $Fe(II)_{aq}$, 1.50 x10^{-4} M Fe(III), and 2.50 x10^{-4} M HS^-), which was performed n = 6 times. The experimental sequence was randomized to eliminate time dependent artifacts. All experiments were conducted in a dark room to minimize photochemical reactions. The correlation between pH variability and measured outcomes (S1-S53, S1-S54) was less than 0.1, indicating pH was not a statistically significant factor across the experimental design.

Results

The multifactorial experiments were justified based on the hypothesis that complex sediment samples could be reductively modeled as equivalent to mixtures of aqueous solutions of Fe(II), HS^- and Fe(III) as they came to thermodynamic equilibrium with dissolved oxygen. Air saturated solutions of HS^- were stable at pH 8.28 in the presence and absence of added hydrogen peroxide (S1-S61). Separate Fe(III) solutions and hydrogen sulfide solutions were monitored over time and no hydrogen peroxide evolution was detected. However the joint addition of Fe(II) and Fe(III) to oxic HS^- solutions

resulted in the oxidation of Fe(II) and HS^- along with the initial rapid reduction of some Fe(III) (Figure 1). The ratio of the first derivatives of [HS^-] and [Fe(II)] plotted vs time approached unity after the initial Fe(III) reduction phase, indicating the catalytic function of Fe(II) in enabling the oxidation of HS^- by O_2 (Figure 1 inset).

The evolution of hydrogen peroxide was monitored under all conditions of the trivariate experiment and observed to range from a minimum below the detection limit and a maximum of 2.3 $x10^{-5}$ M (Figure 2). An ANOVA table was constructed to determine the relationship between the hydrogen peroxide and the initial concentrations of Fe(II), HS^- and Fe(III). The maximum concentration of hydrogen peroxide for each experimental condition was correlated against all three individual factors, their squared terms (curvature) and the possible interactions in accordance with the quadratic fit of the central composite design algorithm (Table 2). The factors could be fit to the maximum hydrogen peroxide yield with an unadjusted R^2 of 0.919. The model was constructed assuming each term (x) had a coefficient, β_x. The statistical significance of each term to the outcome was determined by applying the t-test to the hypothesis that $\beta_x \neq 0$ at the 95% level of confidence. Factors with β_x values that did not test as significantly different from 0 were statistically and practically unimportant to hydrogen peroxide. $[Fe(II)]_{aq}$, $[HS^-]$, $[Fe(II)]_{aq}^2$, $[HS^-]^2$ and the $[Fe(II)]_{aq}$-$[HS^-]$ interaction terms were significant to the outcome at the 95% level of confidence. The sign on the associated β_x values indicated the direction of contribution of that factor to the model outcome. Elimination of the remaining terms yielded an adjusted R^2 of 0.899. When their corresponding uncoded β_x terms and the intercept (Table 2) were included, the resulting empirical model for predicting the maximum concentration of hydrogen peroxide was (eq 7):

$$[H_2O_2]_{max}^{1/2} = -0.3064 + 1.673\,x10^{-2}\left([Fe(II)]_{aq}x10^6\right) \quad (7)$$
$$+ 1.305x10^{-2}([HS^-]x10^6)$$
$$+ 2.243x10^{-5}\left([Fe(II)]_{aq}x10^6\right)([HS^-]x10^6)$$
$$- 4.325x10^{-5}\left([Fe(II)]_{aq}x10^6\right)^2$$
$$- 2.529x10^{-5}([HS^-]x10^6)^2$$

A sum of squares value was obtained from the ANOVA table for the model and each factor (Table S1-S2). The ratio of the value for each factor over the value for the model provided a rough estimate of the percent impact attributable to that factor on the maximum yield of hydrogen peroxide (Table 2).

A series of field-derived sediment samples were characterized (*vide supra*) and suspended in aerated solution of hydrogen sulfide and equilibrated with oxygen. The measured initial values of Fe(II) and HS^- were then entered into the model (eq 7) to generate predicted H_2O_2 maxima. The validity of the initial hypothesis was tested by comparison between the measured and predicted hydrogen peroxide maxima at the 95% level of confidence.

Equilibration experiments were conducted with aqueous suspensions of tidal creek sediment (Bread and Butter Creek (S1-S4), 1.00 wt % suspension; composition 21% C, 2% N, 1.2% total Fe). Sediments were aerated in the dark in the absence or presence of added hydrogen sulfide. Samples removed prior to sulfide addition contained detectable amounts of Fe(II) (detection limit of 2.0 $x10^{-6}$ M, whereas [HS^-] and [H_2O_2] were both below their respective detection limits (3.0 ±1.5 $x10^{-6}$ M and 2.50 ±0.90 $x10^{-7}$ M, S1-S64). Native Fe(II) sources in the samples contributed to an Fe(II) background of 9.1±2.9

$x10^{-6}$ M. Additional suspensions were prepared and sufficient hydrogen sulfide added to raise the nominal initial concentration to 3.00 $x10^{-4}$ M (Figure 3) or 6.00 $x10^{-4}$ M (Figure 4). These conditions were chosen to emulate tidally driven measured groundwater exchange (the outward pulse) through sediments.[14, 50-55] Dissolved O_2 reduction in the latter suspensions was rapid with concurrent oxidation of hydrogen sulfide and formation of $Fe(II)_{aq}$ (Figure 3 and 4). $Fe(II)_{aq}$ fell to pre-sulfide spike concentrations after added hydrogen sulfide was consumed, in agreement with existing models of Fe-catalyzed O_2 driven oxidation (e.g. the Udenfriend reaction and many subsequent works) and the results of the trivariate model.[14, 56-60] Subsequent additions of hydrogen sulfide to the sediment suspensions resulted in essentially identical reactant/product production and consumption profiles (S1-S58, S1-S59, S1-S60) as long as oxygen concentrations were maintained. $Fe(II)_{aq}$ never reached the concentration that would be predicted from the reductive equivalents added (as hydrogen sulfide), presumably due to its simultaneous oxidation by dissolved oxygen (eqs 2, 6). Hydrogen peroxide concentration increased as sulfide concentrations fell to near the detection limit, approaching a maximum of 3.85 and 2.83 $x10^{-6}$ M for 300 and 6.00 $x10^{-4}$ M hydrogen sulfide added respectively (Figures 3 and 4). $Fe(II)_{aq}$ achieved a maximum concentration within 30 s and maintained at a pseudo-stationary state until $[HS^-] < [Fe(II)]_{aq}$, then fell.

Discussion

Aqueous solutions of ferrous and ferric iron, dissolved oxygen and hydrogen sulfide are a thermodynamically unstable mixture that occurs frequently if transiently in natural waters as a result of mass trasport. They are associated with the movement of aqueous solutions across sharp redox gradients, particularly those imposed by microbial

consumption of oxygen or the action of sulfate reducers. Examples include the tidally driven release of submarine groundwater across the sediment-water column interface; the seasonal overturn of hypolimnetic waters, redox zonation in biofilms and other events corresponding to a large range of flow regimes.[61-68] They equilibrate rapidly on mixing with concurrent oxidation of reduced iron and production of superoxide. The corresponding rate of O_2 reduction is controlled by several variables, including the rate of precipitation of resulting Fe(III) or Fe(III)-L in the studied system. Under the conditions of this study (pH 8.28, 5.0 x10^{-2} M total CO_3^{2-} species, $[Fe(II)]_o$ < 3.00 x10^{-4} M) net Fe(II) oxidation in the absence of sulfide was expected to be quite rapid with an Fe(II) lifetime of less than 10 s.[41, 42] Based on this assumption and eq 1-5 the appearance of superoxide and H_2O_2 should have mirrored the rapid loss of Fe(II). However, previous work has shown sulfide capable of rapidly reducing $Fe(III)_{aq}$ to Fe(II).[59, 60] In this study sulfide addition resulted in a net apparent decrease in Fe(II) oxidation rates, with ROS formation coupled to sulfide oxidation and Fe(II) oxidation as a result (as distinguished from previous work reporting ROS formation as a result of Fe(II) oxidation alone).[13, 41, 42, 49] The observation is supported by the results from the multifactorial experiment (Table 2) that indicate HS^- and FeS combined account for nearly 50% of the maximum hydrogen peroxide. Given that the direct reaction of HS^- with O_2 is spin forbidden this large positive impact indicates the intermediacy of Fe(II) as an electron shuttle between reduced S species and O_2 in the system. The relatively minor impact of FeS indicates that the reduction of Fe(III) by sulfide to produce Fe(II) was a more important source of reductive equivalents in the studied system than the direct oxidation of FeS. Given that the oxidation of Fe(II) and FeS both yield superoxide, comparison of the FeS and Fe(II)

terms also suggested that the reduction of superoxide by Fe(II) (eq 3) was a more significant source for H_2O_2 than disproportionation. [69, 70] However, changes in environmental conditions such as those associated with ocean acidification are likely to change the mechanism of H_2O_2 production, probably increasing the relative importance of dismutation if conditions are closer to pH 7.

The lack of significance of Fe(III) to maximum [H_2O_2] (as indicated by analysis of the model in Table 2) supported commutability of the solution-phase model to experiments containing natural sediments. Comparison of predicted H_2O_2 maxima from eq 7 to the outcome of experiments measuring the equilibration of sediments with air; post-sulfide addition, showed close agreement between the two sets of experiments (Table 3). It was particularly notable that doubling the initial HS^- loading had no statistically significant effect on the maximum H_2O_2 yield. This suggested the family of associated reactions had reached a steady state limited by a factor independent of added sulfide, speculatively the rate of FeS oxidation. Although FeS is stable in oxic solution on the timescale of days, freshly prepared (amorphous) FeS is known to oxidize on the timescale of seconds to minutes, depending on solution conditions. The appearance of a steady state was consistent with the self-reactions of ROS that limit their concentrations and with the observation of negative $\partial r / \partial x$ for the significant squared factors (Table 2).

It was notable that the sediments in this study had very a high concentration of organic carbon, approximately 20% by mass. This carbon was not deliberately extracted or modified during the experimental procedure and therefore was presumably a faithful representation of organic carbon in the field environment. Despite the large excess of organic C in the suspensions eq 7 predicted the outcome of both HS^- spike concentrations

to within the 90% confidence interval; and to within the 95% confidence interval for the 3.00 x10^{-4} M HS^- spike, although both sets of predictions were biased slightly low (Table 3). The low bias in eq 7 could have also been a result of H_2O_2 produced during the peroxidation of organic C post-oxidation by HO•, but the bias was so small organic C was probably not a significant contributor to the H_2O_2 maximum. The high concentration of natural organic materials in the studied system indicated they were certainly the primary sink for secondary ROS such as HO• generated during the process yet they did not affect its outcome. These observations have significant implications for micropollutant fate and carbon cycling and suggest an abiotic link between microbial metabolism and carbon oxidation. If the partial oxidation of refractory carbon or other electron donors/acceptors through sulfide driven ROS production leads to modifications making them better microbial energy sources, this suggests an alternative pathway for microbial alteration and consumption of natural and anthropogenic organic carbon.[23, 71, 72]

Table 1. Factor Concentration Range Subdivisions: Experimental factors and initial concentrations corresponding to the ranges chosen for the trivariate experiment.

Coded value for each factor:					
✔	-2	-1	0	1	2
Uncoded value for each factor (i.e. initial molar concentration):					
$[Fe(II)]_{aq}$x10^{-6} M	0	61	150	239	300
[Fe(III)] x10^{-6} M	0	61	150	239	300
$[HS^-]$ x10^{-6} M	0	101	250	399	500

Table 2. Uncoded coefficients (β_x) obtained by modeling the maximum H_2O_2 yield as a function of initial [Fe(II)], [Fe(III)] and [HS^-]. (R^2_{model} = 0.919; $R^2_{adjusted}$ = 0.899)

β_x	Value	Sum of Squares	Estimated % contribution	p-value
$\beta_{0\ (intercept)}$	-0.3064	57.69		<0.0001
$\beta_{Fe(II)}$	1.673×10^{-2}	20.16	34.9	<0.0001
$\beta_{Fe(III)}$	NS[a]	0.08	NS[a]	0.4523
β_{HS-}	1.305×10^{-2}	23.10	40.0	<0.0001
$\beta_{Fe(II)Fe(III)}$	NS[a]	0.15	NS[a]	0.2948
$\beta_{Fe(II)HS-}$	2.243×10^{-5}	2.12	3.7	0.0003
$\beta_{HS-Fe(III)}$	NS[a]	0.31	NS[a]	0.1382
$\beta_{(Fe(II))2}$	-4.325×10^{-5}	3.29	5.7	<0.0001
$\beta_{Fe(III))2}$	NS[a]	0.00	NS[a]	0.9745
$\beta_{(HS-)2}$	-2.529×10^{-5}	8.68	15.0	<0.0001

[a] NS indicates "not significant" at the 95% level of confidence.

Table 3: Comparision of Sediment Experimental Hydrogen Peroxide Data to Model Predictions

[HS-] initial	$[Fe(II)]_{aq}$ initial	[Fe(III)] initial	Sediment Data	Model Prediction
$3.00x10^{-4}$ M	$7 x10^{-6}$ M	$2.2 x10^{-3}$ M	$3±1.8 x10^{-6}$ M	$2±0.9 x10^{-6}$ M
$6.00x10^{-4}$ M	$7 x10^{-6}$ M	$2.2 x10^{-3}$ M	$4±1.8 x10^{-6}$ M	$2±0.9 x10^{-6}$ M

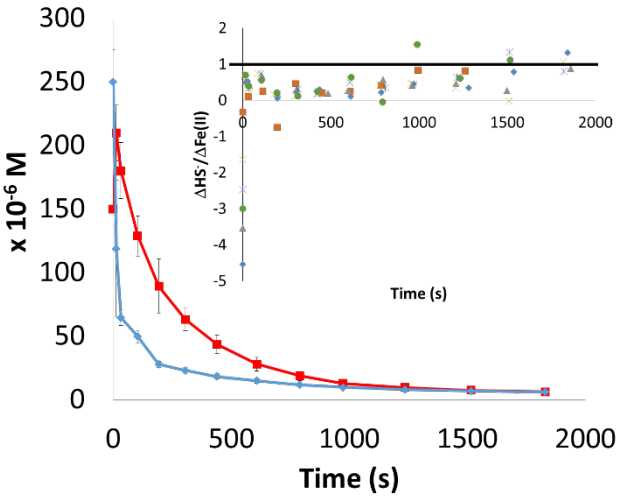

Figure 1. The concentration of (■) $Fe(II)_{aq}$ and (●) $[HS^-]$ during the oxidation of 1.50 $x10^{-4}$ M initial $Fe(II)_{aq}$ and 2.50 $x10^{-4}$ M initial hydrogen sulfide in the presence of 1.50 $x10^{-4}$ M initial Fe(III) is shown. Error bars shown are ±1 standard deviation based on n = 6 experiments. Inset: the ratio of the first derivatives of $[HS^-]$ and [Fe(II)], with a thick solid line to illustrate the approach to unity, six replicates shown.

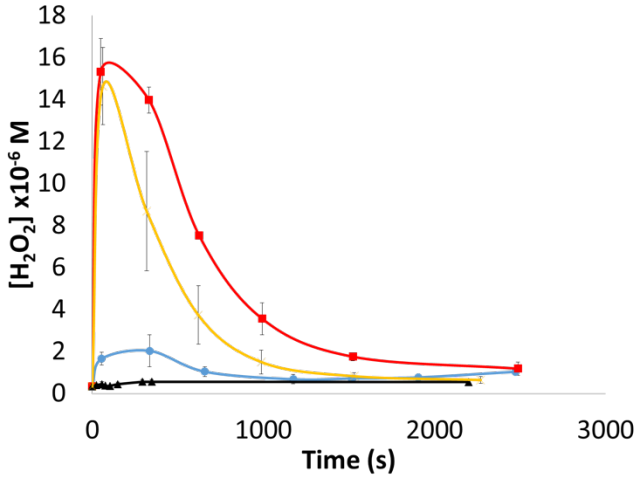

Figure 2. The concentration of peroxide with time. Initial conditions: (■), 1.50 x10^{-4} M $Fe(II)_{aq}$, 2.50 x10^{-4} M HS^-; (×) 1.50 x10^{-4} M $Fe(II)_{aq}$, 1.50 x10^{-4} M Fe(III), 2.50 x10^{-4} M HS^-; (●) 1.50 x10^{-4} M Fe(III), 2.50 x10^{-4} M HS^-; (▲) 1.50 x10^{-4} M $Fe(II)_{aq}$, 1.50 x10^{-4} M Fe(III). Error bars shown are ±1 standard deviation based on n = 3 experiments.

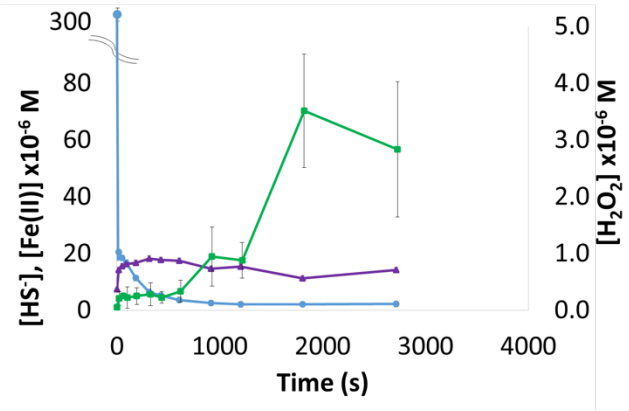

Figure 3. Concentration of (●) hydrogen sulfide, (▲) $Fe(II)_{aq}$, and (■) H_2O_2 during the injection of 3.00 x10^{-4} M hydrogen sulfide into a slurry of Bread and Butter Creek sediment (10.00 g sediment/L). Error bars are ±1 standard deviation based on n = 3 experiments.

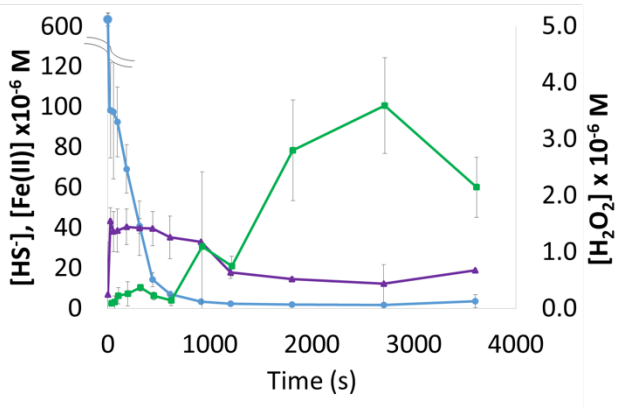

Figure 4. Concentration of (●) hydrogen sulfide, (▲) $Fe(II)_{aq}$, and (■) H_2O_2 during the injection of 6.00 x10^{-4} M hydrogen sulfide into a slurry of Bread and Butter Creek sediment (10.00 g sediment/L) are shown. Error bars shown are ±1 standard deviation based on n = 3 experiments.

ASSOCIATED CONTENT

AUTHOR INFORMATION

Corresponding Author

*ferry@sc.edu; phone: 803-777-2646; fax: 803-777-9521.

Author Contributions

The manuscript was written through contributions of all authors. All authors have given approval to the final version of the manuscript.

Funding Sources

This work was supported by the U.S. National Science Foundation, Grant CHE-1308801.

Notes

The authors declare no competing financial interest.

ACKNOWLEDGMENT

The authors would like to extend special thanks to Kate Washburn and Prof. Tom Chandler for generously providing the Bread and Butter Creek sediment samples, Dr. Lijian He for AVS analysis, and to Joy Ihekweazu for help in the laboratory. We are also grateful to the reviewers for their work helping make a better paper.

Supporting Information. Preliminary work, all $[Fe(II)]_{aq}$, $[HS^-]$, and $[H_2O_2]$ data, matrix outcomes, quality assurance/quality control data re pH, run order, etc; and peroxide consumption experiments can be found in Supporting Information. This material is available free of charge via the Internet at http://pubs.acs.org.

ABBREVIATIONS

ROS, Reactive Oxygen Species; NOM, Natural Organic Matter;

REFERENCES

1. Chen, R. Z.; Pignatello, J. J., Role of quinone intermediates as electron shuttles in Fenton and photoassisted Fenton oxidations of aromatic compounds. *Environ. Sci. Technol.* **1997,** *31*, (8), 2399-2406.

2. Jiang, J.; Kappler, A., Kinetics of microbial and chemical reduction of humic substances: Implications for electron shuttling. *Environ. Sci. Technol.* **2008,** *42*, (10), 3563-3569.

3. Lovley, D. R.; Fraga, J. L.; Blunt-Harris, E. L.; Hayes, L. A.; Phillips, E. J. P.; Coates, J. D., Humic substances as a mediator for microbially catalyzed metal reduction. *Acta. Hydroch. Hydrob.* **1998,** *26*, (3), 152-157.

4. Nevin, K. P.; Lovley, D. R., Potential for nonenzymatic reduction of Fe(III) via electron shuttling in subsurface sediments. *Environ. Sci. Technol.* **2000,** *34*, (12), 2472-2478.

5. Fan, S. M., Photochemical and biochemical controls on reactive oxygen and iron speciation in the pelagic surface ocean. *Mar. Chem.* **2008,** *109*, (1-2), 152-164.

6. Faust, B. C., Photochemistry of clouds, fogs, and aerosols. *Environ. Sci. Technol.* **1994,** *28*, (5), A217-A222.

7. Haag, W. R.; Hoigne, J., Photo-sensitized oxidation in natural water via ·OH radical. *Chemosph.* **1985,** *14*, (11/12), 1659-1671.

8. Petasne, R. G.; Zika, R. G., Fate of superoxide in coastal sea water. *Nature* **1987,** *325*, (6104), 516-518.

9. Wardman, P.; Candeias, L. P., Fenton chemistry: An introduction. *Radiat. Res.* **1996,** *145*, (5), 523-531.

10. Voelker, B. M.; Morel, F. M. M.; Sulzberger, B., Iron redox cycling in surface waters: Effects of humic substances and light. *Environ. Sci. Technol.* **1997,** *31*, (4), 1004-1011.

11. Barb, W. G.; Baxendale, J. H.; George, P.; Hargrave, K. R., Reactions of ferrous and ferric ions with hydrogen peroxide. 2. The ferric ion reaction. *T. Faraday Soc.* **1951,** *47*, (6), 591-616.

12. Barb, W. G.; Baxendale, J. H.; George, P.; Hargrave, K. R., Reactions of ferrous and ferric ions with hydrogen peroxide. 1. The ferrous ion reaction. *T. Faraday Soc.* **1951,** *47*, (5), 462-500.

13. Carey, E.; Burns, J.; DiChristina, T. J.; Taillefert, M., Formation of soluble organic-Fe(III) complexes during microbial iron reduction. *Geochim.Cosmochim. Ac.* **2005,** *69*, (10), A225-A225.

14. Carey, E.; Taillefert, M., The role of soluble Fe(III) in the cycling of iron and sulfur in coastal marine sediments. *Limnol. Oceanogr.* **2005,** *50*, (4), 1129-1141.

15. USGS Nutrients National Synthesis Project. http://water.usgs.gov/nawqa/nutrients/datasets/cycle91/

16. Stumm, W.; Lee, G. F., Oxygenation of ferrous iron. *Ind. Eng. Chem.* **1961,** *53*, (2), 143-146.

17. Staehelin, J.; Hoigne, J., Decomposition of ozone in water - rate of initiation by hydroxide ions and hydrogen-peroxide. *Environ. Sci. Technol.* **1982,** *16*, (10), 676-681.

18. Gonzalez-Davila, M.; Santana-Casiano, J. M.; Millero, F. J., Oxidation of iron(II) nanomolar with H_2O_2 in seawater. *Geochim. Cosmochim. Ac.* **2005,** *69*, (1), 83-93.

19. Yao, W. S.; Millero, F. J., Oxidation of hydrogen sulfide by hydrous Fe(III) oxides in seawater. *Mar. Chem.* **1996,** *52*, (1), 1-16.

20. Luther, G. W.; Glazer, B. T.; Ma, S. F.; Trouwborst, R. E.; Moore, T. S.; Metzger, E.; Kraiya, C.; Waite, T. J.; Druschel, G.; Sundby, B.; Taillefert, M.; Nuzzio, D. B.; Shank, T. M.; Lewis, B. L.; Brendel, P. J., Use of voltammetric solid-state (micro)electrodes for studying biogeochemical processes: Laboratory measurements to real time measurements with an in situ electrochemical analyzer (ISEA). *Mar. Chem.* **2008,** *108*, (3-4), 221-235.

21. Mullaugh, K. M.; Luther, G. W.; Ma, S.; Moore, T. S.; Yucel, M.; Becker, E. L.; Podowski, E. L.; Fisher, C. R.; Trouwborst, R. E.; Pierson, B. K., Voltammetric

(micro)electrodes for the in situ study of Fe^{2+} oxidation kinetics in hot springs and $S_2O_3^{2-}$ production at hydrothermal vents. *Electroanal.* **2008,** *20*, (3), 280-290.

22. Luther, G. W., The Role of One- and Two-Electron Transfer Reactions in Forming Thermodynamically Unstable Intermediates as Barriers in Multi-Electron Redox Reactions. *Aquat. Geochem.* **2010,** *16*, (3), 395-420.

23. Roy, M.; Martin, J. B.; Cable, J. E.; Smith, C. G., Variations of iron flux and organic carbon remineralization in a subterranean estuary caused by inter-annual variations in recharge. *Geochim. Cosmochim. Ac.* **2013,** *103*, 301-315.

24. Morgan, B.; Burton, E. D.; Rate, A. W., Iron monosulfide enrichment and the presence of organosulfur in eutrophic estuarine sediments. *Chem. Geol.* **2012,** *296*, 119-130.

25. Frommichen, R.; Kellner, S.; Friese, K., Sediment conditioning with organic and/or inorganic carbon sources as a first step in alkalinity generation of acid mine pit lake water (pH 2-3). *Environ. Sci. Technol.* **2003,** *37*, (7), 1414-1421.

26. Yucel, M.; Gartman, A.; Chan, C. S.; Luther, G. W., Hydrothermal vents as a kinetically stable source of iron-sulphide-bearing nanoparticles to the ocean. *Nat. Geosci.* **2011,** *4*, (6), 367-371.

27. Sholkovitz, E. R.; Shaw, T. J.; Schneider, D. L., The Geochemistry of Rare-Earth Elements in the Seasonally Anoxic Water Column and Porewaters of Chesapeake Bay. *Geochim. Cosmochim. Ac.* **1992,** *56*, (9), 3389-3402.

28. Moore, W. S.; Shaw, T. J., Chemical signals from submarine fluid advection onto the continental shelf. *J. Geophys. Res-Oceans* **1998,** *103*, (C10), 21543-21552.

29. Windom, H. L.; Moore, W. S.; Niencheski, L. F. H.; Jahrike, R. A., Submarine groundwater discharge: A large, previously unrecognized source of dissolved iron to the South Atlantic Ocean. *Mar. Chem.* **2006,** *102*, (3-4), 252-266.

30. Moore, W. S., A reevaluation of submarine groundwater discharge along the southeastern coast of North America. *Global Biogeochem. Cy.* **2010,** *24*. DOI: 10.1029/2009GB003747.

31. Moore, W. S., The Effect of Submarine Groundwater Discharge on the Ocean. *Annu. Rev. Mar. Sci.* **2010,** *2*, 59-88.

32. Porubsky, W. P.; Joye, S. B.; Moore, W. S.; Tuncay, K.; Meile, C., Field measurements and modeling of groundwater flow and biogeochemistry at Moses Hammock, a backbarrier island on the Georgia coast. *Biogeochem.* **2011,** *104*, (1-3), 69-90.

33. Krest, J. M.; Moore, W. S.; Gardner, L. R.; Morris, J. T., Marsh nutrient export supplied by groundwater discharge: Evidence from radium measurements. *Global Biogeochem. Cy.* **2000,** *14*, (1), 167-176.

34. Duncan, T.; Shaw, T. J., The mobility of rare earth elements and redox sensitive elements in the groundwater/seawater mixing zone of a shallow coastal aquifer. *Aquat. Geochem.* **2003,** *9*, (3), 233-255.

35. Cooper, W. J.; Jones, A. C.; Whitehead, R. F.; Zika, R. G., Sunlight-induced photochemical decay of oxidants in natural waters: Implications in ballast water treatment. *Environ. Sci. Technol.* **2007,** *41*, (10), 3728-3733.

36. Cooper, W. J.; Zika, R. G.; Petasne, R. G.; Plane, J. M. C., Photochemical formation of H_2O_2 in natural-waters exposed to sunlight. *Environ. Sci. Technol.* **1988,** *22*, (10), 1156-1160.

37. Zepp, R. G.; Hoigne, J.; Bader, H., Nitrate-induced photooxidation of trace organic-chemicals in water. *Environ. Sci. Technol.* **1987,** *21*, (5), 443-450.

38. Zepp, R. G.; Faust, B. C.; Hoigne, J., Hydroxyl radical formation in aqueous reaction (pH 3-8) of iron (II) with hydrogen peroxide: the photo-Fenton reaction. *Environ. Sci. Technol.* **1992,** *26*, 313-319.

39. Cline, J. D., Spectrophotometric determination of hydrogen sulfide in natural waters. *Limnol. Oceanogr.* **1969,** *14*, (3), 454-458.

40. Stookey, L. L., Ferrozine - a new spectrophotometric reagent for iron. *Anal. Chem.* **1970,** *42*, (7), 779-781.

41. Burns, J. M.; Craig, P. S.; Shaw, T. J.; Ferry, J. L., Combinatorial parameter space as an empirical tool for predicting water chemistry: Fe(II) oxidation across a watershed. *Environ. Sci. Technol.* **2011,** *45*, (9), 4023-4029.

42. Burns, J. M.; Craig, P. S.; Shaw, T. J.; Ferry, J. L., Short-Term Fe Cycling during Fe(II) Oxidation: Exploring Joint Oxidation and Precipitation with a Combinatorial System. *Environ. Sci. Technol.* **2011,** *45*, (7), 2663-2669.

43. Cooper, W. J.; Moegling, J. K.; Kieber, R. J.; Kiddle, J. J., A chemiluminescence method for the analysis of H_2O_2 in natural waters. *Mar. Chem.* **2000,** *70*, (1-3), 191-200.

44. King, D. W.; Cooper, W. J.; Rusak, S. A.; Peake, B. M.; Kiddle, J. J.; O'Sullivan, D. W.; Melamed, M. L.; Morgan, C. R.; Theberge, S. M., Flow injection analysis of H_2O_2

in natural waters using acridinium ester chemiluminescence: Method development and optimization using a kinetic model. *Anal. Chem.* **2007,** *79*, (11), 4169-4176.

45. Aller, J. Y.; Aller, R. C.; Kemp, P. F.; Chistoserdov, A. Y.; Madrid, V. M., Fluidized muds: a novel setting for the generation of biosphere diversity through geologic time. *Geobiol.* **2010,** *8*, (3), 169-178.

46. Ciglenecki, I.; Bura-Nakic, E.; Margus, M., Zinc sulfide surface formation on Hg electrode during cyclic voltammetric scan: an implication for previous and future research studies on metal sulfide systems. *J. Solid State Electr.* **2012,** *16*, (6), 2041-2046.

47. Teuchies, J.; De Jonge, M.; Meire, P.; Blust, R.; Bervoets, L., Can acid volatile sulfides (AVS) influence metal concentrations in the macrophyte Myriophyllum aquaticum? *Environ. Sci. Tech.* **2012,** *46*, (16), 9129-9137.

48. Luther, G. W.; Glazer, B.; Ma, S. F.; Trouwborst, R.; Shultz, B. R.; Druschel, G.; Kraiya, C., Iron and sulfur chemistry in a stratified lake: Evidence for iron-rich sulfide complexes. *Aquat. Geochem.* **2003,** *9*, (2), 87-110.

49. Burns, J. M.; Craig, P. S.; Shaw, T. J.; Ferry, J. L., Multivariate examination of Fe(II)/Fe(III) cycling and consequent hydroxyl radical generation. *Environ. Sci. Technol.* **2010,** *44*, (19), 7226-7231.

50. Wilson, A. M.; Morris, J. T., The influence of tidal forcing on groundwater flow and nutrient exchange in a salt marsh-dominated estuary. *Biogeochem.* **2012,** *108*, (1-3), 27-38.

51. Tobias, C. R.; Harvey, J. W.; Anderson, I. C., Quantifying groundwater discharge through fringing wetlands to estuaries: Seasonal variability, methods comparison, and implications for wetland-estuary exchange. *Limnol. Oceanogr.* **2001,** *46*, (3), 604-615.

52. Fennessey, C. M.; Jones, M. E.; Taillefert, M.; DiChristina, T. J., Siderophores are not involved in Fe(III) solubilization during anaerobic Fe(III) respiration by Shewanella oneidensis MR-1. *Appl. Environ. Microb.* **2010,** *76*, (8), 2425-2432.

53. Luther, G. W.; Glazer, B. T.; Hohmann, L.; Popp, J. I.; Taillefert, M.; Rozan, T. F.; Brendel, P. J.; Theberge, S. M.; Nuzzio, D. B., Sulfur speciation monitored in situ with solid state gold amalgam voltammetric microelectrodes: polysulfides as a special case in sediments, microbial mats and hydrothermal vent waters. *J. Environ. Monit.* **2001,** *3*, (1), 61-66.

54. Tercier-Waeber, M. L.; Taillefert, M., Remote in situ voltammetric techniques to characterize the biogeochemical cycling of trace metals in aquatic systems. *J. Environ. Monit.* **2008,** *10*, (1), 30-54.

55. Survey, United States Department of the Interior, USGS National Water Quality Assessment Data Warehouse. 2007.

56. Brodie, B. B.; Axelrod, J.; Shore, P. A.; Udenfriend, S., Ascorbic acid in aromatic hydroxylation. 2. Products formed by reaction of substrates with ascorbic acid, ferrous ion, and oxygen. *J. Biol. Chem.* **1954,** *208*, (2), 741-750.

57. Udenfriend, S.; Clark, C. T.; Axelrod, J.; Brodie, B. B., Ascorbic acid in aromatic hydroxylation. 1. A model system for aromatic hydroxylation. *J. Biol. Chem.* **1954,** *208*, (2), 731-739.

58. Kang, S. H.; Choi, W., Oxidative degradation of organic compounds using zero-valent iron in the presence of natural organic matter serving as an electron shuttle. *Environ. Sci. Technol.* **2009,** *43*, (3), 878-883.

59. Sedlak, D. L.; Hoigne, J., Oxidation of S(IV) in atmospheric water by photooxidants and iron in the presence of copper. *Environ. Sci. Technol.* **1994,** *28*, (11), 1898-1906.

60. Sedlak, D. L.; Hoigne, J., The role of copper and oxalate in the redox cycling of iron in atmospheric waters. *Atmos. Environ. a-Gen.* **1993,** *27*, (14), 2173-2185.

61. Lutz, R. A.; Shank, T. M.; Luther, G. W.; Vetriani, C.; Tolstoy, M.; Nuzzio, D. B.; Moore, T. S.; Waldhauser, F.; Crespo-Medina, M.; Chatziefthimiou, A. D.; Annis, E. R.; Reed, A. J., Interrelationships between vent fluid chemistry, temperature, seismic activity, and biological community structure at a mussel-dominated, deep-sea hydrothermal vent along the East Pacific Rise. *J. Shellfish Res.* **2008,** *27*, (1), 177-190.

62. Ma, S.; Luther, G. W.; Keller, J.; Madison, A. S.; Metzger, E.; Emerson, D.; Megonigal, J. P., Solid-state Au/Hg microelectrode for the investigation of Fe and Mn cycling in a freshwater wetland: Implications for methane production. *Electroanal.* **2008,** *20*, (3), 233-239.

63. Ma, S. F.; Noble, A.; Butcher, D.; Trouwborst, R. E.; Luther, G. W., Removal of H_2S via an iron catalytic cycle and iron sulfide precipitation in the water column of dead end tributaries. *Estuar. Coast Shelf S* **2006,** *70*, (3), 461-472.

64. Moore, T. S.; Nuzzio, D. B.; Deering, T. W.; Taillefert, M.; Luther, G. W., Use of voltammetry to monitor O_2 using Au/Hg electrodes and to control physical sensors on an unattended observatory in the Delaware bay. *Electroanal.* **2007,** *19*, (19-20), 2110-2116.

65. Babauta, J. T.; Nguyen, H. D.; Istanbullu, O.; Beyenal, H., Microscale gradients of oxygen, hydrogen peroxide, and pH in freshwater cathodic biofilms. *Chemsuschem.* **2013,** *6*, (7), 1252-1261.

66. Hsieh, P.; Pedersen, J. Z.; Albertano, P., Generation of reactive oxygen species upon red light exposure of cyanobacteria from Roman hypogea. *Int. Biodeter. Biodegr.* **2013,** *84*, 258-265.

67. Koley, D.; Ramsey, M. M.; Bard, A. J.; Whiteley, M., Discovery of a biofilm electrocline using real-time 3D metabolite analysis. *P. Natl. Acad. Sci. USA* **2011,** *108*, (50), 19996-20001.

68. Liu, X. H.; Ramsey, M. M.; Chen, X. L.; Koley, D.; Whiteley, M.; Bard, A. J., Real-time mapping of a hydrogen peroxide concentration profile across a polymicrobial bacterial biofilm using scanning electrochemical microscopy. *P. Natl. Acad. Sci. USA* **2011,** *108*, (7), 2668-2673.

69. Bielski, B. H. J., Reevaluation of spectral and kinetic-properties of HO_2 and $O_2^{-\cdot}$ free radicals. *Photochem. Photobiol.* **1978,** *28*, (4-5), 645-649.

70. Rush, J. D.; Bielski, B. H. J., Pulse radiolytic studies of the reactions of HO_2/O_2^- with Fe(II)/Fe(III) ions - the reactivity of HO_2/O_2^- with ferric ions and its implication on the occurrence of the Haber-Weiss reaction. *J. Phys. Chem.* **1985,** *89*, (23), 5062-5066.

71. Roesler, A. J.; Gammons, C. H.; Druschel, G. K.; Oduro, H.; Poulson, S. R., Geochemistry of flooded underground mine workings influenced by bacterial sulfate reduction. *Aquat. Geochem.* **2007,** *13*, (3), 211-235.

72. Roy, M.; Martin, J. B.; Smith, C. G.; Cable, J. E., Reactive-transport modeling of iron diagenesis and associated organic carbon remineralization in a Florida (USA) subterranean estuary. *Earth Planet Sc. Lett.* **2011,** *304*, (1-2), 191-201.

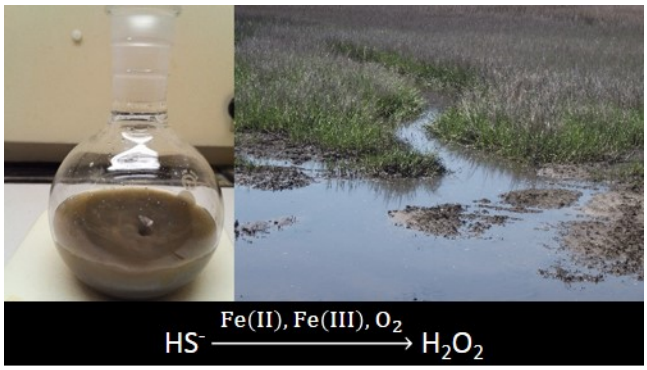

TOC/Abstract Art: Graphic for manuscript

APPENDIX B – GEOCHEMICAL PRODUCTION OF REACTIVE OXYGEN SPECIES FROM BIOGEOCHEMICALLY REDUCED FE (THE PUBLISHED VERSION)

ENVIRONMENTAL Science & Technology

Article

pubs.acs.org/est

Geochemical Production of Reactive Oxygen Species From Biogeochemically Reduced Fe

Sarah A. Murphy, Benson M. Solomon, Shengnan Meng, Justin M. Copeland, Timothy J. Shaw, and John L. Ferry*

Department of Chemistry and Biochemistry, University of South Carolina, Columbia, South Carolina 29208, United States

Supporting Information

ABSTRACT: The photochemical reduction of Fe(III) complexes to Fe(II) is a well-known initiation step for the production of reactive oxygen species (ROS) in sunlit waters. Here we show a geochemical mechanism for the same in dark environments based on the tidally driven, episodic movement of anoxic groundwaters through oxidized, Fe(III) rich sediments. Sediment samples were collected from the top 5 cm of sediment in a saline tidal creek in the estuary at Murrell's Inlet, South Carolina and characterized with respect to total Fe, acid volatile sulfides, and organic carbon content. These sediments were air-dried, resuspended in aerated solution, then exposed to aqueous sulfide at a range of concentrations chosen to replicate the conditions characteristic of a tidal cycle, beginning with low tide. No detectable ROS production occurred from this process in the dark until sulfide was added. Sulfide addition resulted in the rapid production of hydrogen peroxide, with maximum concentrations of 3.85 μM. The mechanism of hydrogen peroxide production was tested using a simplified three factor representation of the system based on hydrogen sulfide, Fe(II) and Fe(III). The resulting predictive model for maximum hydrogen peroxide agreed with measured hydrogen peroxide in field-derived samples at the 95% level of confidence, although with a persistent negative bias suggesting a minor undiscovered peroxide source in sediments.

INTRODUCTION

The cycling of Fe between ferrous and ferric oxidation states constitutes a catalytic mechanism of electron transport in aqueous environments ranging from sediments to surface waters.[1−4] This cycle is coupled to atmospheric oxygen through the reduction of O_2 by ferrous iron. In the photic zone, ferrous iron formation is generally photoinduced through the photolysis of Fe(III)−ligand (L) complexes, particularly when L = carboxylic acids (eq 1).[5−7] The resultant $Fe(II)_{aq}$ is thermodynamically unstable in the presence of dissolved oxygen and its oxidation leads to the production of the superoxide anion radical (eq 2). The superoxide anion radical is the conjugate base of the hydroperoxyl radical (pK_a 4.8). This radical can react with a second $Fe(II)_{aq}$ or disproportionate to generate hydrogen peroxide (eqs 3 and 4).[8−10] Hydrogen peroxide in turn can react with reduced transition metals (M^{x+}) to yield the hydroxyl radical (eq 5).[11,12] In sediments, aquifers, and anoxic porewaters microbial respiration can replace photons as the source of reductive equivalents to drive $Fe(II)_{aq}$ production. This is accomplished through a combination of direct microbial reduction and indirect reduction by microbially produced agents such as hydrogen sulfide (eq 6).[13,14] Reduced sulfur species, derived from anaerobic microbial reduction of sulfate, can occur in groundwaters at concentrations as high as millimolar.[15]

$$Fe(III)L \xrightarrow{h\nu,\mathrm{LMCT}} Fe(II)_{aq} + L_{ox} \quad (1)$$

$$Fe(II)_{aq} + O_2 \rightleftarrows Fe(III) + O_2^{-}\cdot \quad (2)$$

[16]

$$Fe(II) + HO_2\cdot \overset{H^+}{\rightleftarrows} H_2O_2 \quad (3)$$

[17]

$$O_2^{-}\cdot + HO_2\cdot \overset{H^+}{\rightleftarrows} H_2O_2 + O_2 \quad (4)$$

[17]

$$M^{x+}{}_{aq} + H_2O_2 \rightleftarrows M^{(x+1)+} + HO\cdot + HO^- \quad (5)$$

[18]

$$Fe(III) + HS^- \rightleftarrows Fe(II)_{aq} + HS\cdot \quad (6)$$

[19]

Reactions 1−5 suggest microbially generated $Fe(II)_{aq}$ can have the same impact on ROS production as photochemical sources of ROS, but with magnitude mediated by mass transport rather than light intensity.[20−22] Major sources of $Fe(II)_{aq}$ and hydrogen sulfide-rich waters include the outflow of

Received: November 20, 2013
Revised: February 18, 2014
Accepted: March 5, 2014
Published: March 5, 2014

dx.doi.org/10.1021/es4051764 | Environ. Sci. Technol. 2014, 48, 3815−3821

subterranean estuaries,[23] the release of sediment-associated porewater during low tide,[24] mine drainage[25] and the emissions of some hydrothermal vents.[26] Subterranean estuaries and tidally driven mixing are particularly significant among these sources because their releases are in close proximity to high human population densities near coastal regions.[27−29] Recent studies indicate the volume of groundwater associated with subterranean estuary emission represents a major, continuous flux of $Fe(II)_{aq}$ to the groundwater/seawater mixing zone.[30−32] Estimates based on Ra isotope inventories suggest that on the order of 30 kg water $m^{-2}day^{-1}$ is circulated through the shallow aquifer in the South Carolina saltmarsh system alone.[33] This yields an estimate for the entire South Carolina coastline (est. 2000 km^2 saltmarsh) of approximately 6.0×10^{10} kg of water exchanged between the oxic and anoxic conditions per day.[34] The implication is this ecosystem has a potential daily abiotic ROS flux of up to 1.5×10^7 moles day^{-1} (based on the accompanying dissolved oxygen flux). This number is comparable to photochemical sources of ROS, based on measured steady state concentrations of reactive oxygen species in near shore environments.[8,35,36] These numbers are rough estimates yet still suggest an important hypothesis: the number of moles of reactive oxygen species derived from $Fe(II)_{aq}$ rich groundwater is potentially on par with that obtained from photochemical processes, with biogeochemical reductants (e.g., sulfide) acting as initiators in a manner analogous to photons.

Direct measurement of the ROS production capacity of a given environmental compartment is a difficult challenge because of the transient nature of the analytes involved. There is a long tradition in aqueous ROS chemistry of addressing that problem by removing a representative fraction of the system in question from the field and initiating ROS production in a laboratory setting.[7,37,38] This work reports application of that strategy to test the hypothesis expressed in the preceding paragraph. This was done by infusing oxic sediment samples from a protected coastal marsh with sulfidic solutions (the initiation step) and monitoring subsequent ROS formation. Sediment samples were obtained from the surface of a pristine saline tidal creek at low tide (i.e., top five cm of exposed creek bottom, flooded with seawater at high tide, pH 8.0, salinity of 28 ppt). Varying concentrations of hydrogen sulfide were spiked into sediments and hydrogen peroxide generation was measured as a function of added sulfide and time. The duration of peroxide generation increased with increasing sulfide but the maximum concentration was constant, consistent with catalytic Fe oxidation/reduction cycles that continued until the sulfide was depleted. The mechanism of peroxide production was tested by comparing these outcomes to those obtained from a trifactorial experiment based on the cooxidation of $Fe(II)_{aq}$ and sulfide in solution in the presence of Fe(III) (central composite design, 15 conditions interrogated, vide infra).

■ EXPERIMENTAL METHODS

Materials. Iron(III) chloride hexahydrate and sodium sulfide nonahydrate (99.99+% trace metal free) were purchased from Aldrich. Hydrochloric acid (ACS grade) was obtained from BDH. *N,N*-dimethyl-*p*-phenylenediamine sulfate salt was acquired from Acros Organics. Diethylenetriaminepentaacetic acid (98+%) and iron(II) chloride anhydrous (99.5+%) were purchased from Alfa Aesar. Iron(II) chloride was stored in a desiccator. FerroZine iron reagent (98%) was purchased from VWR. All other salts (99%) were obtained from Fisher Scientific. All chemicals were used as received. Solutions were made in Barnstead E-pure (18 MΩ cm^{-1}) water which had been distilled under nitrogen to remove trace H_2O_2.

Analytical Methods. *Iron(II) and Sulfide Measurement.* $Fe(II)_{aq}$ and hydrogen sulfide were monitored colorimetrically using the ferrozine and methylene blue methods respectively.[39−42] Samples were withdrawn from the reactor and added directly to developing solutions (varied by analyte). Absorption spectra were recorded on a Spectramax M5 plate reader.

Hydrogen Peroxide. Hydrogen peroxide was measured by the acridinium ester chemiluminescence technique utilizing a flow injection analysis instrument with a chemiluminescence detector (Waterville Analytical, Waterville, ME).[43,44] Chemiluminescence from the reaction between the hydroperoxyl anion and acridinium ester at pH 11.4 was monitored in a flow through cell by a photon multiplier (PMT). All initial flow rates (sample, carrier, acridinium ester, and buffer) were set at a constant 1.5 mL/min. The flow cell volume was 2 mL, with a PMT integration time of 0.200 s and a constant voltage for every experiment set. Daily calibration was achieved by the use of independently verified (UV absorbance at 2.54×10^{-7} m) peroxide solutions, with hourly drift checks based on standard comparison. New calibrations were performed at least twice/measurement period or when instrument drift exceeded 10%.

All glassware used was cleaned in a muffle furnace and acid washed. After rinsing with 18MΩ deionized water, glassware was handled and stored as trace metal clean glassware to prevent trace metal catalytic oxidation of sulfide in the absence of added metals (Supporting Information (SI) S1−S61).

Sediment Experiments. Sediment samples were collected from a tidal creek (Bread and Butter Creek) in North Inlet, part of the Baruch Institute reserve near the town of Murrell's Inlet, South Carolina (SI S1−S4). Collected sediments included both oxic and anoxic layers. Anoxic portions were sulfidic with a loading of 26.5 μmol/g acid volatile sulfides based on dry weight. Aqueous sediment loading was 10.00 g L^{-1} of air-dried, sieved sediment, consistent with the low range of solid/liquid ratio (99% porosity) observed in the top layers of many coastal surface sediments.[45] Sediments were stirred for 20 min prior to the addition of sulfide and buffered to pH 8.28 with $NaHCO_3$ (0.050 M). Samples were removed from the reactors and spun down on a Baxter Dade Immufuge II centrifuge at 3225 rpm for 30 s to remove suspended solids before subsequent spectroscopic assays.

Quality Assurance/Quality Control. Replicate blanks (n = 3) were obtained for all reagents. Blanks were updated with preparation of fresh reagent solutions. Reference standards were interrogated for peroxide analysis at a frequency of 1 reference check/5 unknown determinations. Peroxide reference standards were externally calibrated against their optical absorbance at 254 nm. The detection limit for each method was defined by the linear dynamic range of the calibration curves.

■ EXPERIMENTAL DESIGN

The multifactorial experiments were designed to interrogate the relationship between peroxide yield and the initial concentrations of $Fe(II)_{aq}$, total Fe(III), and hydrogen sulfide. Specific conditions for each experiment were determined by processing the conditional ranges for each variable through the central composite design algorithm, which solved for specific points in parameter space that required experimentation (Table 1). This

Table 1. Factor Concentration Range Subdivisions: Experimental Factors and Initial Concentrations Corresponding to the Ranges Chosen for the Trivariate Experiment

	coded value for each factor:				
α	−2	−1	0	1	2
uncoded value for each factor (i.e., initial molar concentration):					
$[Fe(II)]_{aq} \times 10^{-6}$ M	0	61	150	239	300
$[Fe(III)] \times 10^{-6}$ M	0	61	150	239	300
$[HS^-] \times 10^{-6}$ M	0	101	250	399	500

design was chosen to allow an estimate of feedback terms, a necessary experimental componenet for systems based on free radical reactions that may involve self-disproportionation in the final observables. This method of interrogation allowed development of models based on the correlation of experimental outcomes with initial conditions without exhaustive understanding of the fundamental equilibria and kinetic constants for every step of the system.

The concentration ranges for each factor were chosen based on reported field measurements to ensure environmental relevance.[15,46−48] Similar models have previously been shown competent for accurately predicting net oxidation rates in complex multistep reaction systems.[41,42,49]

The pH of each reaction was monitored to ensure consistency. A pH probe (Cole Palmer pH electrode, general purpose, combination, refillable, glass body, BNC) was calibrated at the appropriate ionic strength condition and used to monitor pH throughout. Mean pH for the experimental array was 8.28 ± 0.07 reported as one standard deviation. The ionic strength of the solutions was established by the buffer; the sum of all other ionic species added contributed less than 2% to the total. All measurements were performed in triplicate, except the midpoint (initial conditions 1.50×10^{-4} M $Fe(II)_{aq}$, 1.50×10^{-4} M Fe(III), and 2.50×10^{-4} M HS^-), which was performed $n = 6$ times. The experimental sequence was randomized to eliminate time dependent artifacts. All experiments were conducted in a dark room to minimize photochemical reactions. The correlation between pH variability and measured outcomes (SI S1−S53, S1−S54) was less than 0.1, indicating pH was not a statistically significant factor across the experimental design.

RESULTS

The multifactorial experiments were justified based on the hypothesis that complex sediment samples could be reductively modeled as equivalent to mixtures of aqueous solutions of Fe(II), HS^- and Fe(III) as they came to thermodynamic equilibrium with dissolved oxygen. Air saturated solutions of HS^- were stable at pH 8.28 in the presence and absence of added hydrogen peroxide (SI S1−S61). Separate Fe(III) solutions and hydrogen sulfide solutions were monitored over time and no hydrogen peroxide evolution was detected. However the joint addition of Fe(II) and Fe(III) to oxic HS^- solutions resulted in the oxidation of Fe(II) and HS^- along with the initial rapid reduction of some Fe(III) (Figure 1). The ratio of the first derivatives of $[HS^-]$ and [Fe(II)] plotted vs time approached unity after the initial Fe(III) reduction phase, indicating the catalytic function of Fe(II) in enabling the oxidation of HS^- by O_2 (Figure 1 inset).

The evolution of hydrogen peroxide was monitored under all conditions of the trivariate experiment (Table 1) and observed

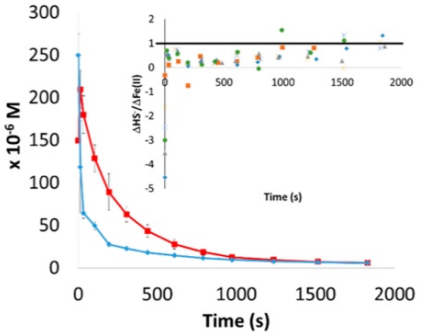

Figure 1. The concentration of (red square) $Fe(II)_{aq}$ and (blue circle) $[HS^-]$ during the oxidation of 1.50×10^{-4} M initial $Fe(II)_{aq}$ and 2.50×10^{-4} M initial hydrogen sulfide in the presence of 1.50×10^{-4} M initial Fe(III) is shown. Error bars shown are ±1 standard deviation based on $n = 6$ experiments. Inset: the ratio of the first derivatives of $[HS^-]$ and [Fe(II)], with a thick solid line to illustrate the approach to unity, six replicates shown.

to range from a minimum below the detection limit and a maximum of 2.3×10^{-5} M (Figure 2). An ANOVA table was

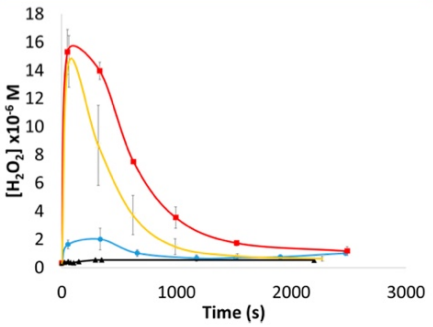

Figure 2. The concentration of peroxide with time. Initial conditions: (red square), 1.50×10^{-4} M $Fe(II)_{aq}$, 2.50×10^{-4} M HS^-; (yellow ×) 1.50×10^{-4} M $Fe(II)_{aq}$, 1.50×10^{-4} M Fe(III), 2.50×10^{-4} M HS^-; (blue circle) 1.50×10^{-4} M Fe(III), 2.50×10^{-4} M HS^-; (black triangle) 1.50×10^{-4} M $Fe(II)_{aq}$, 1.50×10^{-4} M Fe(III). Error bars shown are ±1 standard deviation based on $n = 3$ experiments.

constructed to determine the relationship between the hydrogen peroxide and the initial concentrations of Fe(II), HS^- and Fe(III). The maximum concentration of hydrogen peroxide for each experimental condition was correlated against all three individual factors, their squared terms (curvature) and the possible interactions in accordance with the quadratic fit of the central composite design algorithm (Table 2). The factors could be fit to the maximum hydrogen peroxide yield with an unadjusted R^2 of 0.919. The model was constructed assuming each term (x) had a coefficient, β_x. The statistical significance of each term to the outcome was determined by applying the t-

Table 2. Uncoded Coefficients (β_x) Obtained by Modeling the Maximum H_2O_2 Yield As a Function of Initial [Fe(II)], [Fe(III)] and [HS^-][a]

β_x	value	sum of squares	estimated % contribution	*p*-value
$\beta_{0\ (intercept)}$	−0.3064	57.69		<0.0001
$\beta_{Fe(II)}$	1.673×10^{-2}	20.16	34.9	<0.0001
$\beta_{Fe(III)}$	NS[b]	0.08	NS[b]	0.4523
β_{HS-}	1.305×10^{-2}	23.10	40.0	<0.0001
$\beta_{Fe(II)Fe(III)}$	NS[b]	0.15	NS[b]	0.2948
$\beta_{Fe(II)HS-}$	2.243×10^{-5}	2.12	3.7	0.0003
$\beta_{HS-Fe(III)}$	NS[b]	0.31	NS[b]	0.1382
$\beta_{(Fe(II))2}$	-4.325×10^{-5}	3.29	5.7	<0.0001
$\beta_{(Fe(III))2}$	NS[b]	0.00	NS[b]	0.9745
$\beta_{(HS-)2}$	-2.529×10^{-5}	8.68	15.0	<0.0001

[a] $R^2_{model} = 0.919$; $R^2_{adjusted} = 0.899$. [b] NS indicates "not significant" at the 95% level of confidence.

test to the hypothesis that $\beta_x \neq 0$ at the 95% level of confidence. Factors with β_x values that did not test as significantly different from 0 were statistically and practically unimportant to hydrogen peroxide. $[Fe(II)]_{aq}$, $[HS^-]$, $[Fe(II)]_{aq}^2$, $[HS^-]^2$, and the $[Fe(II)]_{aq}$-$[HS^-]$ interaction terms were significant to the outcome at the 95% level of confidence. The sign on the associated β_x values indicated the direction of contribution of that factor to the model outcome. Elimination of the remaining terms yielded an adjusted R^2 of 0.899. When their corresponding uncoded β_x terms and the intercept (Table 2) were included, the resulting empirical model for predicting the maximum concentration of hydrogen peroxide was (eq 7):

$$[H_2O_2]_{max}^{1/2} = -0.3064 + 1.673 \times 10^{-2}([Fe(II)]_{aq} \times 10^6) + 1.305x \times 10^{-2}([HS^-] \times 10^6) + 2.243 \times 10^{-5}([Fe(II)]_{aq} \times 10^6)([HS^-] \times 10^6) - 4.325 \times 10^{-5}([Fe(II)]_{aq} \times 10^6)^2 - 2.529 \times 10^{-5}([HS^-] \times 10^6)^2 \quad (7)$$

A sum of squares value was obtained from the ANOVA table for the model and each factor (SI Tables S1 and S2). The ratio of the value for each factor over the value for the model provided a rough estimate of the percent impact attributable to that factor on the maximum yield of hydrogen peroxide (Table 2).

A series of field-derived sediment samples were characterized (vide supra) and suspended in aerated solution of hydrogen sulfide and equilibrated with oxygen. The measured initial values of Fe(II) and HS^- were then entered into the model (eq 7) to generate predicted H_2O_2 maxima. The validity of the initial hypothesis was tested by comparison between the measured and predicted hydrogen peroxide maxima at the 95% level of confidence.

Equilibration experiments were conducted with aqueous suspensions of tidal creek sediment (Bread and Butter Creek (SI S1−S4), 1.00 wt % suspension; composition 21% C, 2% N, 1.2% total Fe). Sediments were aerated in the dark in the absence or presence of added hydrogen sulfide. Samples removed prior to sulfide addition contained detectable amounts of Fe(II) (detection limit of 2.0×10^{-6} M, whereas $[HS^-]$ and $[H_2O_2]$ were both below their respective detection limits ($3.0 \pm 1.5 \times 10^{-6}$ M and $2.50 \pm 0.90 \times 10^{-7}$ M, SI S1−S64). Native Fe(II) sources in the samples contributed to an Fe(II) background of $9.1 \pm 2.9 \times 10^{-6}$ M. Additional suspensions were prepared and sufficient hydrogen sulfide added to raise the nominal initial concentration to 3.00×10^{-4} M (Figure 3) or

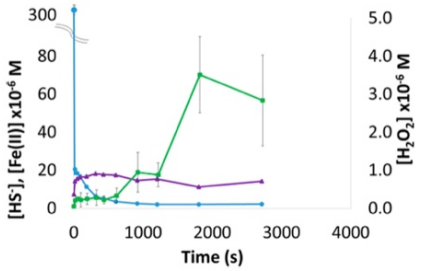

Figure 3. Concentration of (blue circle) hydrogen sulfide, (purple triangle) $Fe(II)_{aq}$, and (green square) H_2O_2 during the injection of 3.00×10^{-4} M hydrogen sulfide into a slurry of Bread and Butter Creek sediment (10.00 g sediment/L). Error bars are ±1 standard deviation based on $n = 3$ experiments.

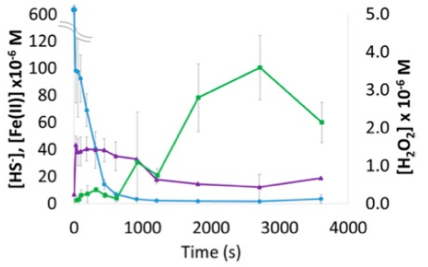

Figure 4. Concentration of (blue circle) hydrogen sulfide, (purple triangle) $Fe(II)_{aq}$, and (green square) H_2O_2 during the injection of 6.00×10^{-4} M hydrogen sulfide into a slurry of Bread and Butter Creek sediment (10.00 g sediment/L) are shown. Error bars shown are ±1 standard deviation based on $n = 3$ experiments.

6.00×10^{-4} M (Figure 4). These conditions were chosen to emulate tidally driven measured groundwater exchange (the outward pulse) through sediments.[14,50−55] Dissolved O_2 reduction in the latter suspensions was rapid with concurrent oxidation of hydrogen sulfide and formation of $Fe(II)_{aq}$ (Figure 3 and 4). $Fe(II)_{aq}$ fell to presulfide spike concentrations after added hydrogen sulfide was consumed, in agreement with existing models of Fe-catalyzed O_2 driven oxidation (e.g., the Udenfriend reaction and many subsequent works) and the results of the trivariate model.[14,56−60] Subsequent additions of hydrogen sulfide to the sediment suspensions resulted in essentially identical reactant/product production and consumption profiles (SI S1−S58, S1−S59, S1−S60) as long as oxygen concentrations were maintained. $Fe(II)_{aq}$ never reached the concentration that would be predicted from the reductive

Table 3. Comparison of Sediment Experimental Hydrogen Peroxide Data to Model Predictions

[HS-] initial	$[Fe(II)]_{aq}$ initial	[Fe(III)] initial	Sediment Data	Model Prediction
3.00×10^{-4} M	7×10^{-6} M	2.2×10^{-3} M	$3 \pm 1.8 \times 10^{-6}$ M	$2 \pm 0.9 \times 10^{-6}$ M
6.00×10^{-4} M	7×10^{-6} M	2.2×10^{-3} M	$4 \pm 1.8 \times 10^{-6}$ M	$2 \pm 0.9 \times 10^{-6}$ M

equivalents added (as hydrogen sulfide), presumably due to its simultaneous oxidation by dissolved oxygen (eqs 2 and 6). Hydrogen peroxide concentration increased as sulfide concentrations fell to near the detection limit, approaching a maximum of 3.85 and 2.83×10^{-6} M for 300 and 6.00×10^{-4} M hydrogen sulfide added, respectively (Figures 3 and 4). $Fe(II)_{aq}$ achieved a maximum concentration within 30 s and maintained at a pseudostationary state until $[HS^-] < [Fe(II)]_{aq}$, then fell.

DISCUSSION

Aqueous solutions of ferrous and ferric iron, dissolved oxygen and hydrogen sulfide are a thermodynamically unstable mixture that occurs frequently if transiently in natural waters as a result of mass trasport. They are associated with the movement of aqueous solutions across sharp redox gradients, particularly those imposed by microbial consumption of oxygen or the action of sulfate reducers. Examples include the tidally driven release of submarine groundwater across the sediment−water column interface; the seasonal overturn of hypolimnetic waters, redox zonation in biofilms and other events corresponding to a large range of flow regimes.[61−68] They equilibrate rapidly on mixing with concurrent oxidation of reduced iron and production of superoxide. The corresponding rate of O_2 reduction is controlled by several variables, including the rate of precipitation of resulting Fe(III) or Fe(III)-L in the studied system. Under the conditions of this study (pH 8.28, 5.0×10^{-2} M total CO_3^{2-} species, $[Fe(II)]_o < 3.00 \times 10^{-4}$ M) net Fe(II) oxidation in the absence of sulfide was expected to be quite rapid with an Fe(II) lifetime of less than 10 s.[41,42] Based on this assumption and eq 1−5 the appearance of superoxide and H_2O_2 should have mirrored the rapid loss of Fe(II). However, previous work has shown sulfide capable of rapidly reducing $Fe(III)_{aq}$ to Fe(II).[59,60] In this study sulfide addition resulted in a net apparent decrease in Fe(II) oxidation rates, with ROS formation coupled to sulfide oxidation and Fe(II) oxidation as a result (as distinguished from previous work reporting ROS formation as a result of Fe(II) oxidation alone).[13,41,42,49] The observation is supported by the results from the multifactorial experiment (Table 2) that indicate HS^- and FeS combined account for nearly 50% of the maximum hydrogen peroxide. Given that the direct reaction of HS^- with O_2 is spin forbidden this large positive impact indicates the intermediacy of Fe(II) as an electron shuttle between reduced S species and O_2 in the system. The relatively minor impact of FeS indicates that the reduction of Fe(III) by sulfide to produce Fe(II) was a more important source of reductive equivalents in the studied system than the direct oxidation of FeS. Given that the oxidation of Fe(II) and FeS both yield superoxide, comparison of the FeS and Fe(II) terms also suggested that the reduction of superoxide by Fe(II) (eq 3) was a more significant source for H_2O_2 than disproportionation.[69,70] However, changes in environmental conditions such as those associated with ocean acidification are likely to change the mechanism of H_2O_2 production, probably increasing the relative importance of dismutation if conditions are closer to pH 7.

The lack of significance of Fe(III) to maximum $[H_2O_2]$ (as indicated by analysis of the model in Table 2) supported commutability of the solution-phase model to experiments containing natural sediments. Comparison of predicted H_2O_2 maxima from eq 7 to the outcome of experiments measuring the equilibration of sediments with air; postsulfide addition, showed close agreement between the two sets of experiments (Table 3). It was particularly notable that doubling the initial HS^- loading had no statistically significant effect on the maximum H_2O_2 yield. This suggested the family of associated reactions had reached a steady state limited by a factor independent of added sulfide, speculatively the rate of FeS oxidation. Although FeS is stable in oxic solution on the time scale of days, freshly prepared (amorphous) FeS is known to oxidize on the time scale of seconds to minutes, depending on solution conditions. The appearance of a steady state was consistent with the self-reactions of ROS that limit their concentrations and with the observation of negative β_x for the significant squared factors (Table 2).

It was notable that the sediments in this study had very a high concentration of organic carbon, approximately 20% by mass. This carbon was not deliberately extracted or modified during the experimental procedure and therefore was presumably a faithful representation of organic carbon in the field environment. Despite the large excess of organic C in the suspensions eq 7 predicted the outcome of both HS^- spike concentrations to within the 90% confidence interval; and to within the 95% confidence interval for the 3.00×10^{-4} M HS^- spike, although both sets of predictions were biased slightly low (Table 3). The low bias in eq 7 could have also been a result of H_2O_2 produced during the peroxidation of organic C postoxidation by HO•, but the bias was so small organic C was probably not a significant contributor to the H_2O_2 maximum. The high concentration of natural organic materials in the studied system indicated they were certainly the primary sink for secondary ROS such as HO• generated during the process yet they did not affect its outcome. These observations have significant implications for micropollutant fate and carbon cycling and suggest an abiotic link between microbial metabolism and carbon oxidation. If the partial oxidation of refractory carbon or other electron donors/acceptors through sulfide driven ROS production leads to modifications making them better microbial energy sources, this suggests an alternative pathway for microbial alteration and consumption of natural and anthropogenic organic carbon.[23,71,72]

ASSOCIATED CONTENT

Supporting Information

Preliminary work, all $[Fe(II)]_{aq}$, $[HS^-]$, and $[H_2O_2]$ data, matrix outcomes, quality assurance/quality control data re pH, run order, etc; and peroxide consumption experiments can be found in the Supporting Information. This material is available free of charge via the Internet at http://pubs.acs.org.

AUTHOR INFORMATION

Corresponding Author

*Phone: 803-777-2646; fax: 803-777-9521; e-mail: ferry@sc.edu.

(36) Cooper, W. J.; Zika, R. G.; Petasne, R. G.; Plane, J. M. C. Photochemical formation of H_2O_2 in natural-waters exposed to sunlight. *Environ. Sci. Technol.* **1988**, *22* (10), 1156−1160.
(37) Zepp, R. G.; Hoigne, J.; Bader, H. Nitrate-induced photooxidation of trace organic-chemicals in water. *Environ. Sci. Technol.* **1987**, *21* (5), 443−450.
(38) Zepp, R. G.; Faust, B. C.; Hoigne, J. Hydroxyl radical formation in aqueous reaction (pH 3−8) of iron (II) with hydrogen peroxide: The photo-Fenton reaction. *Environ. Sci. Technol.* **1992**, *26*, 313−319.
(39) Cline, J. D. Spectrophotometric determination of hydrogen sulfide in natural waters. *Limnol. Oceanogr.* **1969**, *14* (3), 454−458.
(40) Stookey, L. L. Ferrozine - a new spectrophotometric reagent for iron. *Anal. Chem.* **1970**, *42* (7), 779−781.
(41) Burns, J. M.; Craig, P. S.; Shaw, T. J.; Ferry, J. L. Combinatorial parameter space as an empirical tool for predicting water chemistry: Fe(II) oxidation across a watershed. *Environ. Sci. Technol.* **2011**, *45* (9), 4023−4029.
(42) Burns, J. M.; Craig, P. S.; Shaw, T. J.; Ferry, J. L. Short-term Fe cycling during Fe(II) oxidation: Exploring joint oxidation and precipitation with a combinatorial system. *Environ. Sci. Technol.* **2011**, *45* (7), 2663−2669.
(43) Cooper, W. J.; Moegling, J. K.; Kieber, R. J.; Kiddle, J. J. A chemiluminescence method for the analysis of H_2O_2 in natural waters. *Mar. Chem.* **2000**, *70* (1−3), 191−200.
(44) King, D. W.; Cooper, W. J.; Rusak, S. A.; Peake, B. M.; Kiddle, J. J.; O'Sullivan, D. W.; Melamed, M. L.; Morgan, C. R.; Theberge, S. M. Flow injection analysis of H_2O_2 in natural waters using acridinium ester chemiluminescence: Method development and optimization using a kinetic model. *Anal. Chem.* **2007**, *79* (11), 4169−4176.
(45) Aller, J. Y.; Aller, R. C.; Kemp, P. F.; Chistoserdov, A. Y.; Madrid, V. M. Fluidized muds: A novel setting for the generation of biosphere diversity through geologic time. *Geobiol.* **2010**, *8* (3), 169−178.
(46) Ciglenecki, I.; Bura-Nakic, E.; Margus, M. Zinc sulfide surface formation on Hg electrode during cyclic voltammetric scan: An implication for previous and future research studies on metal sulfide systems. *J. Solid State Electrochem.* **2012**, *16* (6), 2041−2046.
(47) Teuchies, J.; De Jonge, M.; Meire, P.; Blust, R.; Bervoets, L. Can acid volatile sulfides (AVS) influence metal concentrations in the macrophyte *Myriophyllum aquaticum*? *Environ. Sci. Technol.* **2012**, *46* (16), 9129−9137.
(48) Luther, G. W.; Glazer, B.; Ma, S. F.; Trouwborst, R.; Shultz, B. R.; Druschel, G.; Kraiya, C. Iron and sulfur chemistry in a stratified lake: Evidence for iron-rich sulfide complexes. *Aquat. Geochem.* **2003**, *9* (2), 87−110.
(49) Burns, J. M.; Craig, P. S.; Shaw, T. J.; Ferry, J. L. Multivariate examination of Fe(II)/Fe(III) cycling and consequent hydroxyl radical generation. *Environ. Sci. Technol.* **2010**, *44* (19), 7226−7231.
(50) Wilson, A. M.; Morris, J. T. The influence of tidal forcing on groundwater flow and nutrient exchange in a salt marsh-dominated estuary. *Biogeochem.* **2012**, *108* (1−3), 27−38.
(51) Tobias, C. R.; Harvey, J. W.; Anderson, I. C. Quantifying groundwater discharge through fringing wetlands to estuaries: Seasonal variability, methods comparison, and implications for wetland-estuary exchange. *Limnol. Oceanogr.* **2001**, *46* (3), 604−615.
(52) Fennessey, C. M.; Jones, M. E.; Taillefert, M.; DiChristina, T. J. Siderophores are not involved in Fe(III) solubilization during anaerobic Fe(III) respiration by *Shewanella oneidensis* MR-1. *Appl. Environ. Microb.* **2010**, *76* (8), 2425−2432.
(53) Luther, G. W.; Glazer, B. T.; Hohmann, L.; Popp, J. I.; Taillefert, M.; Rozan, T. F.; Brendel, P. J.; Theberge, S. M.; Nuzzio, D. B. Sulfur speciation monitored in situ with solid state gold amalgam voltammetric microelectrodes: Polysulfides as a special case in sediments, microbial mats and hydrothermal vent waters. *J. Environ. Monit.* **2001**, *3* (1), 61−66.
(54) Tercier-Waeber, M. L.; Taillefert, M. Remote in situ voltammetric techniques to characterize the biogeochemical cycling of trace metals in aquatic systems. *J. Environ. Monit.* **2008**, *10* (1), 30−54.
(55) Survey, United States Department of the Interior, USGS National Water Quality Assessment Data Warehouse. 2007.
(56) Brodie, B. B.; Axelrod, J.; Shore, P. A.; Udenfriend, S. Ascorbic acid in aromatic hydroxylation. 2. Products formed by reaction of substrates with ascorbic acid, ferrous ion, and oxygen. *J. Biol. Chem.* **1954**, *208* (2), 741−750.
(57) Udenfriend, S.; Clark, C. T.; Axelrod, J.; Brodie, B. B. Ascorbic acid in aromatic hydroxylation. 1. A model system for aromatic hydroxylation. *J. Biol. Chem.* **1954**, *208* (2), 731−739.
(58) Kang, S. H.; Choi, W. Oxidative degradation of organic compounds using zero-valent iron in the presence of natural organic matter serving as an electron shuttle. *Environ. Sci. Technol.* **2009**, *43* (3), 878−883.
(59) Sedlak, D. L.; Hoigne, J. Oxidation of S(IV) in atmospheric water by photooxidants and iron in the presence of copper. *Environ. Sci. Technol.* **1994**, *28* (11), 1898−1906.
(60) Sedlak, D. L.; Hoigne, J. The role of copper and oxalate in the redox cycling of iron in atmospheric waters. *Atmos. Environ., Part A.* **1993**, *27* (14), 2173−2185.
(61) Lutz, R. A.; Shank, T. M.; Luther, G. W.; Vetriani, C.; Tolstoy, M.; Nuzzio, D. B.; Moore, T. S.; Waldhauser, F.; Crespo-Medina, M.; Chatziefthimiou, A. D.; Annis, E. R.; Reed, A. J. Interrelationships between vent fluid chemistry, temperature, seismic activity, and biological community structure at a mussel-dominated, deep-sea hydrothermal vent along the East Pacific Rise. *J. Shellfish Res.* **2008**, *27* (1), 177−190.
(62) Ma, S.; Luther, G. W.; Keller, J.; Madison, A. S.; Metzger, E.; Emerson, D.; Megonigal, J. P. Solid-state Au/Hg microelectrode for the investigation of Fe and Mn cycling in a freshwater wetland: Implications for methane production. *Electroanal* **2008**, *20* (3), 233−239.
(63) Ma, S. F.; Noble, A.; Butcher, D.; Trouwborst, R. E.; Luther, G. W. Removal of H_2S via an iron catalytic cycle and iron sulfide precipitation in the water column of dead end tributaries. *Estuarine, Coastal Shelf Sci.* **2006**, *70* (3), 461−472.
(64) Moore, T. S.; Nuzzio, D. B.; Deering, T. W.; Taillefert, M.; Luther, G. W. Use of voltammetry to monitor O_2 using Au/Hg electrodes and to control physical sensors on an unattended observatory in the Delaware bay. *Electroanal* **2007**, *19* (19−20), 2110−2116.
(65) Babauta, J. T.; Nguyen, H. D.; Istanbullu, O.; Beyenal, H. Microscale gradients of oxygen, hydrogen peroxide, and pH in freshwater cathodic biofilms. *ChemSusChem* **2013**, *6* (7), 1252−1261.
(66) Hsieh, P.; Pedersen, J. Z.; Albertano, P. Generation of reactive oxygen species upon red light exposure of cyanobacteria from Roman hypogea. *Int. Biodeterior. Biodegrad.* **2013**, *84*, 258−265.
(67) Koley, D.; Ramsey, M. M.; Bard, A. J.; Whiteley, M. Discovery of a biofilm electrocline using real-time 3D metabolite analysis. *Proc. Natl. Acad. Sci. U.S.A.* **2011**, *108* (50), 19996−20001.
(68) Liu, X. H.; Ramsey, M. M.; Chen, X. L.; Koley, D.; Whiteley, M.; Bard, A. J. Real-time mapping of a hydrogen peroxide concentration profile across a polymicrobial bacterial biofilm using scanning electrochemical microscopy. *Proc. Natl. Acad. Sci. U.S.A.* **2011**, *108* (7), 2668−2673.
(69) Bielski, B. H. J. Reevaluation of spectral and kinetic-properties of HO_2 and O_2^- free radicals. *Photochem. Photobiol.* **1978**, *28* (4−5), 645−649.
(70) Rush, J. D.; Bielski, B. H. J. Pulse radiolytic studies of the reactions of HO_2/O_2^- with Fe(II)/Fe(III) ions—The reactivity of HO_2/O_2^- with ferric ions and its implication on the occurrence of the Haber-Weiss reaction. *J. Phys. Chem.* **1985**, *89* (23), 5062−5066.
(71) Roesler, A. J.; Gammons, C. H.; Druschel, G. K.; Oduro, H.; Poulson, S. R. Geochemistry of flooded underground mine workings influenced by bacterial sulfate reduction. *Aquat. Geochem.* **2007**, *13* (3), 211−235.
(72) Roy, M.; Martin, J. B.; Smith, C. G.; Cable, J. E. Reactive-transport modeling of iron diagenesis and associated organic carbon remineralization in a Florida (USA) subterranean estuary. *Earth Planet Sci. Lett.* **2011**, *304* (1−2), 191−201.

APPENDIX C – ENVIRONMENTAL SCIENCE AND TECHNOLOGY PERMISSIONS

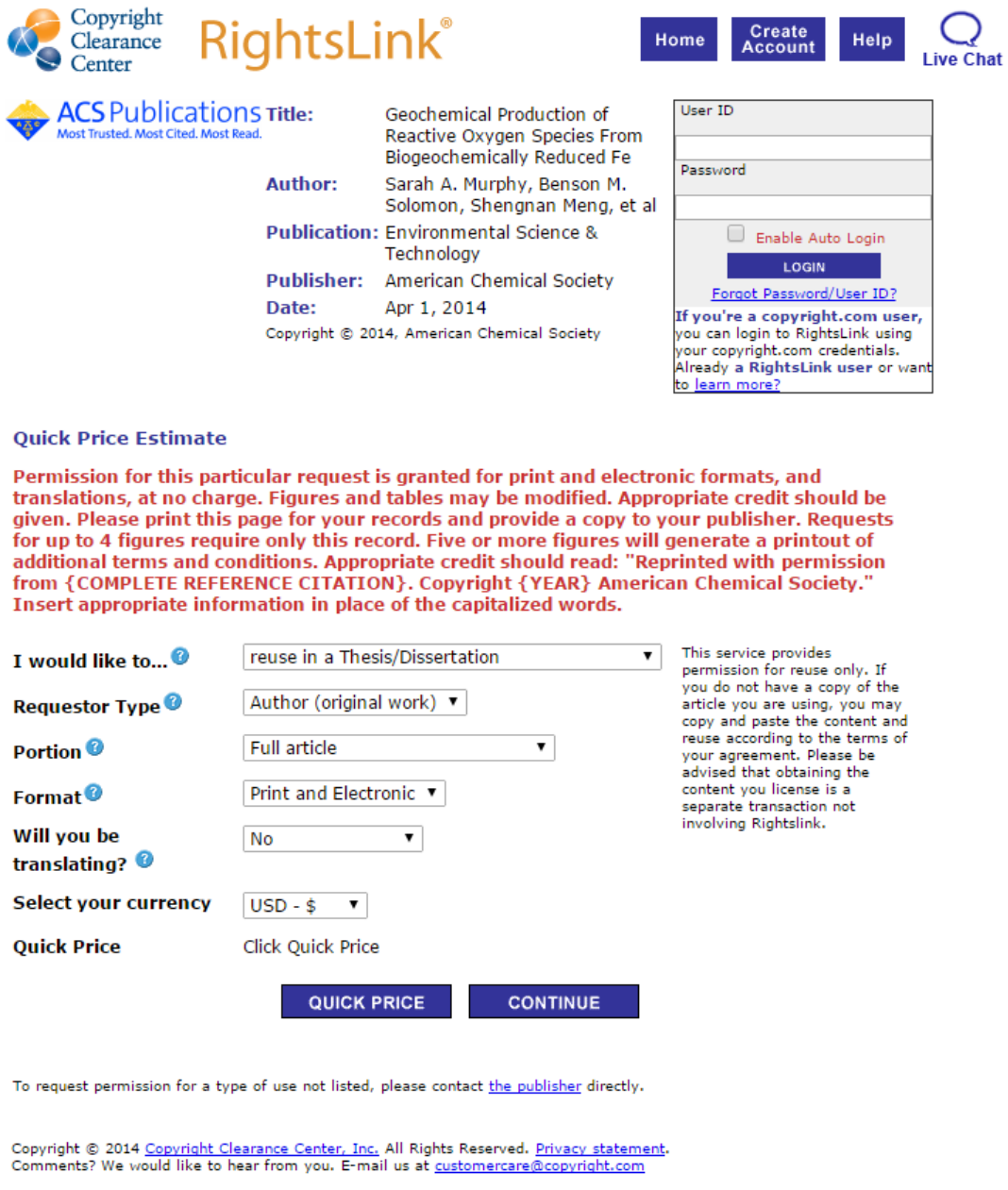

Copyright Clearance Center RightsLink®

Home | Create Account | Help | Live Chat

ACS Publications Most Trusted. Most Cited. Most Read.

Title: Geochemical Production of Reactive Oxygen Species From Biogeochemically Reduced Fe

Author: Sarah A. Murphy, Benson M. Solomon, Shengnan Meng, et al

Publication: Environmental Science & Technology

Publisher: American Chemical Society

Date: Apr 1, 2014

Copyright © 2014, American Chemical Society

User ID

Password

Enable Auto Login

LOGIN

Forgot Password/User ID?

If you're a copyright.com user, you can login to RightsLink using your copyright.com credentials. Already **a RightsLink user** or want to learn more?

Quick Price Estimate

Permission for this particular request is granted for print and electronic formats, and translations, at no charge. Figures and tables may be modified. Appropriate credit should be given. Please print this page for your records and provide a copy to your publisher. Requests for up to 4 figures require only this record. Five or more figures will generate a printout of additional terms and conditions. Appropriate credit should read: "Reprinted with permission from {COMPLETE REFERENCE CITATION}. Copyright {YEAR} American Chemical Society." Insert appropriate information in place of the capitalized words.

I would like to...	reuse in a Thesis/Dissertation
Requestor Type	Author (original work)
Portion	Full article
Format	Print and Electronic
Will you be translating?	No
Select your currency	USD - $
Quick Price	Click Quick Price

This service provides permission for reuse only. If you do not have a copy of the article you are using, you may copy and paste the content and reuse according to the terms of your agreement. Please be advised that obtaining the content you license is a separate transaction not involving Rightslink.

QUICK PRICE | CONTINUE

To request permission for a type of use not listed, please contact the publisher directly.

Copyright © 2014 Copyright Clearance Center, Inc. All Rights Reserved. Privacy statement.
Comments? We would like to hear from you. E-mail us at customercare@copyright.com